Lateral and Temporal Facies Variations in a Quaternary Travertine Deposit, Belen, New Mexico

---

A Thesis

Presented to

the Faculty of the Department of Geosciences

University of Houston

In Partial Fulfillment

of the Requirements for the Degree

Master of Science

By

Megan A. Cook

December 2013

Lateral and Temporal Facies Variations

in a Quaternary Travertine Deposit,

Belen, New Mexico

Megan A. Cook

APPROVED:

Dr. Henry Chafetz, Chairman

Dr. William Dupré, Committee Member

Dr. James Strasen, Committee Member

Dean, College of Natural Sciences and Mathematics

ACKNOWLEDGEMENTS

I would like to express my sincere gratitude to my thesis advisor, Dr. Henry Chafetz, for all of his time and guidance throughout my studies and research. I truly appreciate his enthusiasm for sharing his experience and insight into both travertines and research as a whole. My special thanks goes to my thesis committee members, Dr. William Dupré and Dr. James Strasen, for their invaluable time and encouragement. I would like to thank Dr. James Meen and Dr. Karoline Mueller at the Texas Center for Superconductivity for the training and support for my SEM and XRD analyses. I would like to acknowledge New Mexico Travertine Company for allowing me to have access to their amazing quarries and for providing assistance during my time in the field. I am also very grateful to TOTAL for the generous grant that made this research possible.

I would like to acknowledge my friend and field assistant, Fanjin Meng. Her positive attitude and significant assistance in the field is what allowed my research to come so far. I would also like to thank Xinyang Chen and Chris Trantham for all of their help and support throughout my research.

My heartfelt appreciation is offered to my parents, Doug and Sandi Cook, and sisters, Chelsea Dillon and Mary Cook, for encouraging and motivating me in all aspects of my life. I would not be in the position I am today without them. Last, but certainly not least, I would like to thank my husband, Jose Antonio Sierra, for being both my sounding board and my rock.

Lateral and Temporal Facies Variations

in a Quaternary Travertine Deposit,

Belen, New Mexico

An Abstract of a Thesis

Presented to

the Faculty of the Department of Geosciences

University of Houston

In Partial Fulfillment

of the Requirements for the Degree

Master of Science

By

Megan A. Cook

December 2013

ABSTRACT

This study examines the spatial relationships within travertine deposits, including variations in facies, constituents, and porosity, in two Quaternary travertine quarries near Belen, New Mexico. It integrates a combination of field examination and laboratory analyses, which allows for the interpretation of multiple scales of features. The travertine was deposited as tongues on the hanging wall of a fault on the western edge of the Rio Grande Rift. The quarries are composed of primary travertine and interbedded conglomerate layers that have been cross-cut by multiple generations of fractures, resulting in abundant veins filled with carbonate precipitates.

A wide variety of constituents, including both biotically and abiotically induced features, are present within the field area. The travertine within the quarries transitions, both laterally and temporally, between terrace mound and sloping mound morphologies. The terrace mound morphology exhibits distinct pools and rimstone dams. The pools have vertically stacked horizontal layers that are composed of bacterial shrubs, pisoids, rafts, and foam rock. Rimstone dams are composed of thin, vertical layers of ray-crystal crusts that separate the pools. The location of the terrace pools and rimstone dams was fairly stationary, but through time the height of the rimstone dam decreased and the morphology of the deposit transitioned into a sloping mound. The sloping mound is composed of layers that dip between 5 and 20 degrees. The layers range from smooth slopes that are composed of feather dendrites to microterraced slopes with rapidly

fluctuating pools and rimstone dams. The length of the microterrace pools depends heavily on the slope of the layer, but regardless of length, they are composed of crystal fans, rafts, and pisoids.

Both primary and secondary processes form the porosity within the quarry. The shape and connectivity of the pores is heavily dependent upon the constituents and degree of cementation. The permeability is anisotropic due to the layered natured of the travertine deposit, but the presence of abundant vertical fractures increases the vertical permeability. The knowledge gained from this study can be used in conjunction with other studies to provide a model that will be beneficial in areas where data are difficult to obtain, such as in the subsurface.

TABLE OF CONTENTS

ACKNOWLEDGEMENTS....iii

ABSTRACT v

TABLE OF CONTENTS vii

LIST OF FIGURES x

CHAPTER 1: INTRODUCTION TO THE PROJECT AND FIELD AREA 1

1.1 Introduction 1

1.2 Regional Geologic Setting and Location of Field Site 2

1.2.1 Location of Field Site 2

1.2.2 Regional Geologic Setting 2

1.2.3 Influence of Regional Stress on Rift Formation 4

1.2.4 Volcanism within the Rio Grande Rift 5

1.2.5 Travertine Occurrence and Formation within the Area 7

1.3 Details for Field Site 10

1.3.1 Ivory Quarry 12

1.3.2 Gold Quarry 13

1.3.3 Pink Quarry 14

1.3.4 Conduit Quarry 14

1.3.5 Vista Grande Quarry 14

1.3.6 Beef Steak Quarry 18

CHAPTER 2: INTRODUCTION TO TRAVERTINES 19

2.1 Overview 19

2.2 Precipitation 20

2.3 Travertine Classifications 23
2.4 Constituents 28
2.4.1 Shrubs and Crusts 28
2.4.2 Other Constituents 30
CHAPTER 3: METHODS 33
3.1 Fieldwork 33
3.2 Laboratory Work 34
CHAPTER 4: DATA AND INTERPRETATION 37
4.1 Travertine 37
4.1.1 Gold Quarry Travertine 37
4.1.2 Ivory Quarry Travertine 41
4.1.3 Mineralogy 47
4.1.4 Constituents 48
4.1.4.1 Rafts 48
4.1.4.2 Foam Rock 51
4.1.4.3 Coated Grains 55
4.1.4.4 Pisoids 57
4.1.4.5 Spherulites 59
4.1.4.6 Shrubs and Crusts 61
4.1.4.6.1 Bacterial Shrubs 61
4.1.4.6.2 Feather Dendrites 64
4.1.4.6.3 Ray Crystal Fans and Crusts 66
4.1.5 Porosity 73
4.1.6 Depositional Morphologies and Facies 79
4.1.6.1 Ivory Quarry Facies 79

4.1.6.2 Gold Quarry Facies 86
4.2 Conglomerates 89
4.2.1 Gold Quarry Conglomerates 89
4.2.2 Ivory Quarry Conglomerates 92
4.3 Veins 95
4.3.1 Gold Quarry Veins 97
4.3.2 Ivory Quarry Veins 101
CHAPTER 5: SUMMARY AND CONCLUSIONS 104
5.1 Gold Quarry 104
5.2 Ivory Quarry 105
5.3 Constituents 106
5.4 Porosity 107
5.5 Gold Quarry Conglomerates and Veins 108
5.6 Ivory Quarry Conglomerates and Veins 109
5.7 Final Words 109
REFERENCES 111
APPENDIX I: GOLD QUARRY MEASURED SECTIONS 119
APPENDIX II: IVORY QUARRY MEASURED SECTIONS 132

LIST OF FIGURES

1 Location Map of the Study Area……..03

2 Schematic Map and Cross Section of Travertine……09

3 Location Map of the Six Quarries……11

4 Schematic Outline and Image of the Ivory Quarry……12

5 Schematic Outline and Image of the Gold Quarry……13

6 Images of the Pink Quarry……15

7 Images of the Conduit Quarry……..……16

8 Images of the Vista Grande Quarry……..…17

9 Image of Gold Quarry- Walls B and C: Dip of Travertine Layers…....40

10 Image of Gold Quarry- Wall D ……41

11 Image of Ivory Quarry- Wall C: Dip of Travertine Layers…….43

12 Image of Ivory Quarry- Wall B2: Rimstone Dams Dipping in Opposite Directions…….44

13 Image of Ivory Quarry- Wall E2: Travertine Structure……..45

14 Image of Ivory Quarry- Wall E2: Transition from Terrace Mound to Sloping Mound……46

15 Image of Ivory Quarry- Wall C: Downstream Migrating Rimstone Dams……..47

16 Image of Ivory Quarry- Wall B: Upstream Migrating Rimstone Dam……..47

17 Image of Ivory Quarry- Wall E2: Aggrading Rimstone Dams……..47

18 Image of Conduit Quarry: Aragonite Ray……..…….49

19 Photomicrograph of a Raft with Concentric Growth…….51

20 Photomicrograph of a Raft with Isolated Fan-shaped Growth…….51

21 Photomicrograph of a Vertical Tube with Concentric Outline…….53

22 Photomicrograph of a Vertical Tube with Irregular Outline…….53

23 Photomicrograph of a Vertical Tube with Clumpy Outline……..53

24 Image of Foam Rock Layers……54

25 Photomicrograph of Microbial Mats in a Foam Rock Layer……56

26 Photomicrograph of a Rimstone Dam and Coated Grains……..57

27 Photomicrograph of Large Pisoids……..58

28 Photomicrograph of a Pisoid with a Raft as the Nucleus…….59

29 Photomicrograph of Spherulites……..61

30 SEM Images of Spherulites…….62

31 Photomicrograph of Bacterial Shrub Layers…….63

32 Photomicrograph of Bacterial Shrubs…….64

33 SEM Image of Bacterial Shrub Leaves Surrounded by Cement……65

34 SEM Image of Microporosity in Bacterial Shrub Leaves…….66

35 Photomicrograph of Feather Dendrites……..67

36 Photomicrograph of Ray Crystal Fans…….68

37 Photomicrograph of Ray Crystal Fan Growth……69

38 Photomicrograph of Ray Crystal Crusts…….70

39 Photomicrograph of Ray Crystal Fans Transitioning
into Ray Crystal Crusts…….71

40 Photomicrograph of Ray Crystal Clusters……..73

41 Photomicrograph of Porosity Under a Raft……75

42 Image of Vertical Fractures……..76

43 Photomicrograph of 11.8 Percent Porosity……77

44 Photomicrograph of 0.9 Percent Porosity……..78

45 Photomicrograph of 5.3 Percent Porosity……..79

46 Image of Ivory Quarry: Terrace Mound Pool and Rimstone Dam Indicating Paleo-water Depth……81

47 Image of Ivory Quarry: Peloid, Bacterial Shrub, and Raft Sequence…….83

48 Image of Ivory Quarry: Raft Layer……...84

49 Image of Ivory Quarry: Foam Rock layers with Three Pools……..…84

50 Image of Ivory Quarry: Microterraces…….86

51 Image of Gold Quarry: Terrace Mound……..88

52 Image of Gold Quarry: Sloping Mound……...89

53 Image of Gold Quarry: Microterraces…….89

54 Images of Gold Quarry- Walls B and C: Pinching out Breccia……..…92

55 Image of Ivory Quarry……94

56 Image of Ivory Quarry- Wall E2: Imbricated Clasts in Conglomerate……..…95

57 Geologic Map Showing Faults and Quarry Locations……..97

58 Image of Gold Quarry- Wall D: Multiple Generations of Vein-Fill……..……...99

59 Image of Gold Quarry- Wall D: Travertine Rotation due to Vein-Fill……..99

60 Image of Gold Quarry- Wall F: Red Veins…….……100

61 Image of Gold Quarry: Red Veins Associated with Conglomerates……...101

62 Image of Ivory Quarry- Wall C: Vein-Fill…….……103

63 Image of Ivory Quarry- Wall E2: Vein-Fill at Contact Between Travertine and Conglomerate…….……103

64 Image of Ivory Quarry: Travertine Rotation due to Vein-Fill……104

CHAPTER 1: INTRODUCTION TO THE PROJECT AND FIELD AREA

1.1 Introduction

Travertines, spring-fed carbonate deposits, are formed by an intricate system and can reveal an abundance of information about conditions at the time of their formation. Understanding the presence and characteristics of these deposits can aid in the interpretation of the tectonic activity, water chemistry, and overall depositional environment of the area. Interest in travertines has existed for thousands of years. They were heavily quarried during the Roman Empire and travertine was the most common building material in ancient Rome (Pentecost, 2005). The popularity of travertine as a building material has continued to the modern day, as it is frequently used for tile floors and building facades. More recently, travertines have also been found to be an excellent hydrocarbon reservoir rock.

Even though travertine deposits have been explored and exploited for thousands of years, there are still many aspects of these deposits that are poorly understood. The purpose of this study is to provide a better understanding of the temporal and lateral facies variations within a travertine deposit. In addition to characterizing the depositional fabrics, an emphasis is placed on understanding the variations in porosity resulting from morphological changes within the deposit. Finally, this study draws conclusions about the depositional environment, paleo-environmental conditions, and diagenetic history of the travertine deposit.

The results of this project help provide a model for the spatial distribution of the facies relationships and associated porosity found within travertine accumulations. Such a model is applicable to similar travertine deposits found at the surface and in the subsurface. This is of significant importance to the oil and gas industry as it is attempting to better understand the spatial extent of the subsurface travertine deposits, in particular, the pre-salt travertine deposit in the Campos Basin, offshore Brazil.

1.2 Regional Geologic Setting and Location of Field Site

1.2.1 Location of Field Site

The field area for this project is an active travertine quarry in Valencia County, New Mexico, and is operated by New Mexico Travertine Company. The quarry is located approximately 40 kilometers west of the city of Belen, at the base of Mesa Aparejo (Figure 1). This deposit is situated on the western edge of the Albuquerque-Belen subbasin, which is the central section of the Rio Grande Rift.

1.2.2 Regional Geologic Setting

The Rio Grande Rift has experienced two main phases of extension. An early phase of extension occurred during the late Oligocene to early Miocene, 25 to 19 million years ago. It is characterized by closely spaced, low-angle normal faults, which formed broad, shallow rift basins (Baldridge et al., 1980; Morgan et al., 1986). The low-angle nature of the faults resulted in significant tilting and

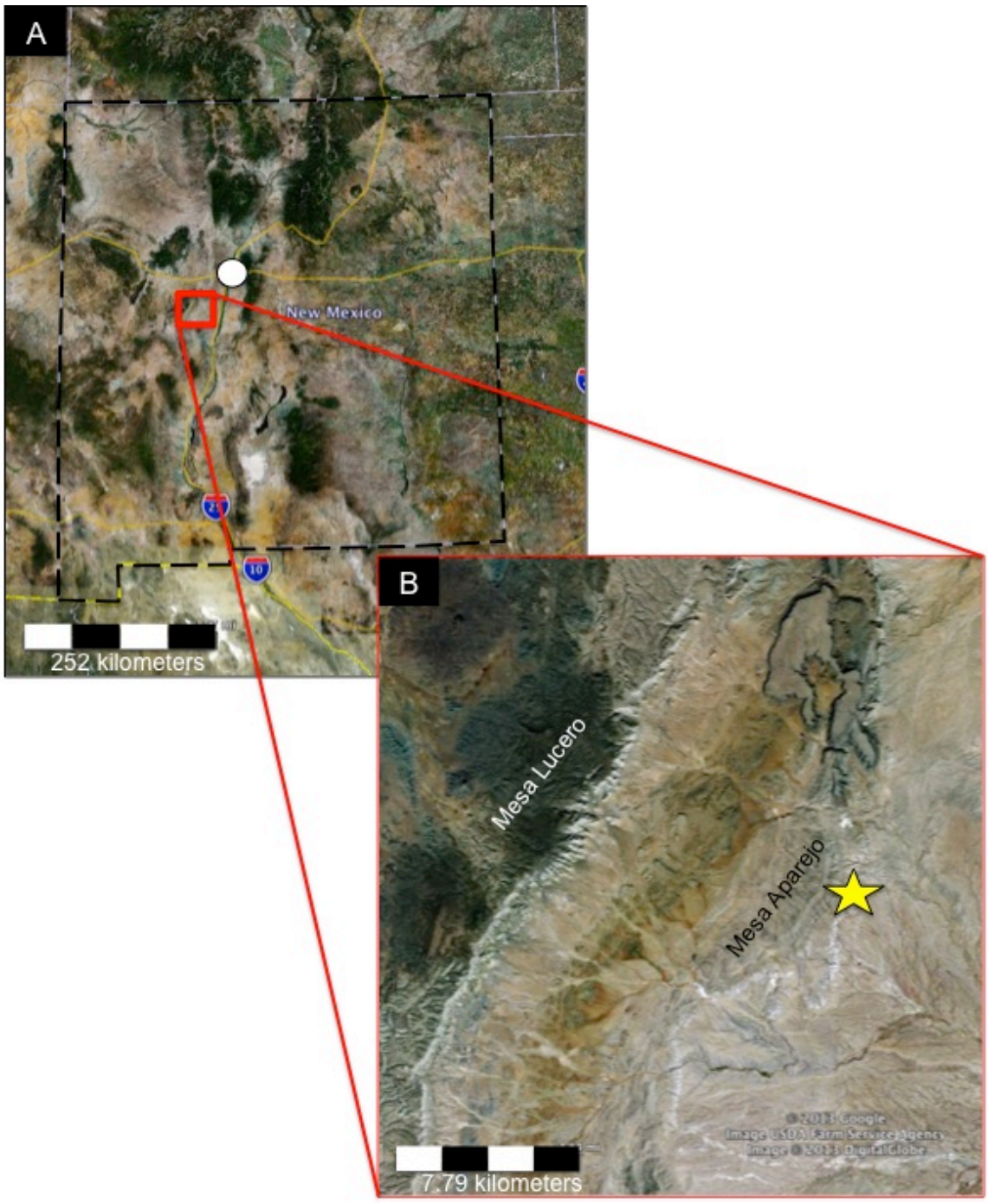

Figure 1: (A) Google Earth image showing the location of the field site in west-central New Mexico. The black dashed line is the outline of the state of New Mexico. The white dot indicates the location of Albuquerque. The red box indicates the location of the zoomed in image of the field site shown in image B. (B) Google Earth image of the area surrounding the field location (marked with a yellow star). The field area is immediately to the east of Mesa Aparejo.

rotation of the strata that were deposited within the basin. Although the faults cannot be directly dated, relative dating gives them an age of 31 to 10 million years ago (Morgan et al., 1986). Following the early phase of extension, the area experienced a 6 million year lull in magmatism, which has been interpreted as a slowing down or hiatus in extension (Baldridge et al., 1980). The late phase of extension occured during the late Miocene (13 million years ago) to the present and is characterized by the renewal of volcanism and the uplift of mountains (Baldridge et al., 1980). This phase is marked tectonically by the formation of widely spaced, high-angle normal faults. These faults offset the low-angle faults that formed during the early phase of extension (Morgan et al., 1986). The faulting that occurred during the late phase of extension caused the formation of narrow, deep, asymmetric basins. These resulting basins exhibit large vertical offsets between the basins and surrounding areas, but not a lot of extension due to the high angle of the faults (Morgan et al., 1986).

1.2.3 Influence of Regional Stress on Rift Formation

During the formation of the Rio Grande Rift, the direction of least principal stress has rotated in a clockwise direction (Ingersoll, 2001). At the time of the early rift phase, extension was oriented in an ENE-WSW direction. This direction of extension is thought to be derived from a perpendicular maximum stress caused by subduction along the western continental margin (Golombek et al., 1983). Approximately 8 to 10 million years ago, the least principal stress direction rotated to WNW-ESE. This is thought to have resulted in the acceleration of

extension and the initiation of faults in a new direction within the Rio Grande Rift basins (Ingersoll, 2001). This change in stress direction corresponds to the change in plate motion between the Pacific and North American plates (Ingersoll, 2001).

1.2.4 Volcanism within the Rio Grande Rift

The volcanism within the Rio Grande Rift can be generally classified into 3 main phases: prior to rifting, early phase rifting, and late phase rifting. The volcanism that occurred prior to rifting has been used to date the age of rift initiation. These volcanic deposits are widespread and can be identified both within rift basins and outside of rift basins, indicating that the volcanism occurred before rifting began (Morgan et al., 1986). During this time, the upper mantle was influenced by the subduction of the Farallon Plate, which resulted in a heterogeneous mantle that contained an influence from both MORB-type and OIB-type components (Kil and Wendlandt, 2007). The composition of volcanic rocks deposited during the pre-rift phase is mostly intermediate (calc-alkaline) basalt (Keller et al., 1991).

The early phase of magmatism, approximately 30 million years ago until 18 million years ago, occurred primarily along the rift axis and was the cause of 80 percent of the volcanic rocks deposited in the southern Rio Grande Rift (Kil and Wendlandt, 2007). During the early phase, the lithospheric thickness was reduced under the rift axis by asthenospheric upwelling (Kil and Wendlandt, 2007). This is indicated by a depleted (asthenospheric) signature of the volcanic

rocks derived from along the rift axis and an enriched (lithospheric) signature for those sourced from the outer flanks of the Rio Grande Rift (Wilson et al., 2005). The late phase of volcanism occurred from 12 million years until the present, with the majority occurring within the last five million years (Morgan and Golombek, 1984). Baldridge et al. (1987) found that Pliocene to Holocene volcanism in the Lucero area (located just to the west of the field area) has occurred in two main pulses: 4 to 3 million years ago and 1.1 million years ago to present (Baldridge et al., 1987). The compositions of the volcanic deposits within this area are primarily basalts, that being said, a shift within the basaltic composition can be seen through time. In the Lucero area, the composition has progressed from alkali olivine basalts in the Miocene to tholeiitic basalts in the Pliocene (4 to 3 Ma pulse). Finally, the composition has shifted to a combination of tholeiitic rocks and high-alkali, nepheline-normative basalts in the most recent phase (Baldridge et al., 1991). Where volcanism is present within the Rio Grande Rift, it is found in significantly less volumes than is common among continental rift systems (Keller et al., 1991).

Questions have been raised as to whether the lack of volcanism within the Rio Grande Rift is caused by magmatic material not being produced, or that the magmatic material has not made its way to the surface. There has been a large magma body interpreted to be near Socorro, New Mexico (located just to the south of the field area), which leads some authors to believe that the amount of volcanism that has been erupted to surface does not represent the amount of

magmatic material within the system (Keller et al., 1991). The magma body has been described as a broad, tabular body that extends over an area of 1,700 km^2. The magma body appears to be present within the middle section of the crust, at a depth of approximately 20 kilometers (Hermance and Neumann, 1991). Conversely, Slack et al. (1996) used seismic tomography to make interpretations about the temperatures within the central sections of the Rio Grande Rift. They found that the lithosphere beneath the rift is near the solidus temperature but that it is unlikely to have significant partial melting (Slack et al., 1996).

1.2.5 Travertine Occurrence and Formation within the Area

Travertine deposits are a fairly common occurrence within New Mexico, scattered across the entire state on both the eastern and western edges of the Rio Grande Rift system. Within Valencia County, there are three main areas of deposition: Mesa Lucero, Sierra Lucero, and Mesa Aparejo (McLemore et al., 1986). The combination of deep-seated faulting and high heat flow resulted in an abundance of hot springs in the area and made it a prime location for travertine precipitation.

The timing of travertine formation in the area is highly related to fault activity. Many lines of evidence, such as the inclusion of travertine pebbles within surrounding formations, have been identified and indicate that travertine formation began by the late Pliocene (Wright, 1946). Wright (1946) found that travertine precipitation continued during the Pleistocene and resulted in accumulations approximately 30 to 45 meters thick (Wright, 1946). Today, there

are a few locations that are currently producing travertine, but the majority of the area is inactive.

The water in the travertine system is composed of meteoric water mixed with deeply sourced water that is enriched with mantle-derived CO_2 (Newell et al., 2005). Wright (1946) determined that the source for the deep-seated water within the area came from a depth of at least 640 meters (2,100 feet), based on the water temperature and the geothermal gradient of the area (Wright, 1946). A fault system near Mesa Aparejo, the Comanche fault system, is thought to be the conduit for the carbonate-charged waters that precipitated travertine at the study locale (Austin and Barker, 1990). As the water ascended towards the earth's surface, it came into contact with multiple limestones that can be found within the stratigraphic section, including the Madera Formation (Austin and Barker, 1990) and San Andres Limestone (Barker, 1986 after Kottlewski, 1962). The interaction of the water with these limestones resulted in their dissolution and allowed for the increased carbonate saturation within the ascending water. The water reaches the surface at isolated spring orifices and begins to precipitate tongues of travertine in a down slope direction on the hanging wall of the fault (Figure 2).

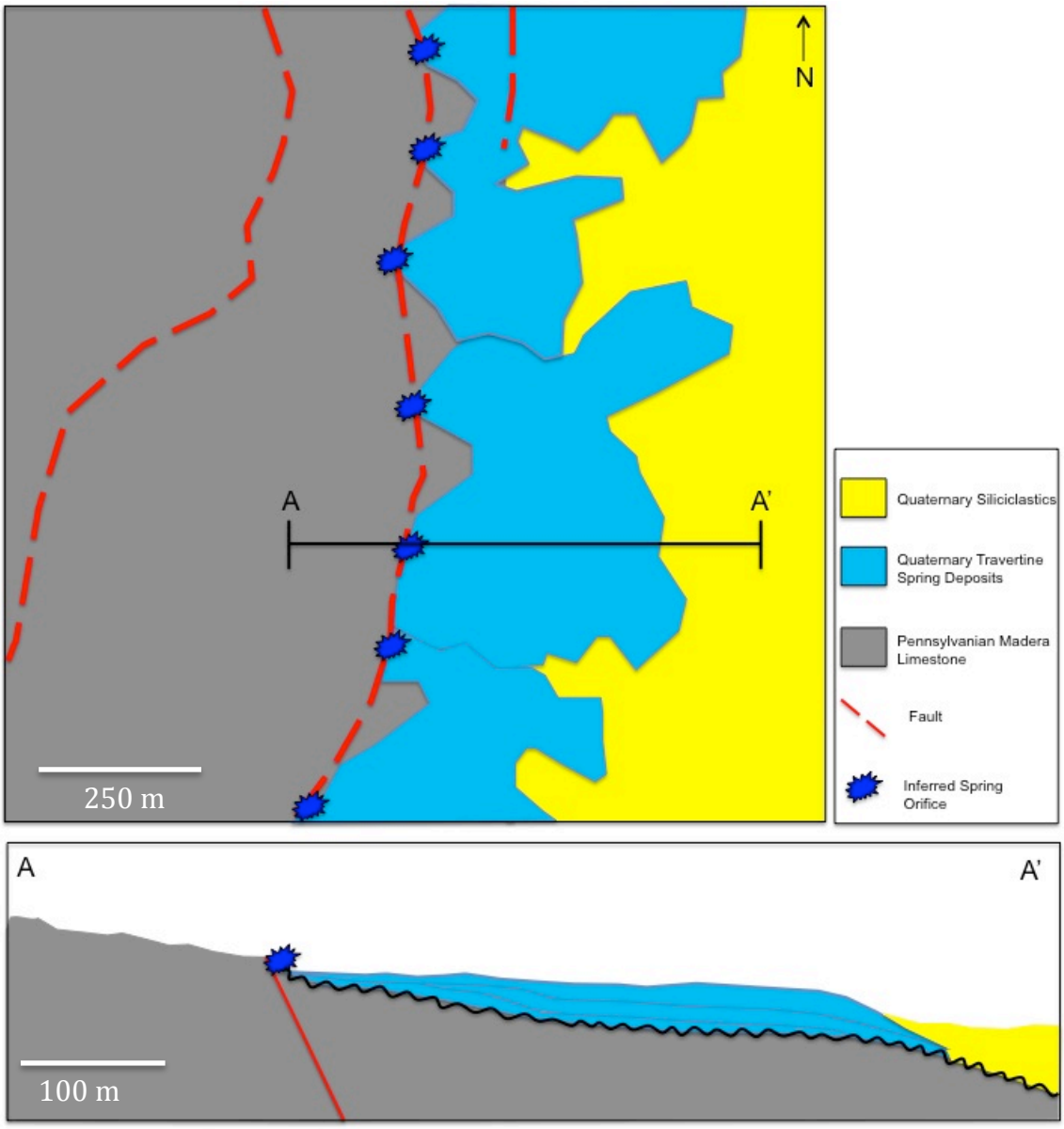

Figure 2: Schematic map and cross section showing the formation of travertine on the downthrown fault block. The deep-seated water ascends to the surface at isolated spring orifices along the fault. The water then flows down slope and precipitates tongues of travertine. Each tongue has a somewhat different composition due to variations in water chemistry, such as changes in color due to fluctuations in iron percentage.

1.3 Details for Field Site

The field site for this research is a Quaternary-aged travertine deposit that covers approximately 1,140 acres (4.6 km^2) and may total 200 million short tons ($181.4x10^9$ kilograms) (Austin and Barker, 1990). The travertine within the area is formed by springs associated with faults within the Comanche fault system. The initial maps that were drafted by Kelley and Wood (1946) indicated that the fault system was composed of numerous thrust faults, but since then it has been interpreted as a normal fault system (Austin and Barker, 1990). This interpretation is backed up by its location on the edge of the Rio Grande Rift system and by the presence of travertine, which have been strongly tied to normal faults (Hancock et al., 1999; Brogi and Capezzuoli, 2009).

The travertine deposit is being actively mined by New Mexico Travertine Inc. and has been separated into six individual quarries: Pink, Gold, Ivory, Vista Grande, Conduit, and Beef Steak (Figure 3). Each quarry represents a different variation of travertine that has its own unique characteristics. The variations are due to a range of factors, including changes of water geochemistry due to the ascent of water through diverse pathways resulting in the influence of different Paleozoic strata at each distinct spring orifice. Other variations can be attributed to the distance of the quarry from the fault. Austin and Barker (1990) noted that each of the six varieties of travertine are laterally continuous for hundreds of meters down slope into the basin (Austin and Barker, 1990). This project will focus on the lateral and temporal variations within the Gold and Ivory quarries,

with minor information about the other quarries as are relevant to the study.

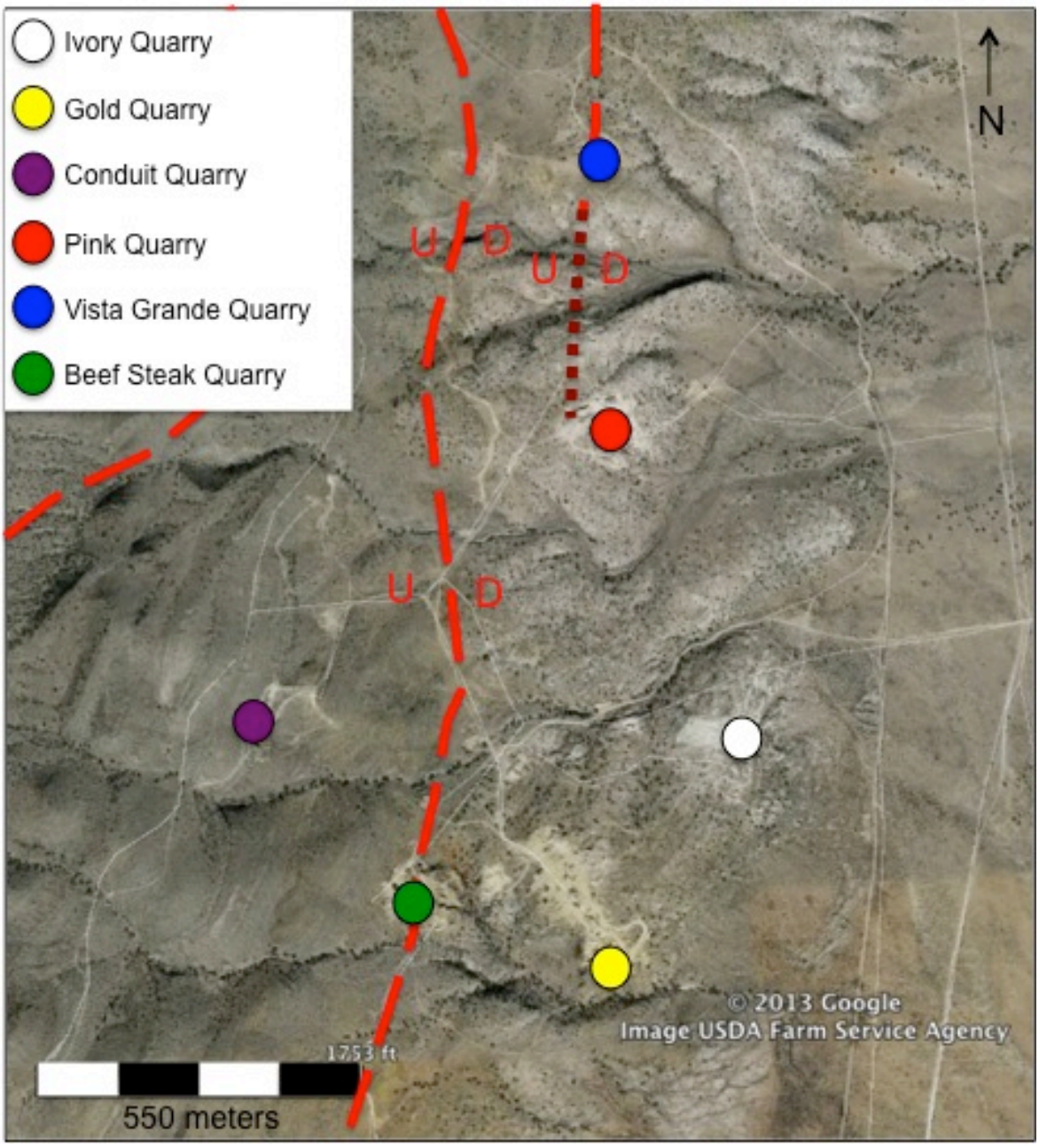

Figure 3: Google Earth image showing the distance and relationship between the 6 quarries at the field site (34°39'58.84"N, 107° 5'43.11"W).

1.3.1 Ivory Quarry

The Ivory Quarry is composed of eight distinct walls that are oriented in a variety of directions (N-S, E-W, NW-SE, NE-SW) (Figure 4). The walls range in width from 6 to 25 m and height from 4 to 8 m. The walls display cream (ivory) colored travertine that is overlain by a large conglomerate layer. Both the travertine and conglomerate are continuous throughout the extent of the Ivory Quarry. The area also exhibits multiple carbonate veins that cut both the initial travertine and the conglomerate.

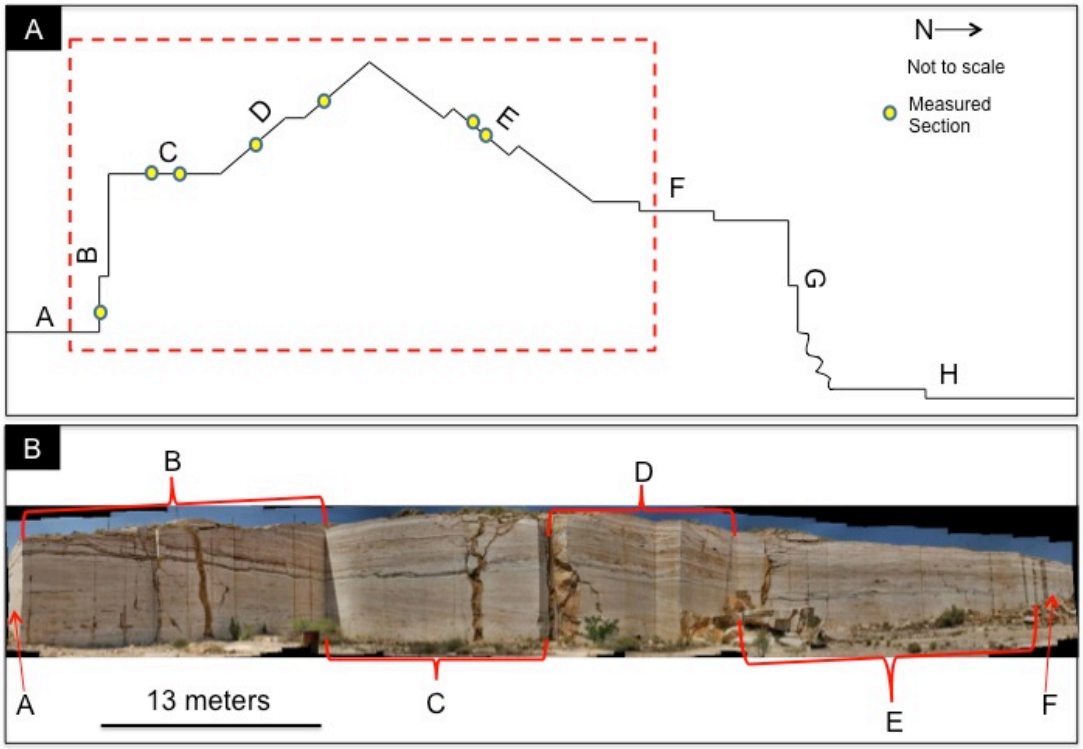

Figure 4: (A) Schematic outline of the walls in the Ivory Quarry. Dashed red box indicates the location of image B. Yellow dots indicate the location of measured sections. (B) Panoramic image showing the Ivory Quarry.

1.3.2 Gold Quarry

The Gold Quarry is composed of seven distinct walls that are oriented in either a N-S or E-W direction (Figure 5). The travertine within this quarry has a variety of different colors, ranging from cream to pink to brown. There are multiple conglomeratic layers scattered throughout the travertine. The area is heavily broken-up by carbonate veins that cut through both the initial travertine and the conglomerate.

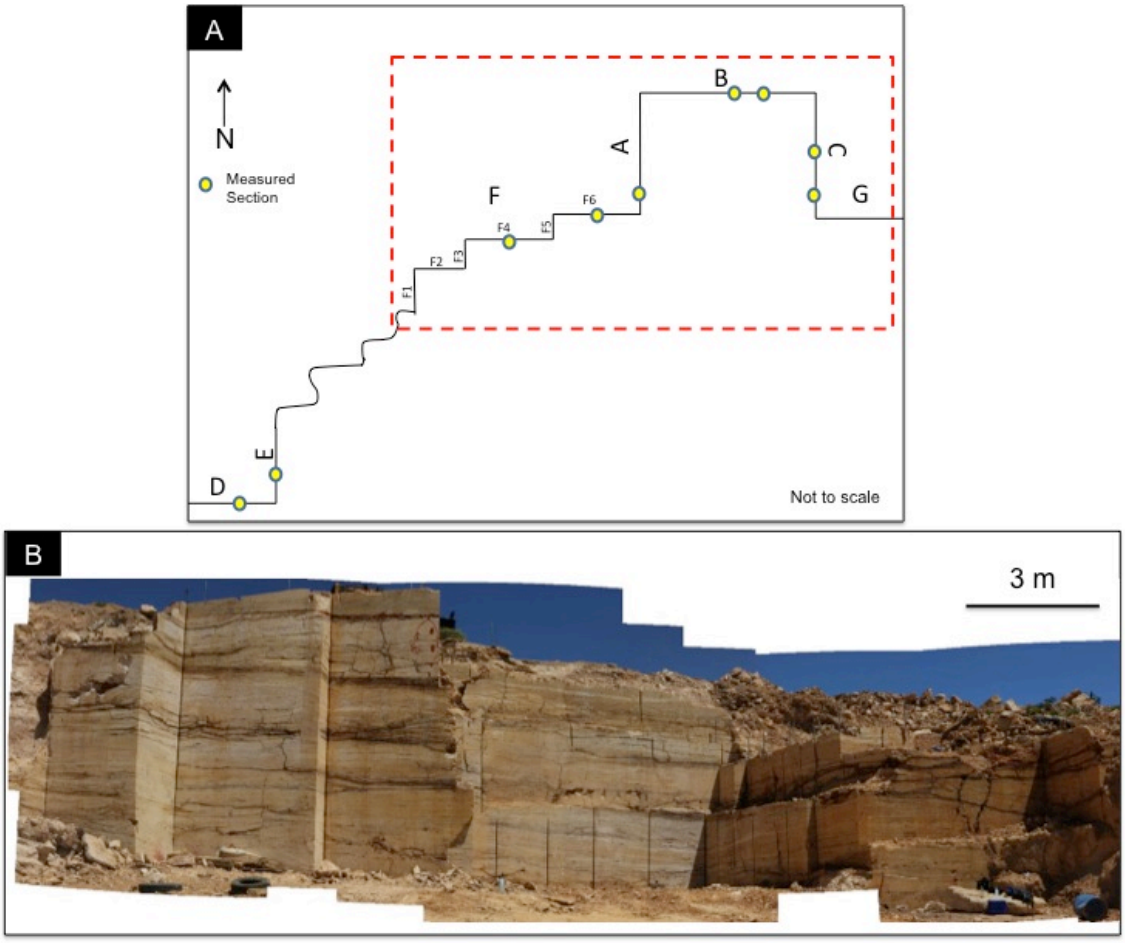

Figure 5: (A) Schematic outline of the walls in the Gold Quarry. Dashed red box indicates the location of image B. Yellow dots indicate the location of measured sections. (B) Panoramic image showing the Gold Quarry.

1.3.3 Pink Quarry

The Pink Quarry is a large quarry composed of twelve walls that are oriented in a N-S or E-W direction (Figure 6). This quarry has undergone severe alteration and most of the original travertine has been broken into pieces. There are multiple small conglomerate layers throughout the quarry, some of which also appear to have been disrupted. There is a large conglomerate unit near the top of the quarry that truncates the travertine below. The conglomerate has a red matrix and large intraclasts that are composed of travertine and dark grey limestone. There is a thin layer of travertine on top of the conglomerate that is cream-colored and has planar layers.

1.3.4 Conduit Quarry

The Conduit Quarry is located on the edge of Mesa Aparejo. It displays large carbonate-filled conduits that cut through the Grey Mesa Member of the Madera Limestone (Figure 7). The limestone is grey in color and finely crystalline. It contains some fossil fragments and abundant stylolites. The conduits are filled or partially filled with very coarsely crystalline carbonate crystals growing into an open cavity from multiple directions. There is obvious banding of different colored crystals, likely indicating changing water conditions during precipitation.

1.3.5 Vista Grande Quarry

The Vista Grande Quarry is intensely altered and appears to contain no

original travertine (Figure 8). This quarry is composed of multiple generations of carbonate veins that cut across each other at a variety of different orientations. The veins display a variety of colors including: cream, black, orange, brown, red, and yellow.

Figure 6: (A) Overview of the eastern part of the Pink Quarry. (B) An erosional surface is present near the top of the walls in the pink quarry. It separates the travertine below from the conglomerate above, labeled with a "C". (C) Closer view of the travertine and carbonate veins within the Pink Quarry. Field assistant for scale is approximately 2 m tall.

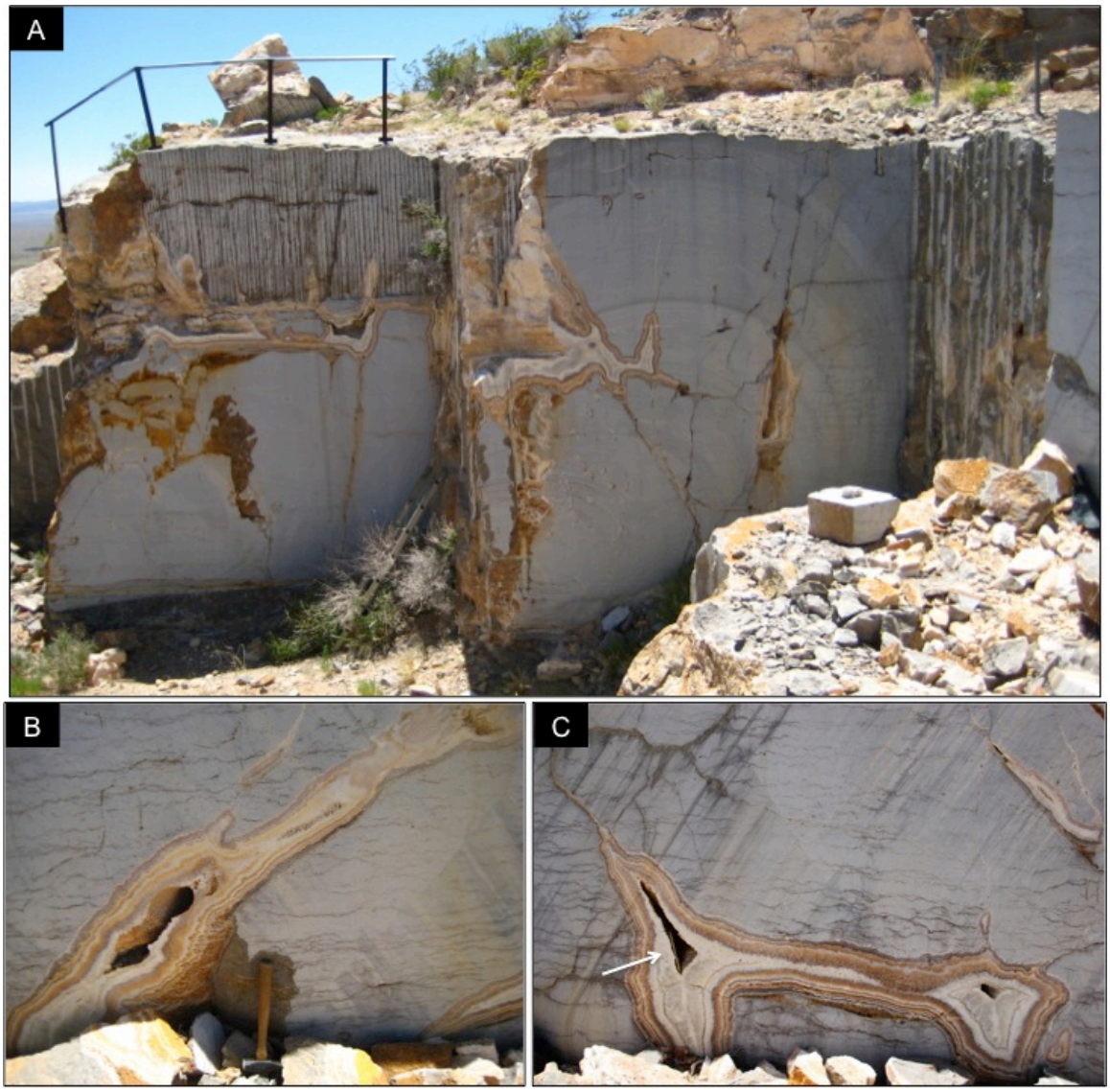

Figure 7: (A) Conduit quarry with distinct calcium carbonate-filled ducts in the Madera Limestone. Height of metal fence post is approximately 1 meter. (B-C) Calcium carbonate filling ducts in the Madera Limestone. The cement has distinct laminations indicating the formation was equal on all sides of the cavity, starting adjacent to the Madera Limestone and ending with the occlusion of the pore space. (B) Rock hammer for scale. (C) White arrow pointing to pen for scale.

Figure 8: (A-E) Images of the Vista Grande Quarry showing multiple generations of veins cutting across each other at a variety of orientations. Field assistant for scale is approximately 2 m tall.

1.3.6 Beef Steak Quarry

The Beef Steak Quarry is a relatively small quarry that has cream- and red-colored travertine and conglomerates. This quarry has an abundance of thin veins that cut through it at a variety of orientations, giving it a “Beef Steak” appearance.

CHAPTER 2: INTRODUCTION TO TRAVERTINES

2.1 Overview

Travertine deposits are spring-fed carbonate accumulations formed by hot or ambient temperature waters. Certain parameters are fairly constant for the creation of a travertine deposit. Active tectonics and volcanism within the area provide faults and fractures, which can be used as conduits for water transport from the subsurface to the surface (Chafetz and Folk, 1984; Hancock et al., 1999). They can also aid in increasing the geothermal gradient, resulting in heated groundwater, which is common for travertine deposits. The area must have an ancient carbonate deposit or, in rare cases, other calcium-rich rock types (Pentecost, 2005). The dissolution of the ancient deposit provides the needed calcium and CO_3 ions resulting in enriched water. Water can be derived from either a deep-seated groundwater source or from meteorically refreshed aquifers. The two sources of water are not exclusive of each other, as it is common to find that travertine deposits waters have mixed origins.

One model for the process of travertine formation is as follows. Water travels up the stratigraphic section along deep-seated faults. As it comes into contact with one or more carbonate formations, it dissolves the ancient deposit resulting in water that is enriched with calcium and CO_3. Once the water reaches the surface, the influence of biotic and abiotic processes results in super-saturation of calcium carbonate and leads to precipitation.

2.2 Precipitation

Travertine precipitation occurs following the reaction:

$$Ca^{2+} + 2HCO^{-}_{3} = CaCO_3 + CO_2 + H_2O$$

There are many factors that can cause the precipitation of travertine, but they can be broken into two main groups, abiotic (physiochemical) processes and biotic processes. The initiation of abiotic calcium carbonate precipitation requires that the water is super-saturated with respect to calcite by five to ten times, as this allows it to overcome the influences which inhibit precipitation (Zhang et al., 2001). A common driving mechanism for this disequilibrium is the degassing of CO_2, which drives the calcium into super-saturation (Florsheim et al., 2013).

There are many physical processes that affect the stability of CO_2 within water. Carbon dioxide is significantly more soluble in solutions that are under high pressures. In the subsurface, the water is highly pressured and therefore is capable of retaining more CO_2. As the water ascends to the earth's surface, the pressure is drastically decreased and the CO_2 escapes from the water, causing super-saturation with respect to calcium carbonate. This results in travertine deposition at vent locations. Carbon dioxide can also be lost from the water into the atmosphere due to differences in the partial pressure of CO_2 between the two (Zhang et al., 2001). Temperature can also be a controlling factor as CO_2 is less soluble in higher temperature solutions. In these high-temperature systems, the insolubility of CO_2 caused by the high water temperature will decrease the effects

of decreasing pressure at the vent, nevertheless, rapid deposition in the near vent environments are common (Pentecost, 1995). In ambient temperature systems, the near-vent deposition is significantly less than their high-temperature counterparts, and can be attributed to the solubility of CO_2 in the water. These systems do experience distal degassing due to increases in temperature from solar heating. Evaporation of water in the distal portions of the system can result in the super-saturation with respect to calcite and promote precipitation (Chafetz and Lawrence, 1994).

Agitation of the water at sites of increased slopes, or surface irregularities is another significant mechanism. Chen et al. (2004) found in areas that experience turbulent flow, such as waterfalls, the hydrodynamic processes drive carbonate precipitation. The turbulent nature of the flow results in aeration and separation of the water into drops, allowing for a larger surface area of the water in contact with the air. This results in the diffusion of CO_2 from the water to the atmosphere moving the system towards equilibrium in the pCO_2 (Chen et al., 2004). There is also an influence from the increased water velocity, which results in a drop in pressure, causing CO_2 to be less soluble in the water (Chen et al., 2004). It was determined that the hydrodynamic processes played a dominant role in areas of turbulent flows, but that other mechanisms are likely more prevalent in quieter areas (Chen et al., 2004).

Biotic activity is a dominant mechanism for the precipitation of travertine under specific conditions. Biotic influences include bacteria, algae, moss, and

other higher plant taxa. Algae, mosses, and higher orders of plant life alter their surrounding microenvironment by the removal of CO_2 during photosynthesis. This causes a gradient in the alkalinity between the organism and the solution and leads to super-saturation with respect to calcium carbonate allowing for precipitation (Riding, 2000; Florsheim et al., 2013). This process has been found to not be effective in high alkaline environments, as the influence of the photosynthesis cannot produce a significant enough gradient in alkalinity to result in super-saturation (Riding, 2000). Algae, mosses, and higher order plant life also increase the abundance of nucleation sites for calcium carbonate precipitation. These organisms are commonly found in ambient temperature environments that have normal water geochemistry (Chafetz and Folk, 1984).

Bacteria have been found to alter their surrounding microenvironment by metabolic processes, acting as a catalyst for carbonate precipitation (Chafetz and Folk, 1984; Chafetz and Guidry, 1999). The negative charge of the cell walls of the bacterial body attracts the positively charged calcium ions, pulling the calcium out of the solution and resulting in precipitation (Folk, 1993). The influence of bacteria has been observed in both natural and laboratory settings and has been found to form crystal aggregates (Buczynski and Chafetz, 1991). Buczynski and Chafetz (1991) found that samples with live bacteria resulted in precipitation of calcium carbonate, whereas sterilized samples under the same laboratory conditions did not. This indicates that the metabolic activity of bacteria is responsible for the precipitation of calcium carbonate and that the presence of

bacteria does not result in passively induced precipitation (Buczynski and Chafetz, 1991). The influence of bacteria is commonly found to dominate in harsh environments, such as high-temperature and sulfur-rich waters (Chafetz and Guidry, 1999). This is because higher plant life cannot survive in such harsh conditions, and therefore is not able to overpower the influence of the bacteria, as is seen in normal water conditions.

Travertine precipitation is generally a result of a complex combination of the above-mentioned processes. The influence of one mechanism over another is highly dependent upon the environmental conditions at the time of precipitation. For any given location, as these environmental conditions change through time, the driving mechanism can also change. Abiotic processes dominate in areas that are experiencing rapid degassing, including proximal to the vent and in areas of turbulent flow conditions. Biotic processes are most abundantly observed in areas with an overall lower saturation with respect to calcium and calmer water conditions (Chafetz and Guidry, 1999).

2.3 Travertine Classifications

Classifications of geologic features are continuously evolving, updated as more is studied and understood about the feature. Certain criteria must be met for a classification to be considered successful. The classification must be applicable to both ancient and modern deposits. It must be broad enough that it is functional, resulting in a reasonable number of end members, so that it is easy to use. That being said, it must be detailed enough to provide meaningful

information, making it useful.

There have been many attempts at classifications for travertine deposits, however many of them were unsuccessful in achieving each of the above criteria. A classification has been proposed based on the water temperature responsible for travertine precipitation, i.e., hot water deposits versus ambient temperature deposits (Pedley, 1990). This is not an effective classification as it is difficult to apply to ancient deposits. Another classification was attempted using vegetation that was associated with the deposit (Pedley, 1990). This was unsuccessful as the vegetation broke down through time, making recognition difficult in ancient deposits. Also, many travertine deposits are formed in conditions too harsh for vegetation to survive, leaving a void in the classification. While each of these classifications provides meaningful information about the deposit, they do not encompass the broad scope that is necessary for travertine accumulations.

Chafetz and Folk (1984) described five depositional morphologies that account for the variety of travertine deposits. They identified: waterfall/cascade deposits, lake-fill deposits, sloping mound/cone/fan deposits, fissure ridge deposits, and terraced mound deposits (Chafetz and Folk, 1984). This classification meets the necessary requirements for travertine classification and provides a good starting point for identifying travertine accumulations.

Waterfall and cascade deposits are rapidly growing travertine deposits that form at the site of water rapids or waterfalls. These deposits can be very large and are commonly formed by the accumulation of travertine in multiple

events. These deposits have a lifecycle of accumulation of travertine, break through of the deposit due to flooding and then renewed accumulation (Love and Chafetz, 1988). The water within this system is generally ambient temperature and of normal chemical make-up. The main mechanism for the formation of waterfall and cascade deposits is degassing of CO_2 due to increased agitation. The influence of evaporation and higher-order plants, such as algae and moss, may play a small role but are not a dominant control (Chen et al., 2004). Waterfall and cascade deposits are characterized as chaotic bedding accumulations that display irregular textures due to the rapid encrustation of algae and moss. Waterfall and cascade deposits will also incorporate any debris that comes into contact with the deposit (Chafetz and Folk, 1984).

Lake-fill deposits form as water from a spring orifice is introduced into a standing body of water. Many travertine-producing lakes have multiple spring orifices scattered throughout the lake bottom. The location of the orifices can move through time and can be identified within the rock record (Chafetz and Folk, 1984). There are two types of lake-fill deposits, those formed in ambient temperature waters and those formed in hot waters, each of which is characterized by distinct features (Chafetz and Folk, 1984). Deposits formed in ambient temperature waters generally exhibit a massive-bedded appearance. They are dominantly micritic with a minor admixture of oncoids. Hot water deposits are finely bedded and display interbedded layers of bacterial shrubs and micritic peloids (Chafetz and Folk, 1984). Lake-fill deposits can be laterally

continuous for hundreds of meters, maintaining layer thicknesses and morphologies, with only minor disturbances. Proximity to a spring orifice can be indicated by the observation of foam rock, intraclasts, and pisoids. Lake-fill deposits commonly experience multiple events in which the depression fills-up, dries-out, is eroded, and then fills-up again (Chafetz and Folk, 1984).

Sloping mounds, fans, and cones form due to an elevated, subaerial spring orifice that allows the super-saturated water to flow downhill, precipitating travertine along the way. The dimensions of these features differ widely as the deposits can vary from gently dipping, laterally extensive sloping mounds to steeply sloping, tall but narrow cones (Chafetz and Folk, 1984). It is common to find multiple cones aligned in a linear orientation, as the location of the cones is related to the underlying faults and fractures (Hancock et al., 1999; Guo and Chafetz, 2012). Many of these deposits form as isolated active lobes of deposition that avulse periodically, so it is common to identify discontinuous surfaces of non-deposition. Sloping mounds, fans, and cones commonly have layers that pinch out laterally and are characterized by irregular laminations (Chafetz and Folk, 1984).

Fissure ridges form as water emerges to the surface along a linear feature, such as a joint or a fault (Chafetz and Folk, 1984; Hancock et al., 1999). These deposits are commonly very long, ranging from 100 to 2000 meters, but commonly narrow with widths of 5 to 400 meters (Hancock et al., 1999). Thin layers of travertine are formed parallel to the ridge sides and can range in habit

from irregular to microterrace features (Guo and Riding, 1999). The sides of the ridge can range from shallow to steeply sloping depending on the flow rate from the fissure. A fast flow rate results in a short, broad fissure ridge, whereas a slow flow rate results in a tall, narrow fissure ridge (Hancock et al., 1999). The presence of these features greatly aids in the understanding of the tectonics in the area and can be used to age date fault activation (Hancock et al., 1999; Brogi and Capezzuoli, 2009).

Terraced mound deposits form down flow from springs in a stair-step pattern with small horizontal pools separated by steep rimstone dam buildups (Chafetz and Folk, 1984). The pools act similar to small lake-fill deposits and form a variety of travertine constituents, including rafts, pisoids, and shrub structures. The rimstone dams form around the edges of the pool deposits and commonly migrate in a downstream direction (Hammer et al., 2010). The increased agitation as the water spills over the edge results in a rapid buildup of the rimstone dams. They are composed of dense calcite and aragonite ray crystals (Chafetz and Folk, 1984). Terrace mound features can be found at many different scales, ranging from a few square centimeters to thousands of square meters, but still maintain the same characteristics (Hammer et al., 2010).

It is important to note that these five depositional morphologies are not independent of each other and can be, in fact, very closely related. An example of this is the lake-fill and waterfall deposits. The accumulation of waterfall deposits can act as a dam, resulting in the ponding of water behind it, which has

lake-fill deposit characteristics.

2.4 Constituents

Travertine deposits are composed of a wide range of constituents that can provide an abundance of information about the environment in which the travertine was deposited. The main constituents include shrubs, crusts, rafts, carbonate-encrusted bubbles, and coated grains.

2.4.1 Shrubs and Crusts

Shrubs and crusts have been the subject of numerous studies by many authors over the past few decades (Chafetz and Folk, 1984; Folk et al., 1985; Pentecost, 1990; Guo and Riding, 1992; Guo and Riding, 1994; Jones and Renaut, 1994; Jones and Renaut, 1995; Chafetz and Guidry, 1999; Rainy and Jones, 2009). They have been separated both by origin (biotic versus abiotic) and morphology, though the two groups are closely related. Chafetz and Guidry (1999) separated the shrubs into three end members: bacterial shrubs, crystal shrubs, and ray-crystal shrubs. Each of the end members has their own unique characteristics and influences on their formation. These distinctions can provided important data about conditions at the time of shrub formation.

Bacterial shrubs are formed by the influence of bacteria, which act as a catalyst for calcium carbonate precipitation. These features are commonly found in environments that have shallow pools of chemically harsh hot water such as lake-fill deposits and terrace mound pools (Chafetz and Folk, 1984). The

bacterial shrub morphology is dominated by bacterial influence, resulting in an irregular morphology with branching clumps of micrite extending from a central trunk (Chafetz and Guidry, 1999). The individual shrubs can range in form from short and wide to tall and thin but generally grow in laterally continuous layers. Daily growth of the shrubs can commonly be observed within individual shrubs as micron-thin laminations, whereas seasonal changes can be seen within layers. Shrub-rich layers form during the growing season, as this is the time when bacteria flourish. Each shrub-rich layer is separated by a layer of silt-sized, bacterially induced peloids that forms during the non-growing season. These daily and seasonal variations highlight the influence of bacteria on the shrub growth (Chafetz and Folk, 1984).

Crystal shrubs are similar to bacterial shrubs in size and lateral continuity of layers, but display a more geometric, crystal habit morphology (Chafetz and Guidry, 1999). The morphology of a crystal shrub displays branches that have distinct, straight edges and are constructed of a single calcite crystal. Bacteria play a role in the precipitation of crystal shrubs, but abiotic processes control the morphology of these features (Chafetz and Guidry, 1999). The crystal shrubs display a range of morphologies and encompass features similar to the crystallographic and non-crystallographic dendrites described by Jones and Renaut (1995). Whereas the morphology is similar, many of the dendrites have been interpreted as completely abiotically precipitated.

Ray-crystal shrubs exhibit a fan-shaped, coarsely crystalline morphology.

They can be separated into two sub-groups; large ray crystal crusts and fine ray crystal fans (Folk et al., 1985). The large ray crystal crusts average in size from 2 to 8 cm, but have been observed up to a meter in height. Bacteria have been found within the large ray crystal crusts, but the radiating crystal morphology is controlled by abiotic precipitation (Folk et al., 1985; Chafetz and Guidry, 1999). The fine ray crystal fans have thicknesses of 1 to 3 mm and are commonly found in horizontal layers. Similar to the large ray crystal crusts, the fine ray crystal fans have been formed by radiating calcite crystals but no bacteria have been found incorporated within them (Folk et al., 1985). The ray crystal shrubs are commonly associated with turbulent flows, such as rimstone dams and near vents (Chafetz and Guidry, 1999).

2.4.2 Other Constituents

Rafts are thin sheets of calcium carbonate that are formed on the surface of shallow pools of water, such as terrace mound pools (Chafetz et al., 1991). They are formed due to changes in the microenvironment at the air-water contact, the result of the loss of CO_2 from the water into the atmosphere. This drives the solution to super-saturation with respect to calcium carbonate, resulting in precipitation (Chafetz et al., 1991). The initial stage of raft development is very rapid and is commonly composed of aragonite. As the rafts continue to form, the top surface of the raft stays flat and all of the crystal growth occurs downward into the water (Taylor and Chafetz, 2004). The presence of the raft acts a barrier between the water and the air, and slows the loss of CO_2

resulting in a change in the mineralogy to dominantly calcite (Chafetz et al., 1991). Eventually, the rafts will be disturbed at the surface, causing them to break into pieces and sink to the bottom of the pool. This allows the rafts to be preserved within the deposit. In thin section, the preserved rafts have a dark, micrite center that is surrounded on both sides by calcite crystals (Folk et al., 1985).

Carbonate-encrusted bubbles are gas bubbles that have been preserved by being encrusted with calcium carbonate. Chafetz et al. (1991) interpreted these bubbles as being pure oxygen bubbles produced by photosynthetic processes from the underlying algae. The pCO_2 difference between the surrounding water and the oxygen bubble results in diffusion of CO_2 into the bubble, altering the immediately surrounding microenvironment (Chafetz et al., 1991). They also found that the encrustation of the oxygen bubble resulted in three distinct layers. The layer closest to the bubble is composed of aragonite needles that are forming tangential to the bubble. It is formed due to extremely high super-saturation with respect to calcium carbonate in the microenvironment surrounding the bubble. As the diffusion between the water and the oxygen bubble slowed, the morphology changed to aragonite hemispheres that are composed of fan-shaped aragonite needles forming perpendicular to the previous layer. The final layer is composed of calcite rhombohedrons and is thought to have formed once the microenvironment began to stabilize (Chafetz et al., 1991).

Foam rock is a travertine texture that is observed as vertical tubes that are 2 to 3 mm wide and 10 to 15 mm long. It forms in distinctive layers that can be up to 80 percent porosity due to the compact nature of the bubbles (Chafetz and Folk, 1984). The layers can be laterally continuous for several meters. This texture is formed as gas bubbles penetrate though a microbial mat, deforming the mat around the puncture holes. It is interpreted to form near vents, which explains the abundance of gas attempting to escape to the surface.

Coated grains are a broad classification used to describe spherical to ellipsoidal constituents that have formed by chemical or biogenic processes (Tucker and Wright, 1990). The term encompasses a wide range of particles and does not provide significant information about their formation or the surrounding conditions. Oncoids are irregular, generally round to elongate-shaped constituents whose cortices are formed due to biogenic influence. The cortices making up oncoids are highly irregular due to their strong biogenic influence (Tucker and Wright, 1990). The symmetric or asymmetric nature of the cortices can provided insight into the movement of the oncoid during formation. Oncoids commonly have a distinct nucleus, although the composition of the nuclei can be highly variable. Pisoid is a term commonly used to describe non-marine ooids. They are generally greater than 2 mm in diameter and commonly have irregular laminations due to their size (Tucker and Wright, 1990). Spherulites are constituents that are composed of fibro-radiating arrays of crystals forming from a small nucleus that is only visible in high magnification (Verrecchia et al., 1995).

CHAPTER 3: METHODS

3.1 Fieldwork

Fieldwork was conducted for this project in the summer of 2012. A reconnaissance trip was conducted in May 2012 and was used to become familiar with the area and determine what was needed for the fieldwork. Each of the six quarries was visited and preliminary sampling was performed. The majority of the fieldwork was conducted in July 2012 and was concentrated on the Gold and Ivory quarries. The process included the creation of detailed stratigraphic sections, the acquisition of high-resolution panoramic images, and the collection of samples for laboratory analysis.

Detailed stratigraphic sections were created of both the Gold and Ivory quarries. The sections are spaced throughout each quarry in an effort to capture the lateral changes within the travertine system. The sections were measured from ground level upward to approximately 3 meters in height. The focus of the sections was to collect data about packages that could be identified within the sequence, including identification and differentiation of constituents, layer thickness, and porosity. In the Gold Quarry, nine stratigraphic sections were created, resulting in 1 or 2 sections per wall (Figure 5). In the Ivory Quarry, seven stratigraphic sections were created (Figure 4).

Three resolutions of panoramic images were created for the Gold and Ivory quarries. First, a broad overview of the entire quarry (when available) was

captured to show large-scale features and the relationship of the walls within the quarry. Next, each wall was photographed in an attempt to display the lateral relationships of layers within the quarry. Finally, high-resolution panoramic photographs were created for each of the stratigraphic sections that were described. For these pictures, the area being photographed was sprayed down with water in an effort to bring out the details of the travertine. The photographs were taken with a Canon T2i camera and a 100mm Canon lens. The photographs were acquired in a grid pattern with an approximately 30 percent overlap between pictures. This provides a level of control during the stitching process for the creation of the panoramic images. The photographs were stitched together using Photoshop CS5 and were adjusted for lens distortion, vignette, and brightness.

The process of collecting hand samples proved challenging. As the fieldwork was being conducted in a quarry, breaking off in situ samples was not an option. Therefore, all of the samples were collected from loose rubble that had been created during the quarrying process. The hand samples were correlated back to individual layers within the quarry walls. This allows the data collected from the laboratory work on the hand samples to have significance to the large-scale lateral relationships.

3.2 Laboratory Work

Thin sections were created from the hand samples collected at the Gold and Ivory quarries. The thin section locations were optimized to capture a variety

of constituents and fabrics. A total of 54 thin sections were created, with 16 from the Ivory Quarry and 38 from the Gold Quarry. The thin sections were impregnated with a blue epoxy to highlight porosity and to ensure that none of the porosity is a result of the thin section preparation.

Panoramic images of the thin sections were created by stitching together individual images in Photoshop CS6. Digital porosity analysis was performed on the panoramic images in Photoshop CS6 in an attempt to quantify the amount of porosity present within the samples. As the thin sections were impregnated with blue epoxy, a hue-based color selection was used to identify the pores. Manual quality control was performed to ensure that only porosity was selected. The number of pixels in the porosity selection was divided by the number of pixels within the entire thin section to give a porosity percentage. Five thin sections were point counted for porosity, using between 550 and 750 points per thin section, in an effort to compare and verify the results between the two methods. The maximum difference between the porosity percentage obtained by the two methods was 0.53 percent.

X-ray diffraction (XRD) was preformed on samples from the Conduit, Gold, and Ivory quarries in an attempt to determine the calcite-to-aragonite ratios at each location. A handheld drill was used to powder the samples and to ensure the precise position of each sample. The powder was then further ground with a mortar and pestle to guarantee its uniformity. After the samples were prepared, they were analyzed using a Siemens D5000 XRD. The samples analyzed from

the Conduit Quarry were taken from different generations of the void-filling cement. This sampling strategy allowed for the capture of changes that occurred between the cement precipitated adjacent to the host rock compared to the most recently precipitated cement. Within the Gold and Ivory quarries, samples were taken from a variety of different travertine constituents, such as rafts, oncoids, and shrubs. Analysis was also performed on veins and pore-filling cements from the Gold and Ivory quarries.

A scanning electron microscope (SEM) was used on samples from the Gold and Ivory quarries to aid in the interpretation of an abiotic versus biotic origin for the precipitates. It also allowed for a more detailed view of the microstructures present within the samples. The samples prepared for the SEM contained a wide range of travertine constituents, including multiple samples of shrubs, rafts, and oncoids. A combination of freshly broken and lightly etched samples was used for SEM analysis. The etched samples were etched using a mixture of 10 percent hydrogen chloride (HCl) and 90 percent water. The samples were exposed to the HCl mixture for 10 seconds before being placed under running water for 1 minute to stop the reaction. The samples were carbon coated and then examined using a JEOL JSM6330F SEM.

CHAPTER 4: DATA AND INTERPRETATION

The Gold and Ivory quarries are composed of two main lithologies, travertine and conglomerate. The travertine can then be divided into two stages, primary precipitation and secondary, vein-fill precipitation. The primary travertine and the conglomerate are interbedded throughout the stratigraphic section and the vein-fill travertine cuts across them both.

4.1 Travertine

4.1.1 Gold Quarry Travertine

The travertine in the Gold Quarry is dipping in an east-northeast direction. This is evident by the presence of good dip sections on the east-west striking walls. The north-south walls are sub-parallel to strike, but there is slight dip of the beds, which indicates a small northern component for deposition (Figure 9). Walls D and E highlight this point, as on wall D the large conglomerate package has an obvious eastern dip and the same conglomerate on wall E (perpendicular to wall D) is mostly planar (Figure 10).

This deposit is primarily a sloping mound morphology with only slight and rare terrace mound features present. The travertine layers are dipping approximately 5 to 12 degrees. Some of the sloping layers have microterrace structures, with pools of approximately 5 cm in length and rimstone dams that are approximately 0.5 cm high. On wall D, two terrace rimstone dams are present, with the largest one having a maximum exposed offset of 50 cm. The rimstone

dams begin to become shallower up section, but are eroded before displaying the full transition to a sloping mound deposit. These are the only large terrace rimstone dams present within the Gold Quarry (Figure 10).

The travertine layers within this deposit are 0.1 to 5 cm thick. The color of the travertine is highly variable, including colors such as cream, tan, red, orange, and brown. The constituents present within this quarry are also variable and contain rafts, shrubs, oncoids, and foam rock. Many of these features indicate that water collected in shallow ponds at the time of deposition. Many of the layers within the Gold Quarry are laterally continuous and can be traced along the different walls. One of the main examples of this is the “pink/brown layer”. This layer is visible on walls F, A, B, and C. In some areas, while the layers of travertine may be continuous, the abundant vein-fill and alteration makes it difficult to trace them.

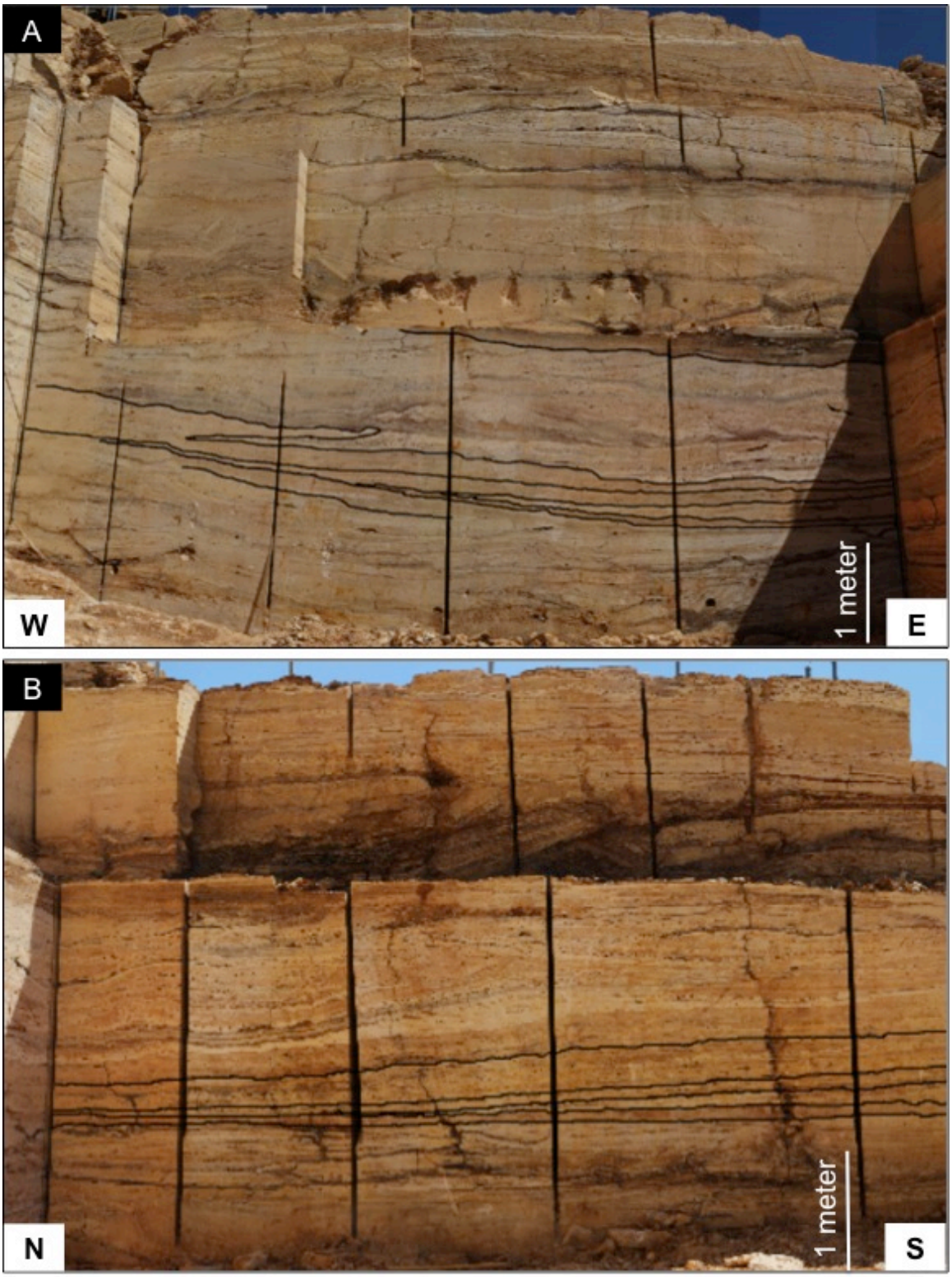

Figure 9: (A) Gold Quarry- Wall B has layers that dip to the east. (B) Gold Quarry-Wall C has layers that are gently dipping to the north. The black lines are annotations added to the interpreted layers used to show the dip of the beds and the sloping mound morphology.

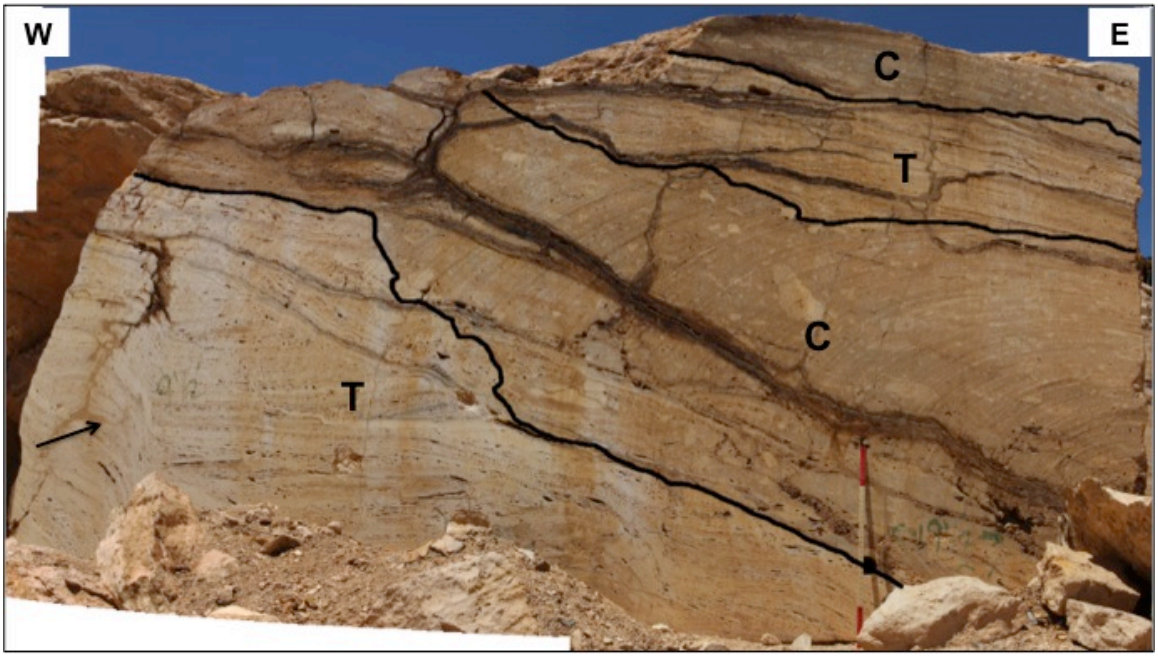

Figure 10: Panoramic image of Gold Quarry- Wall D. A large conglomerate layer dipping at approximately 19 degrees to the east, towards the central axis of the Rio Grande Rift. Black lines marks the boundaries between lithologies. Conglomerates are marked with "C" and travertines are marked with "T". The travertine has a characteristic rimstone dam (black arrow) with adjacent near horizontal pool layers. Meter stick for scale with the top and bottom 20 cm colored in red.

4.1.2 Ivory Quarry Travertine

The travertine in the Ivory Quarry was primarily deposited in a northeast direction. Multiple lines of evidence support this interpretation, including the presence of dipping layers both on walls striking north and walls striking east (Figure 11). Evidence is also visible on wall E, where the presence of large terrace rimstone dams indicates the flow direction (Figure 12). On wall D, which is oriented perpendicular to wall E, the majority of the layers are fairly planar and rimstone dams can be identified dipping in both directions in a single layer. This feature is interpreted to be the strike view of a terrace deposit. On wall B a feature similar to wall D is present and would indicate a northward flow direction (Figure 13). This feature is likely the result of the locally three dimensional, sinuous nature of the flow path, as the rest of the travertine on wall B is dipping in a northeast direction.

The deposit is a combination of a sloping mound and terrace mound morphology. Through time, the deposit fluctuates between large terrace pools with steep vertical rimstone dams to layers dipping approximately 10 degrees and covered with microterraces. The transition between these two morphologies is subtle but has been documented on Wall E (Figure 12). The transition between a terrace mound and a sloping mound morphology occurs by the expansion of layers in the downstream pool, adjacent to the rimstone dam. This causes the rimstone dam to eventually decrease in height to the point of non-existence (Figure 14). After this occurs, the fluids continue to flow down slope, depositing

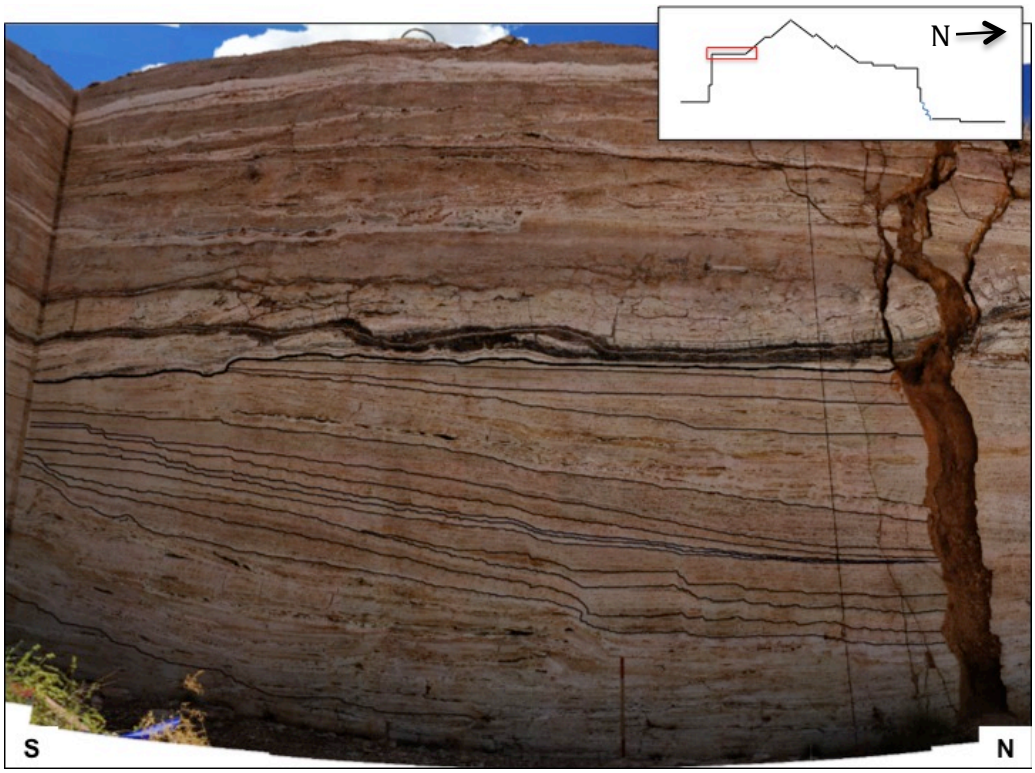

Figure 11: Ivory Quarry- Wall C has a 4 m thick travertine deposit that shows a sloping mound morphology. The layers show an apparent dip to the north. The black lines are interpreted layers used to show the dip of the beds. Meter stick for scale.

dipping layers. Multiple scales of terraces are present within the quarry. Microterraces are commonly seen on the steeper dipping layers. They have pools that are 1 to 3 cm long and rimstone dams that are 0.25 to 0.27 cm high. As the layer begins to flatten out, both vertically and laterally, the pools get longer (approximately 10 to 40 cm) and the rimstone dams increase in height (2 to 5 cm). Larger terraces are also present with pools measuring 1.5 to 2.5 meters and rimstone dams measuring 0.25 to 0.5 meters high. The trajectory of the rimstone

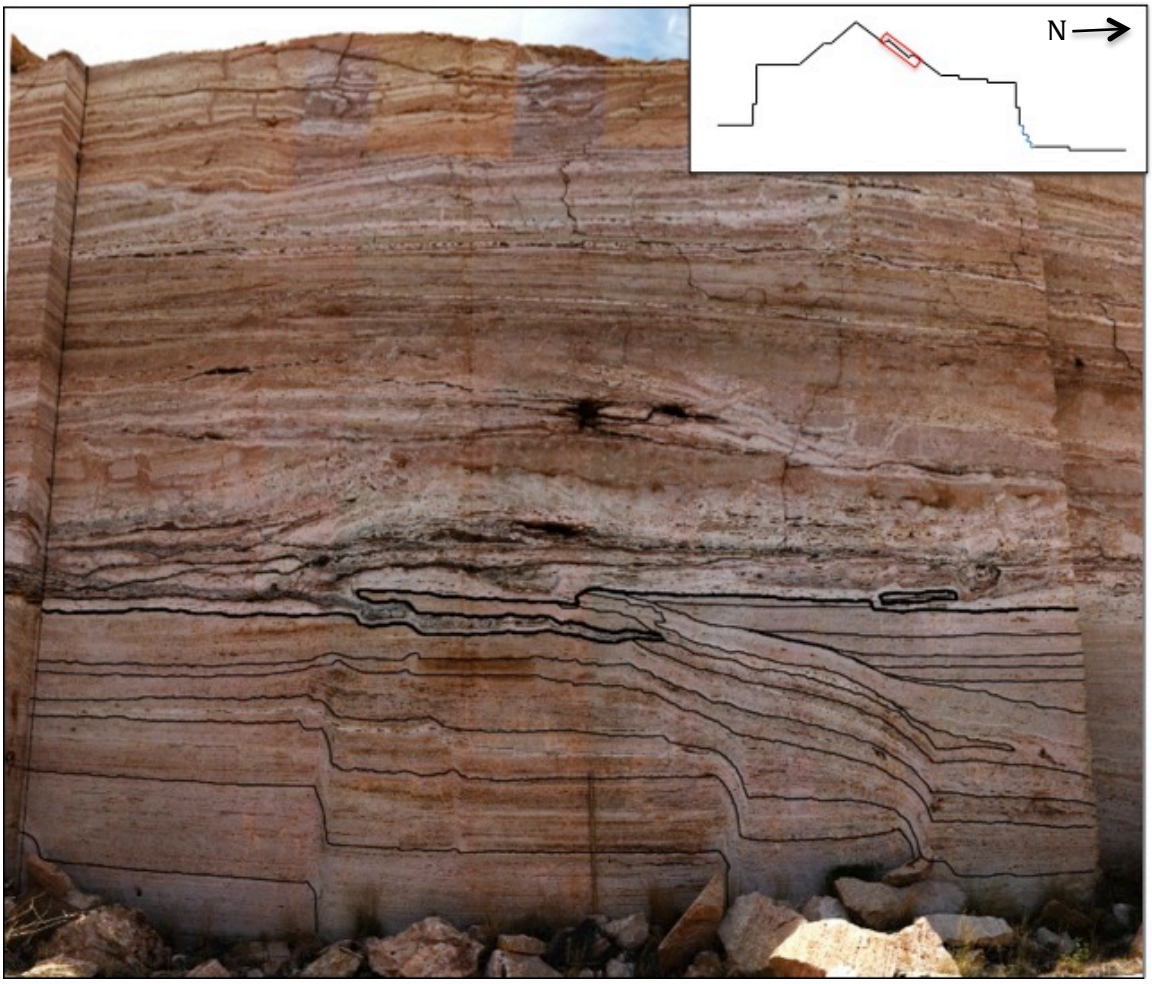

Figure 12: Panoramic image of Ivory Quarry- Wall E2 displays distinct terrace rimstone dams and pools. In the lower right corner of the photograph, it is evident that the rimstone dams decrease in height and transition into sloping layers. Some of the layers within the travertine are marked with black lines to show the structure.

dams varies throughout the quarry, both laterally and vertically. Some of the rimstone dams are building outward in the downstream direction (Figure 15), whereas others are stepping backwards in the upstream direction (Figure 16). Finally, some of the rimstone dams are aggrading, building vertically but not shifting position (Figure 17).

The travertine in the Ivory Quarry is thoroughly laminated with layers ranging in thickness from 0.5 to 7 cm. It is predominately cream-colored, with only slight variations to tan. The constituents present are highly variable, including oncoids, shrubs, rafts, etc. Individual layers vary between containing only a single constituent to containing a mixture of constituents.

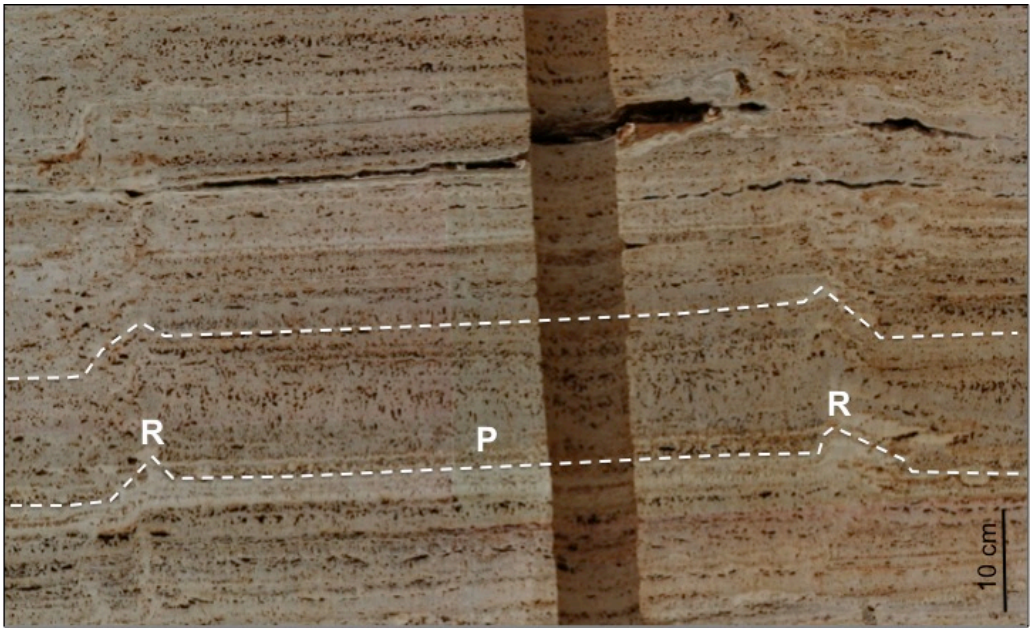

Figure 13: Ivory Quarry- Wall B2. Rimstone dams (R) that dip in opposite directions on either side of a pool (P). White dashed lines are used to mark the structure.

Figure 14: Ivory Quarry- Wall E2. (A-B) Examples of terrace rimstone dams decrease in height upwards until the rimstone dam no longer exists and it is just a slope. Some of the layers are marked with black lines to show the structure.

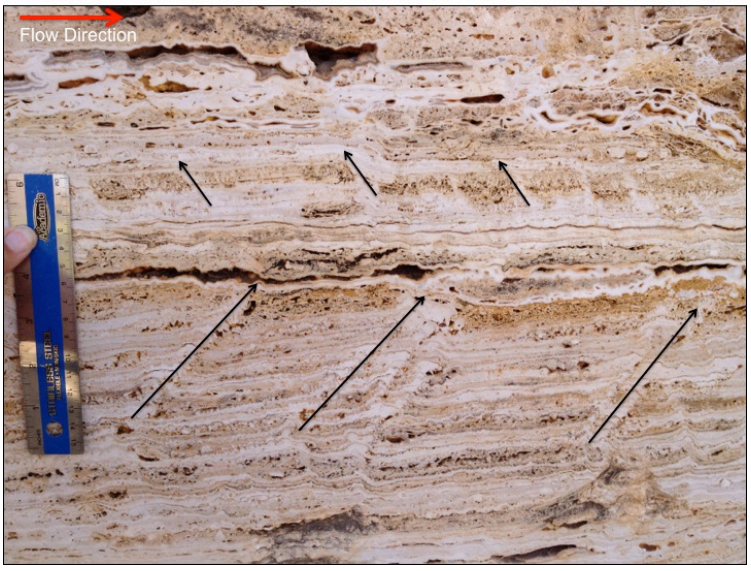

Figure 15: Ivory Quarry- Wall C displays prograding rimstone dams that change trajectory into retrograding rimstone dams. Rimstone dam trajectory is marked with black arrows. Red arrow indicates the more prominent flow direction. The ruler is 15 cm.

Figure 16: Ivory Quarry- Wall B displays rimstone dams in which their location is migrating upstream. Rimstone dam trajectory is marked with black arrows. Red arrow indicates flow direction.

Figure 17: Ivory Quarry- Wall E2 displays aggrading rimstone dam in which the location stays stationary and just builds upwards vertically. Rimstone dam trajectory is marked with a black arrow. Red arrow indicates flow direction.

4.1.3 Mineralogy

All of the samples tested in the Gold and Ivory quarries were found to be composed completely of calcite. Care was taken to include samples of different constituents (rafts, oncoids, etc.), cement surrounding the constituents, and the vein-fill precipitate cutting across the primary travertine deposit, but no difference was identified in the mineralogy between these groups. Additionally, no difference was identified between the samples collected from the Gold Quarry versus the Ivory Quarry. A sample of the red matrix was taken from one of the conglomerate deposits in the Gold Quarry and was found to be predominately calcite with a minor amount of an additional unidentified mineral.

Samples within the Conduit Quarry show a combination of calcite and aragonite. Two distinct types of samples were analyzed. The first sample type was a 15 cm crystal ray (Figure 18). Analysis was performed on multiple locations throughout the ray to identify any possible mineralogical changes. This sample was primarily aragonite with minor amounts of calcite present and the mineralogy stayed consistent throughout the sample.

The second sample type were rocks that contained multiple centimeter-thick carbonate layers that filled veins. The layers were obviously crystalline but did not show a crystal ray habit. The oldest vein-fill, found adjacent to the host rock, is composed of calcite. The subsequent vein-fills, excluding the most recently precipitated, are also composed of calcite. In contrast, the most recently precipitated vein-fill is composed of a mixture of calcite and aragonite. This was

found to be the case both in samples where the youngest vein-fill completely occluded the remaining porosity in the vein, and those where porosity was still present.

Figure 18: Example of an aragonite ray that was present within the Conduit Quarry.

4.1.4 Constituents

4.1.4.1 Rafts

The rafts found within the Gold and Ivory quarries range in length from 0.7 mm to 3 cm and thickness from 0.1 to 0.8 mm. The layers containing rafts can vary from a mixture of rafts among other constituents to layers that contain 100 percent rafts. The presence of rafts indicates the existence of ponds of water within the area at the time of formation. Rafts are more prevalent in the Ivory Quarry than the Gold Quarry, which is understandable due to the higher abundance of terraces and microterraces in the Ivory Quarry.

Rafts can be identified in thin section as straight, elongate features, which are significantly longer than they are thick. They have a dark line that forms in the center of the raft and serves as a nucleating surface for all further growth on the raft. This dark line is likely the initial raft development and formed rapidly compared to the material surrounding it. Growth on the central raft has been observed to take many different forms. Sometimes, the raft is surrounded by concentric laminations completely surrounding it (top, bottom, and forming rounded sides) (Figure 19). The presence of the concentric laminations indicates that the raft was fully submerged underwater when the precipitation formed. In other cases, the raft has isolated fan-shaped growths that are nucleating from the central raft. These fans can be observed forming on the top of the raft, bottom of the raft, or both sides of the raft (Figure 20). When deposited, rafts commonly have abundant porosity beneath them. While the top part of the raft has the potential for sediment to fall on it, or shrub growth to form on it, the porosity underneath the raft is only occluded by cementation.

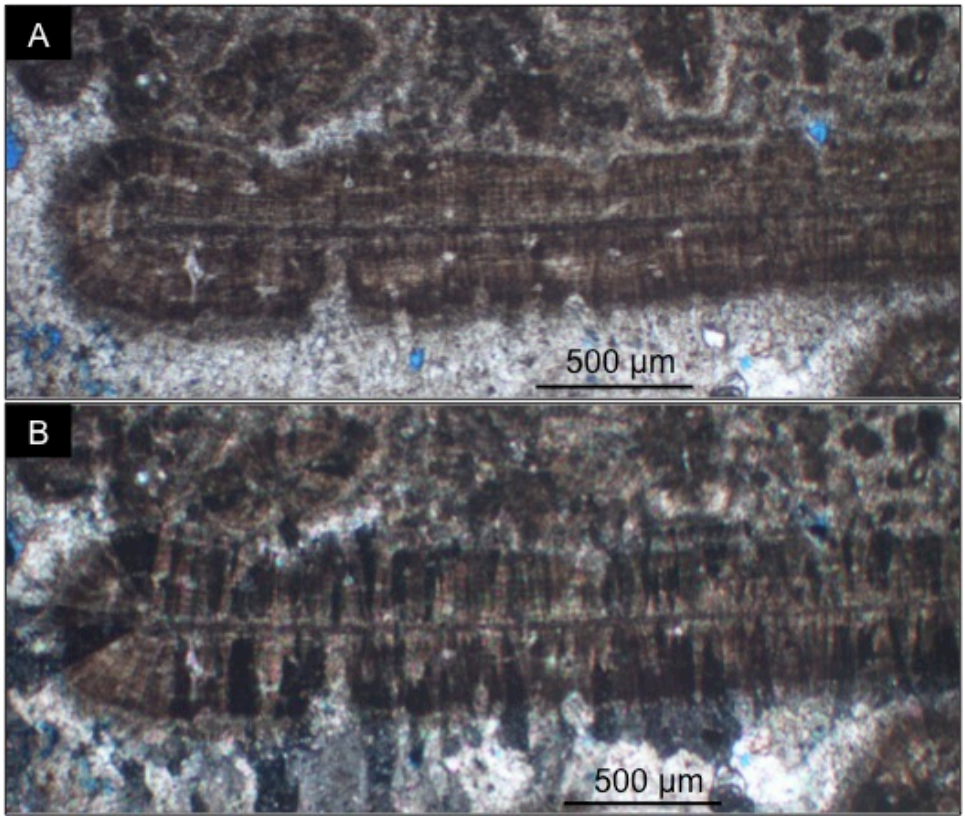

Figure 19: (A) Photomicrograph in plane light of a raft that has a distinct central core surrounded by concentric growth. (B) Photomicrograph (same field of view as image A) under cross-polarized light of a raft showing even growth of calcite blades surrounding the central core.

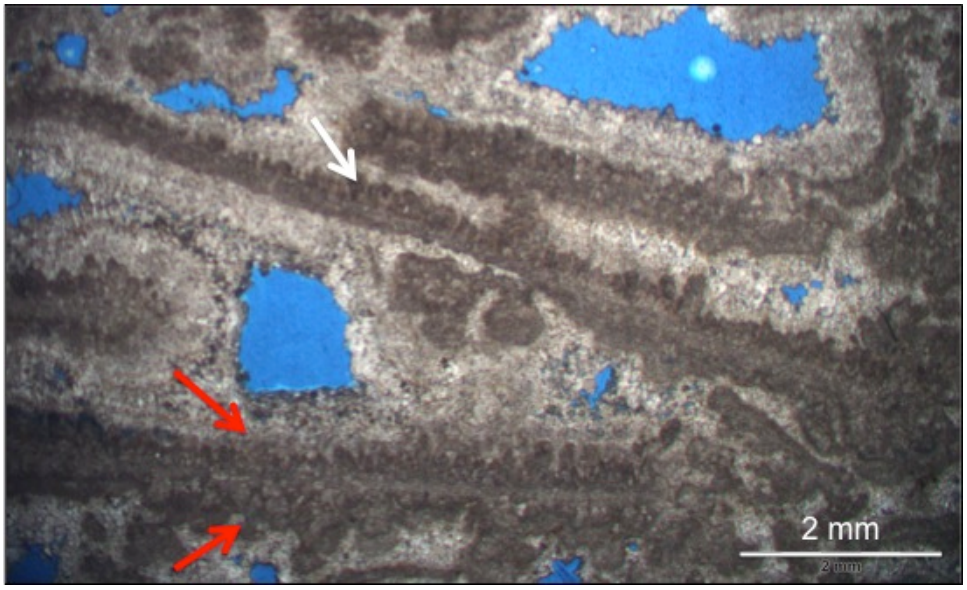

Figure 20: Photomicrograph in plane light of rafts with isolated fan-shaped growth on one (white arrow) or both sides (red arrows) of the raft.

4.1.4.2 Foam Rock

The vertical tubes associated with foam rock vary in length from 0.2 to 1.5 cm and are fairly consistent in width with a narrow range of 0.15 to 0.35 cm. The majority of the vertical tubes have a highly elongate shape, although some rounded forms have been observed. They commonly occur in densely packed layers, termed foam rock, but are sporadically found as isolated features among other constituents. Even within a single layer, the vertical tubes can range from completely open pore space to completely cement-filled. Occasionally, the bottom of the vertical tubes can be filled with sediment, providing an excellent geopetal structure.

The outline of the vertical tubes is commonly well-defined but its appearance is highly diverse between different vertical tubes. Some of the vertical tubes are surrounded by concentric outlines that are composed of multiple, constant thickness micritic layers that surround the entire feature (Figure 21). Other vertical tubes have a single dark micritic line marking the side of the feature, followed by irregular growth on the outside of the line and then a second dark micritic line marking the outer boundary (Figure 22). Another type of boundary that was identified was a 0.25 mm thick, dark brown outline composed of 25 to 50 micron dark brown clumps of micrite. The boundary was fairly homogenous throughout and did not have darker outlines at the edges (Figure 23).

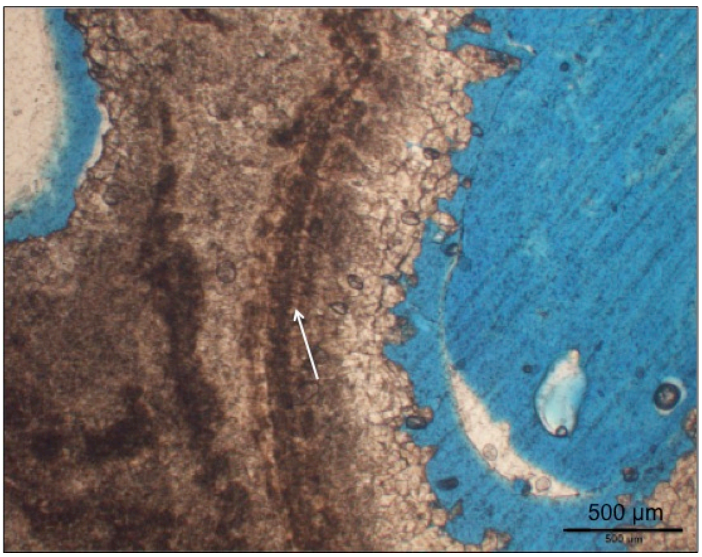

Figure 21:
Photomicrograph in plane light of a vertical tube with a concentrically laminated, micritic outline (white arrow). A minor amount of cement is present inside the tube outline, but the majority of the vertical tube contains open pore space.

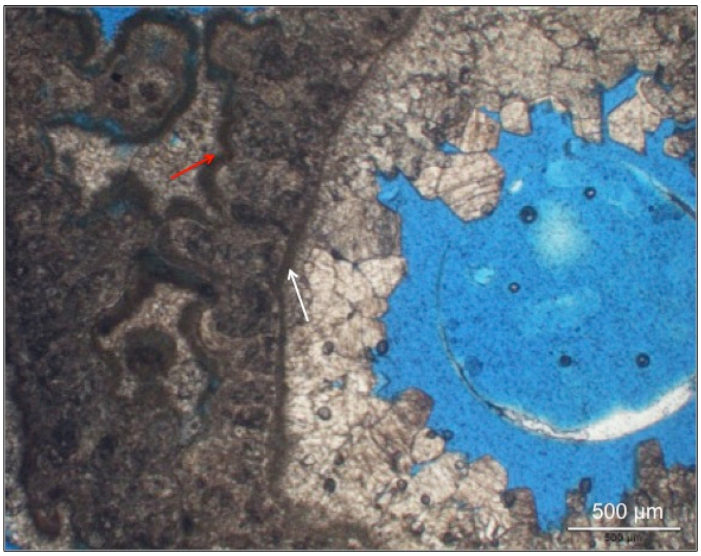

Figure 22:
Photomicrograph in plane light of a vertical tube with a dark, micritic line marking the inside border (white arrow) of the tube, followed by irregular growth and another dark, micritic line marking the outer border (red arrow) of the tube.

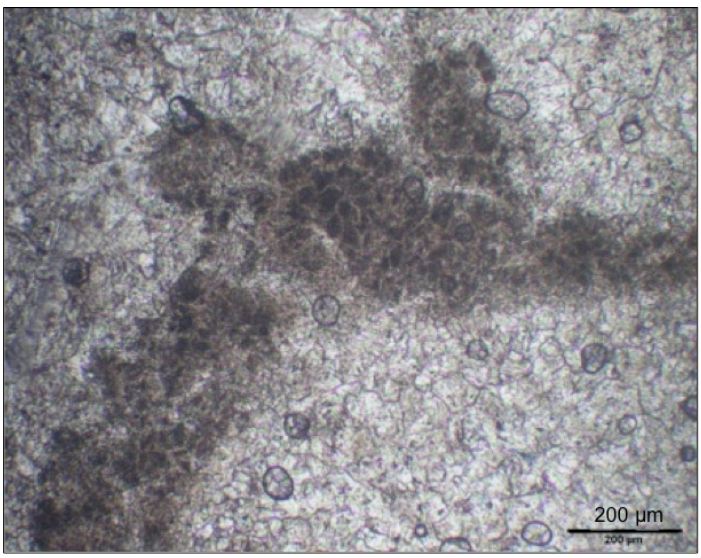

Figure 23:
Photomicrograph in plane light of a vertical tube with a clumpy brown micrite outline and no distinct border. The cement inside and outside of the vertical tube are equally crystalline.

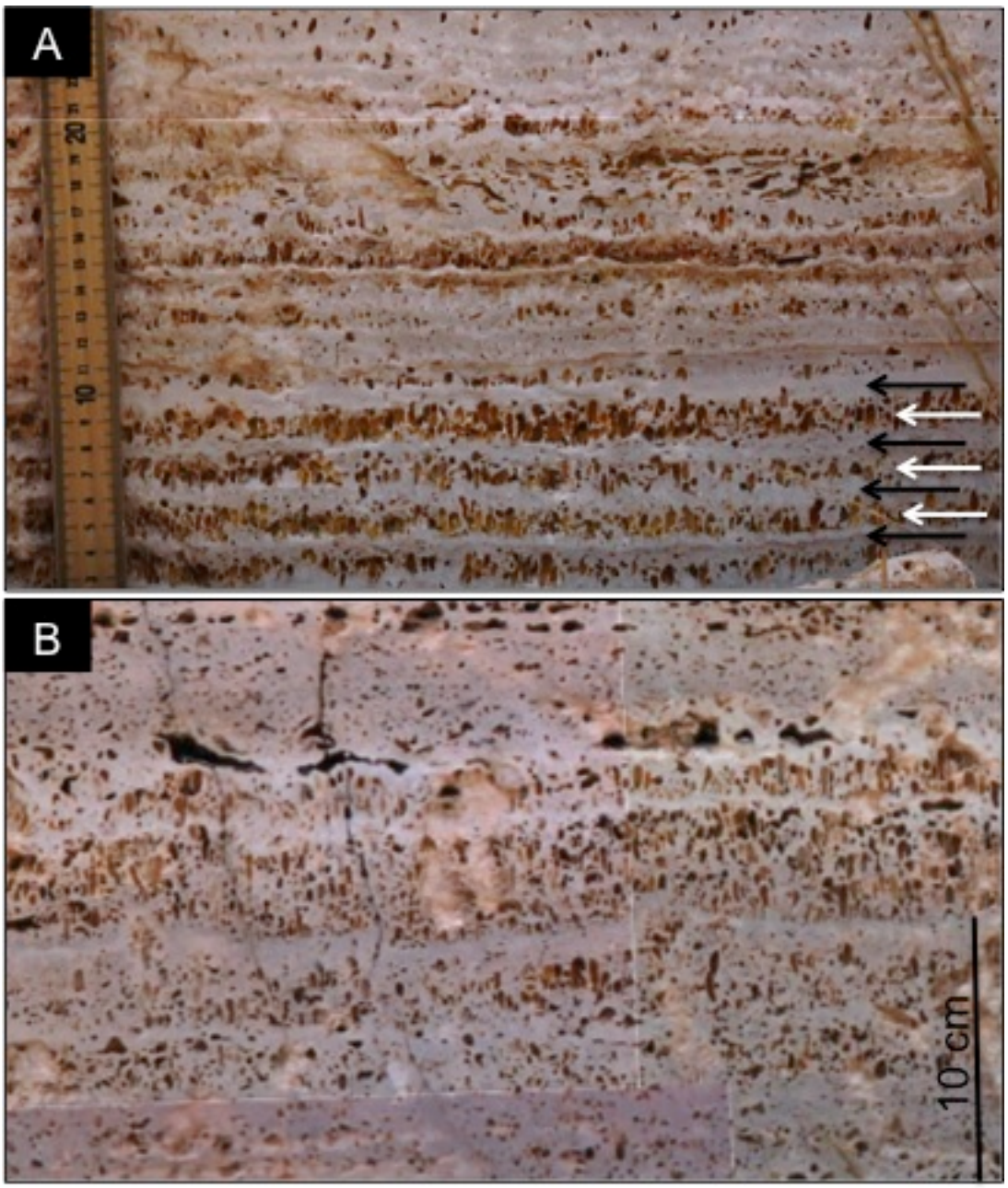

Figure 24: (A) Foam rock layers in a terrace pool showing the differences in layer thickness. The foam rock layers (white arrows) are separated by dense micrite layers (black arrows). (B) Foam rock layers that range in thicknesses.

Foam rock layers are defined by the presence of tightly packed vertical tubes and are commonly bounded by a dense, micrite laminae above and below. The layers range in thickness from 1 to 8 cm. A single layer can be composed of either a single row of vertical tubes, or multiple offset stacked bubbles (Figure 24). They are commonly found as multiple layers of foam rock stacked in a stratigraphic section, but occasionally are found as isolated foam rock layers surrounded by layers of other constituents. In thin section, the material surrounding the vertical tubes in the foam rock layers displays an irregular, lacy, micritic texture (Figure 25). The majority of it is composed of clumpy, brown irregular layers of micrite but some areas have preserved individual layers that are forming on top of each other. This feature is likely caused by microbial mats, which in some areas have been deformed by the upward migration of gas bubbles.

The foam rock layers are abundant within parts of the Ivory Quarry. They are found almost exclusively in terrace pools, and are not commonly found in microterraces or on steeply sloping surfaces. The Gold Quarry has many layers with vertical tubes present, but most of the vertical tubes are isolated and do not form densely packed foam rock layers. The lack of foam rock layers in the Gold Quarry is related to the presence of sloping surfaces instead of terrace structures.

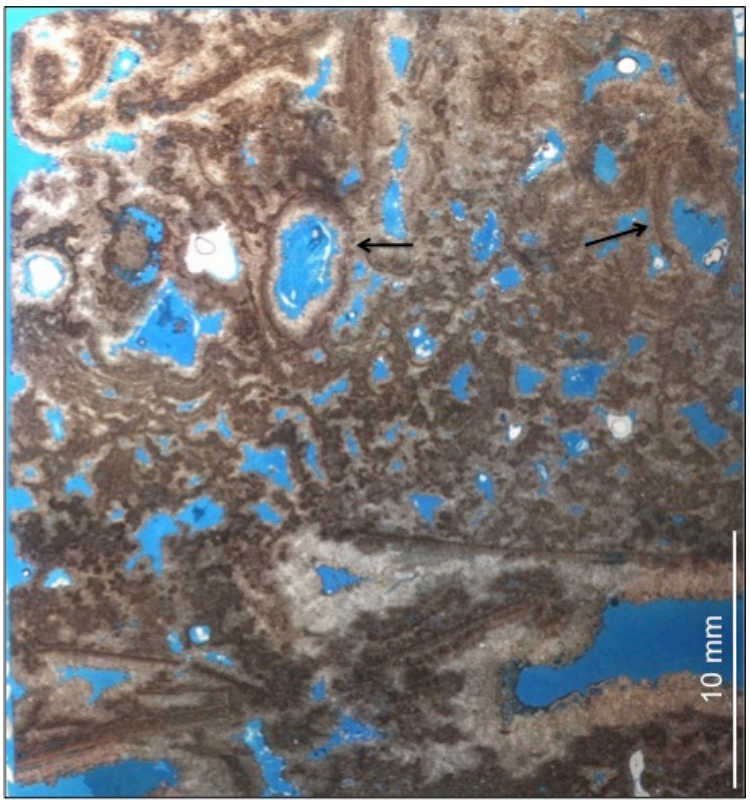

Figure 25: Photomicrograph in plane light showing that the material surrounding the vertical tube (black arrows) in a foam rock layer has an irregular, micritic, lacy texture.

4.1.4.3 Coated Grains

The coated grains found within the samples are relatively small in size (0.1 to 1 mm) and are composed of distinct nuclei and cortices. The nuclei are composed of a single calcite crystal and range in shape from rounded to rhombohedral (Figure 26). The cortices are dark brown micrite and surround the nuclei in an even and consistent nature. This causes a slightly concentric appearance, although it is not highly obvious in every coated grain.

The round shape and constant thickness of the cortices surrounding the coated grains indicates that they were in near constant motion. This is consistent with the location of the coated grains present within the Ivory Quarry, as they are

found adjacent to terrace rimstone dams. Terrace rimstone dam features are associated with rapid, turbulent fluid flow, as they are the location of water movement from a higher elevation to a lower elevation over a very short distance. The coated grains commonly collected in clusters on the down slope side of the rimstone dam and subsequently were surrounded by cement.

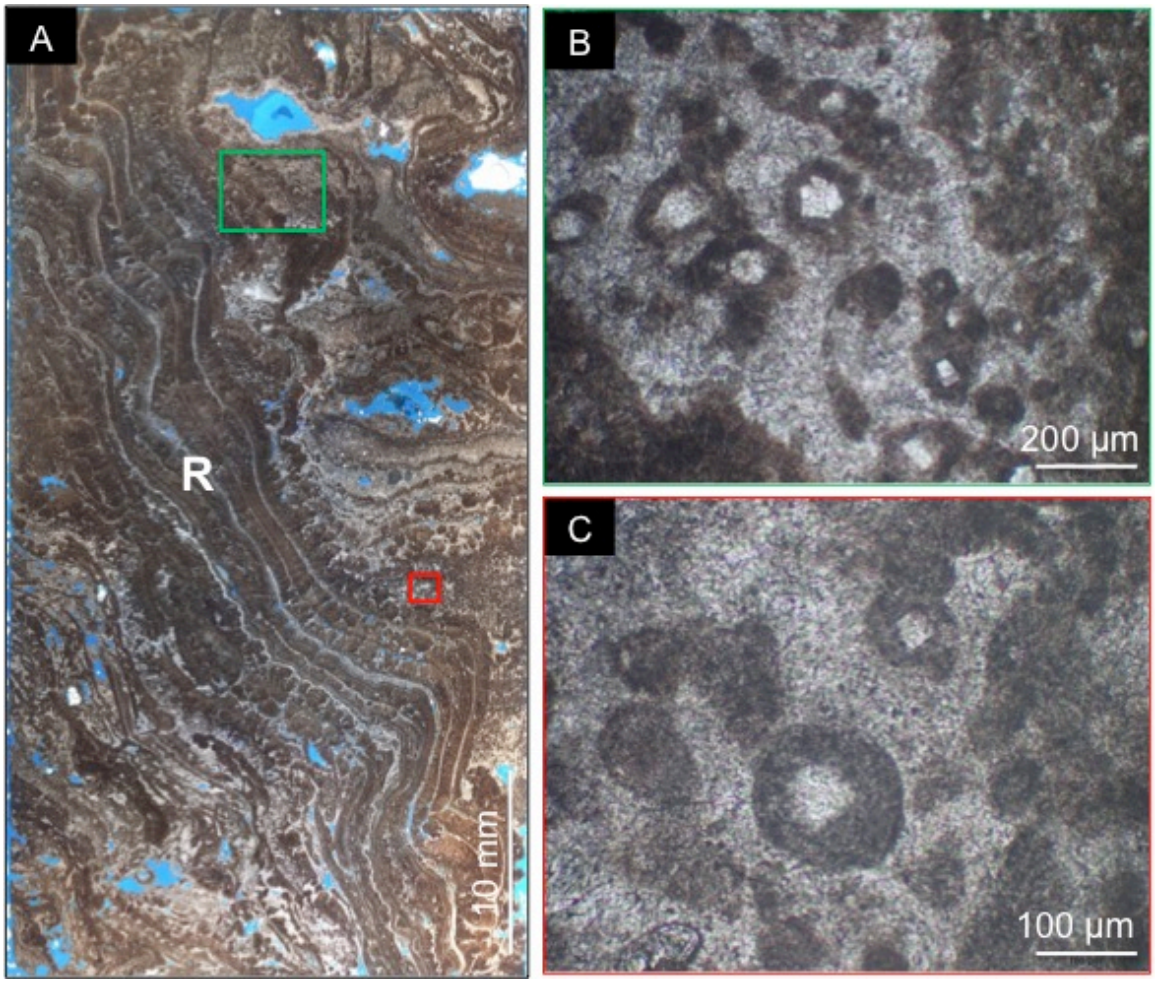

Figure 26: (A) Photomicrograph in plane light of a terrace rimstone dam ("R") with coated grains collecting adjacent to it. The green box indicates the location of Figure B. Red box indicates the location of figure C. (B-C) Photomicrographs in plane light showing coated grains with a single calcite crystal as the nucleus and dark, slightly concentric, micritic cortices.

4.1.4.4 Pisoids

The pisoids present within the Gold and Ivory quarries range in size from 1 mm to 3 cm (Figure 27). They are found both in layers that are primarily composed of pisoids, and layers that have a highly variable mixture of constituents. The pisoids have been observed to vary in shape from round to elongate. This can be due to a number of factors, including the shape of the nucleus and the amount of motion experienced. Whereas most of the pisoids within the Gold and Ivory quarries are well preserved, some of them have undergone significant alteration. In some instances, recrystallization of the pisoids has resulted in the destruction of almost all distinguishing features.

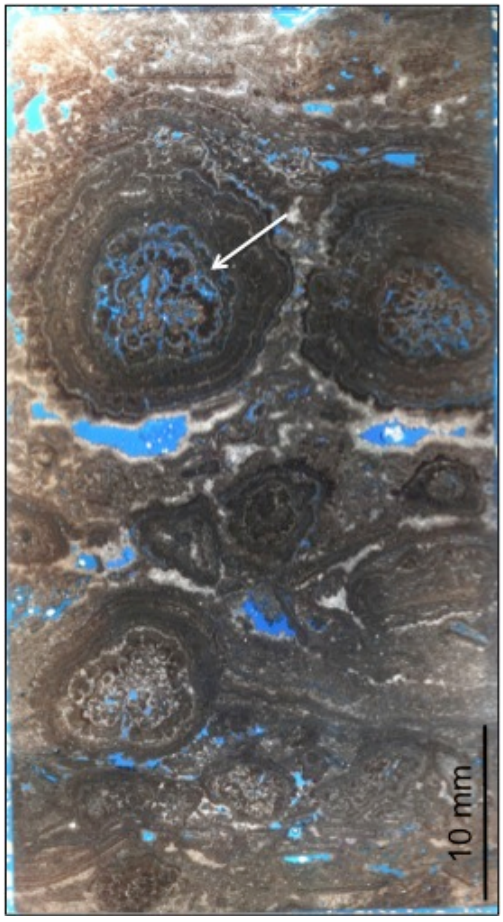

Figure 27: Photomicrograph in plane light showing large pisoids with micritic nuclei. The pisoids have intraparticle porosity in the nuclei (white arrow). The cortices are concentric but irregular.

The nuclei of the pisoids are commonly distinct and can be composed of either another constituent or clumps of micrite. Rafts are the most common constituents that comprise a nucleus. As rafts are elongate features, they result in elongate pisoids (Figure 28). The clumps of micrite are irregularly shaped and appear to have a less dominate control on the pisoids final shape. They also generally result in more porous nuclei than those formed by other constituents.

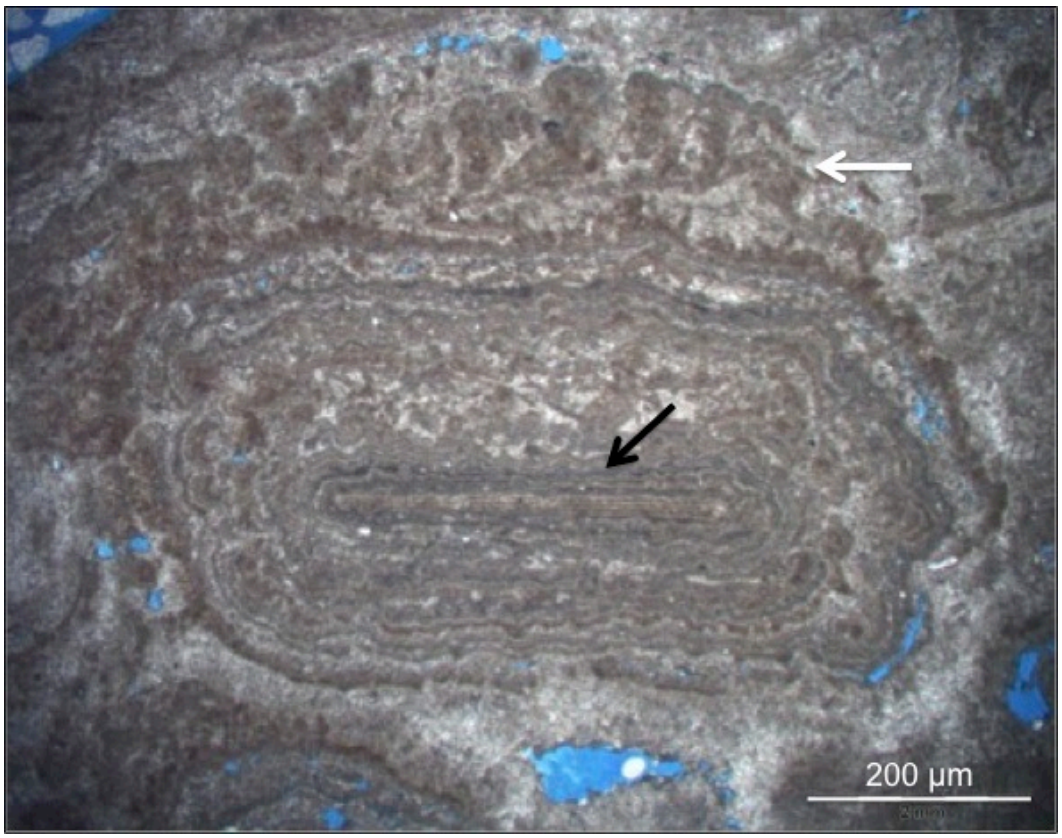

Figure 28: Photomicrograph in plane light of a pisoid with a raft as the nuclei (black arrow). The shape of the nuclei caused the pisoid to be more oblate than spherical. The pisoid also has growth on the top of it (white arrow), indicating that the pisoid became stationary.

Highly irregular, yet concentric cortices surround the pisoids. The irregular habit of the cortices could have been caused by a number of factors, with one of the most likely being the influence of biotic activity in their formation. The concentric nature is due to the near constant motion of the pisoids during their formation. Some of the pisoids have cortices with preferential growth in the upward direction and layers gently draping over the pisoids. These are indications that the pisoids continued to grow while stationary.

4.1.4.5 Spherulites

Spherulites within the Gold and Ivory quarries are not visible within the hand samples, and can only be seen in thin section and SEM. They range in size from 30 microns to 2 mm and spherical to oblate in shape. They have been formed in association with a wide variety of other constituents, including coated grains, crystal ray fans, and bacterial shrubs. The internal structure of the spherulites is composed of radiating calcite crystals around a central nucleus that is only visible under high magnification. In cross-polarized light, the spherulites display a pseudo-uniaxial cross due to the radiating nature of the crystals (Figure 29).

The nuclei of the spherulites are visible under the high magnification of the SEM. They are 5 to 30 microns in diameter and are composed of clusters of spherical to elliptical forms that are less than a micron in size (Figure 30). These forms are interpreted to represent bacteria that are responsible for inducing the initial calcite precipitation of the spherulites. Bacterial forms similar to those seen

within the spherulites in the Gold and Ivory quarries have been documented by Folk (1993, 1999).

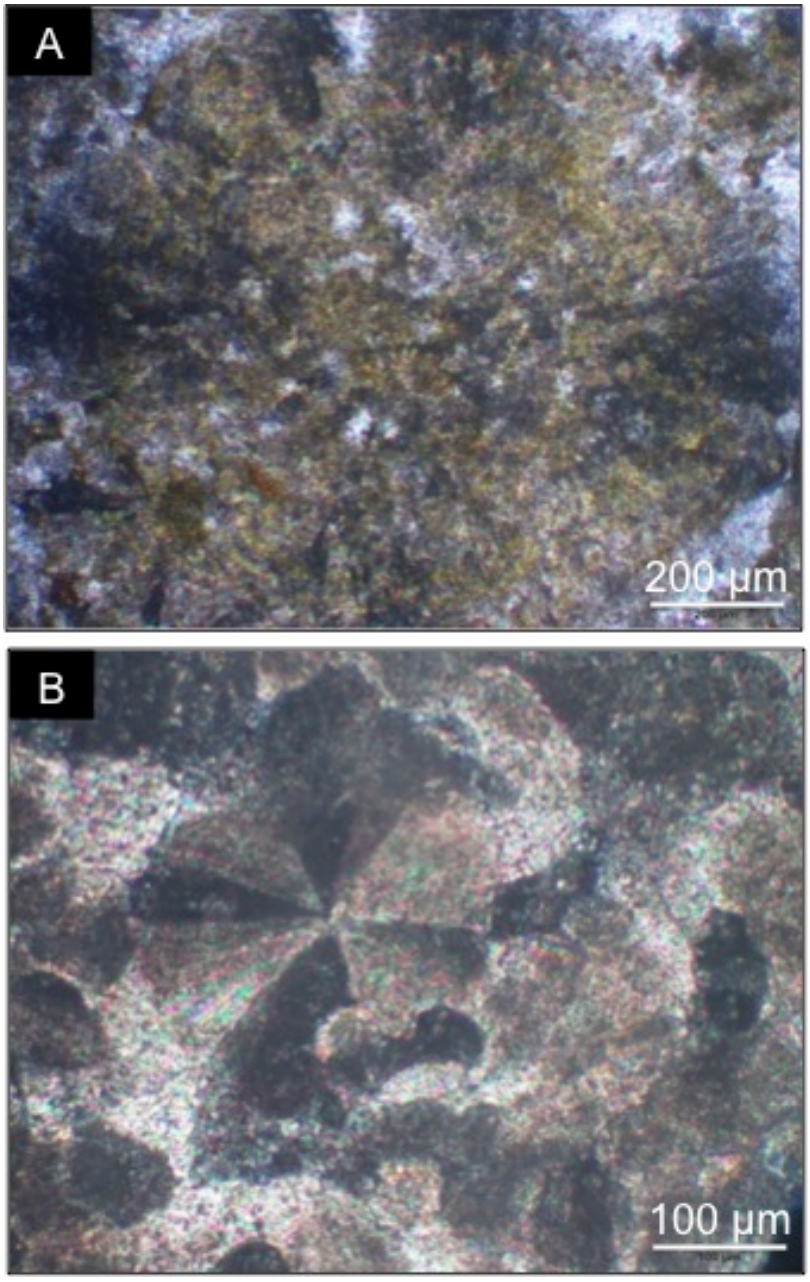

Figure 29: (A-B) Photomicrographs in cross-polarized light showing spherulites that displays a pseudo-uniaxial cross due to the radial nature of the crystals surrounding the nucleus.

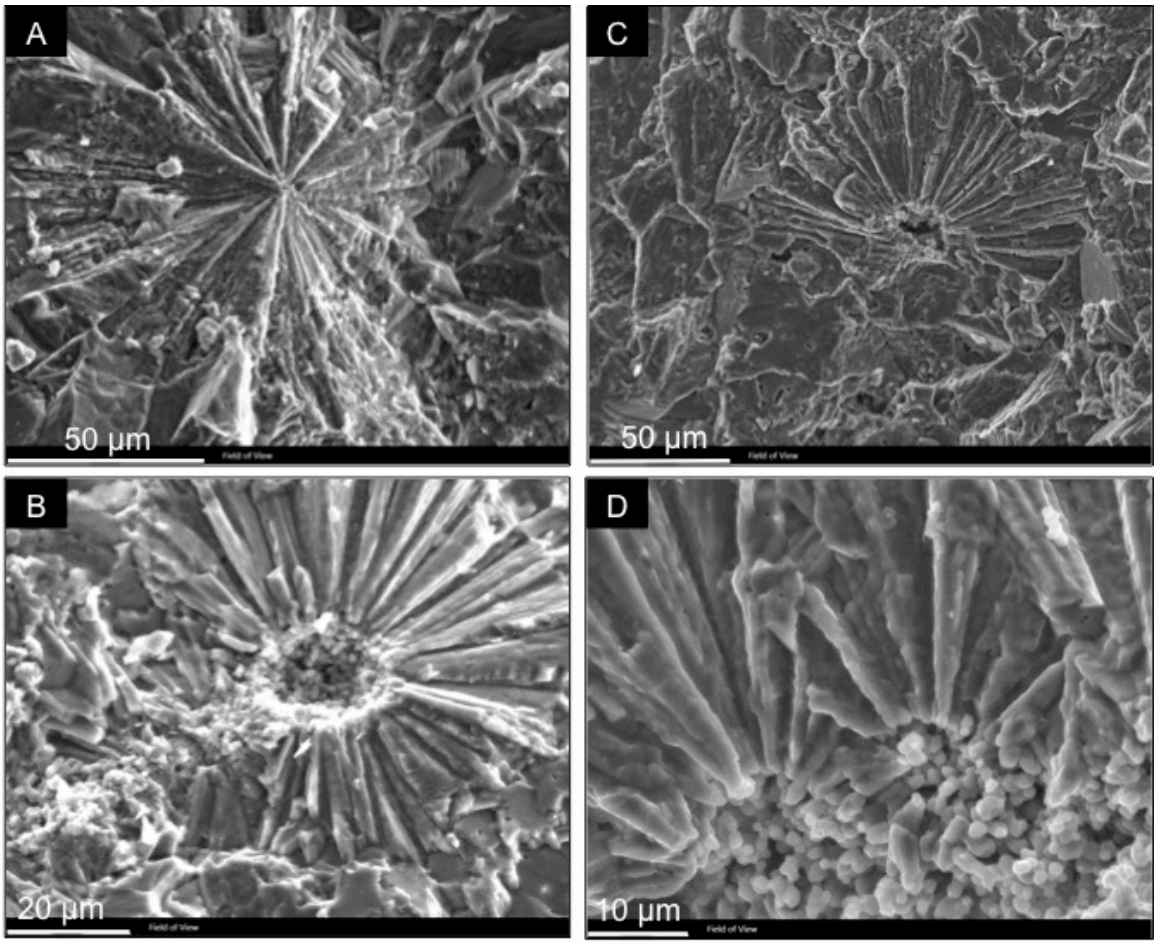

Figure 30: (A-D) Spherulites in SEM. The nuclei of the spherulites are composed of small spherical to elliptical forms.

4.1.4.6 Shrubs and Crusts

The Gold and Ivory quarries display a range of shrub and crust features, including bacterial shrubs, crystal shrubs, and ray crystal fan/crusts.

4.1.4.6.1 Bacterial Shrubs

The bacterial shrubs are found in 1 to 1.5 cm thick, laterally continuous layers. The layers are composed of either a single shrub that has a thickness

equal to the overall layer, or multiple shrubs stacked on top of each other to account for the thickness of the shrubby layer. The shrub layers are bounded below by a laminae of densely packed, micritic peloids (Figure 31). The bacterial shrubs are composed of clumps of micritic material forming an overall branching outward morphology. Some of the bacterial shrubs have a distinct overall morphology, whereas other shrubs are so densely packed that the large-scale morphology is obscured.

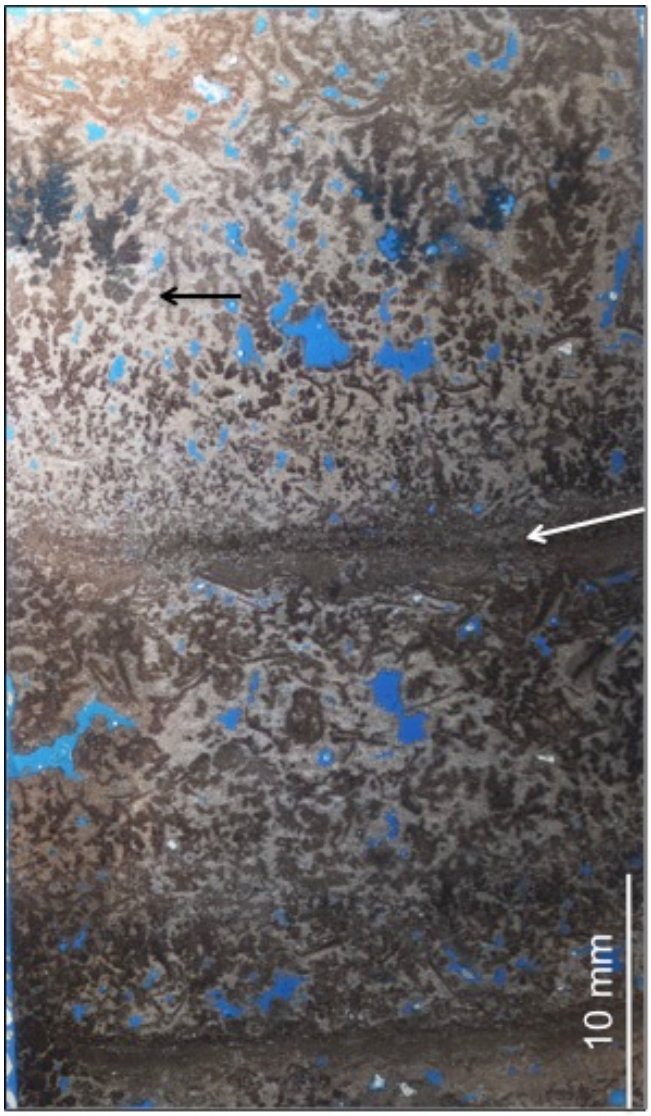

Figure 31: Photomicrograph in plane light of bacterial shrub layers (black arrow) separated by a dense peloid layer (white arrow).

The individual shrub leaves commonly range in size from 0.05 to 0.5 mm and display a wide variety of shapes (Figure 32). In thin section, they are dark brown in color and do not have a distinct internal structure or growth lines. The shrubs are surrounded by spar cement (Figure 33). The shrub leaves vary between being connected to other leaves on one side to being completely surrounded by cement. This is due to a variety of possible factors, including the three-dimensional nature of the feature, how well the shrub is formed, and diagenesis.

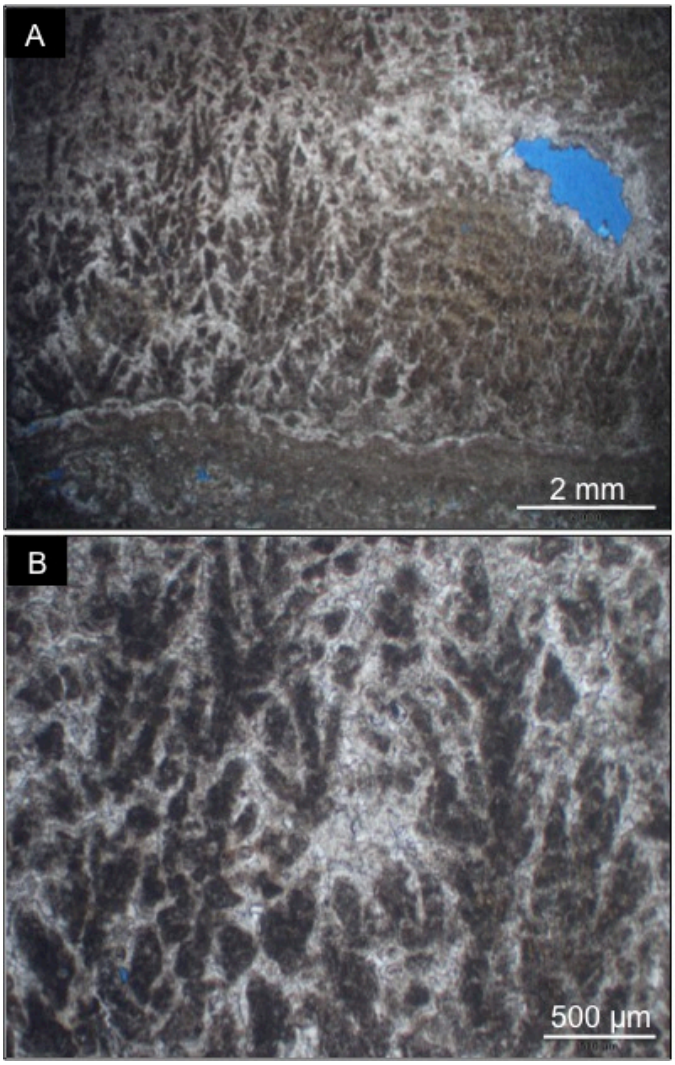

Figure 32: (A and B) Photomicrographs in plane light of bacterial shrubs displaying distinct leaves surrounded by spar.

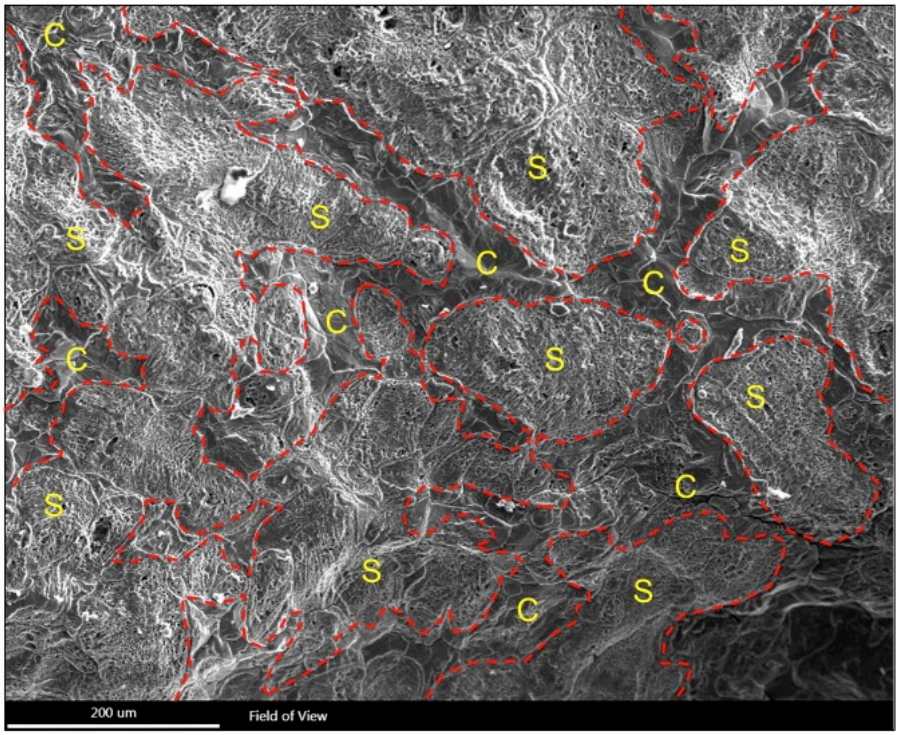

Figure 33: SEM image of a vertical section showing microporous bacterial leaves (S) of a shrub surrounded by spar cement (C). The contacts between the bacterial leaves and the cement is outlined in red dashed lines

SEM analysis of the bacterial shrubs showed that the micritic shrub leaves contain abundant microporosity and that the surrounding cement does not (Figure 34). This finding is consisting with that of Chafetz and Folk (1984) and Chafetz (2013), and was interpreted to be due to the presence of bacteria in the shrub leaves. The bacteria quickly decay and create microporosity at their former site.

4.1.4.6.2 Feather Dendrites

Feather dendrites have been identified within the Gold Quarry. They form in laterally continuous layers on sloping mound intervals that lack microterraces. The full length of the feather dendrites cannot be determined in thin section, as they are at the top of a thin section and have been cut off. Assuming the length of

the feather dendrite is equal to the thickness of the layer, they have a length of about 1.4 cm. They form as thin (0.2 mm), long central crystals and have small branches emanating from the central stalk (Figure 35).

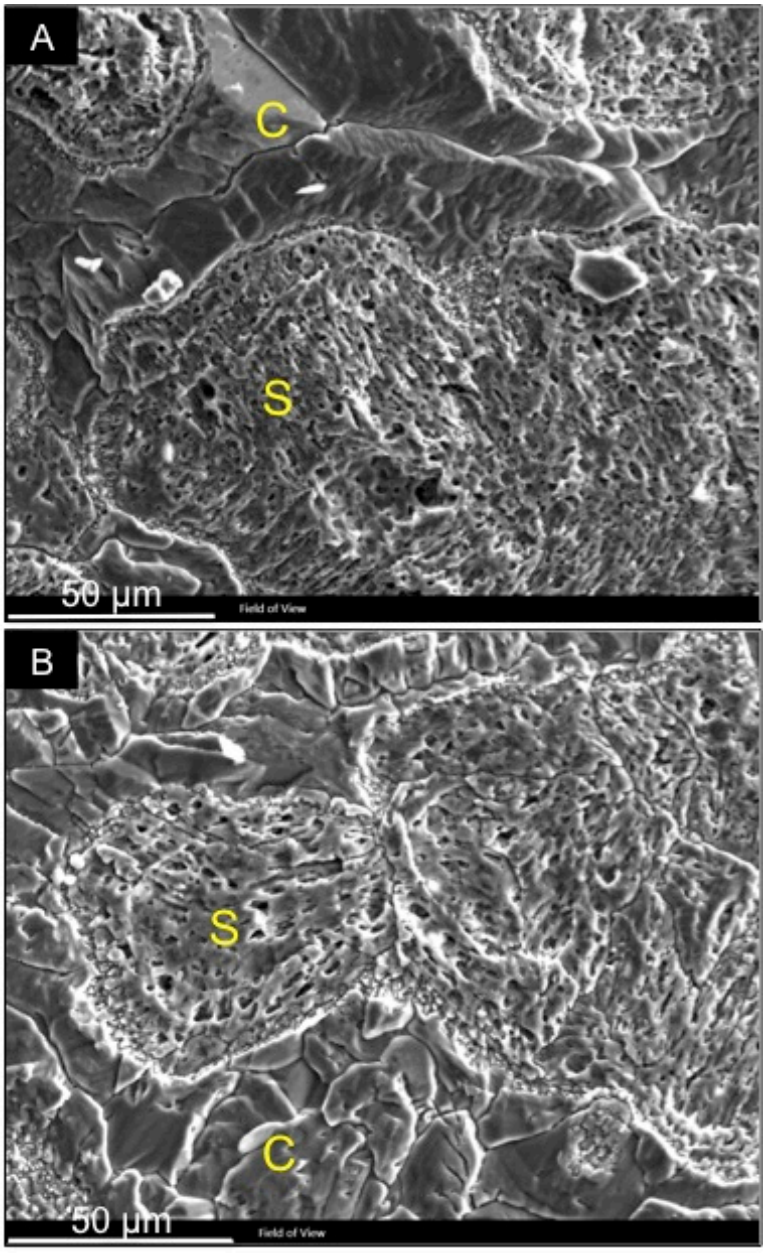

Figure 34: (A and B) SEM images of the bacterial leaves of a shrub (S) surrounded by spar cement (C). The leaves are full of micropores due to the influence of bacteria in their formation. The surrounding cement lacks micropores as it was abiotically precipitated.

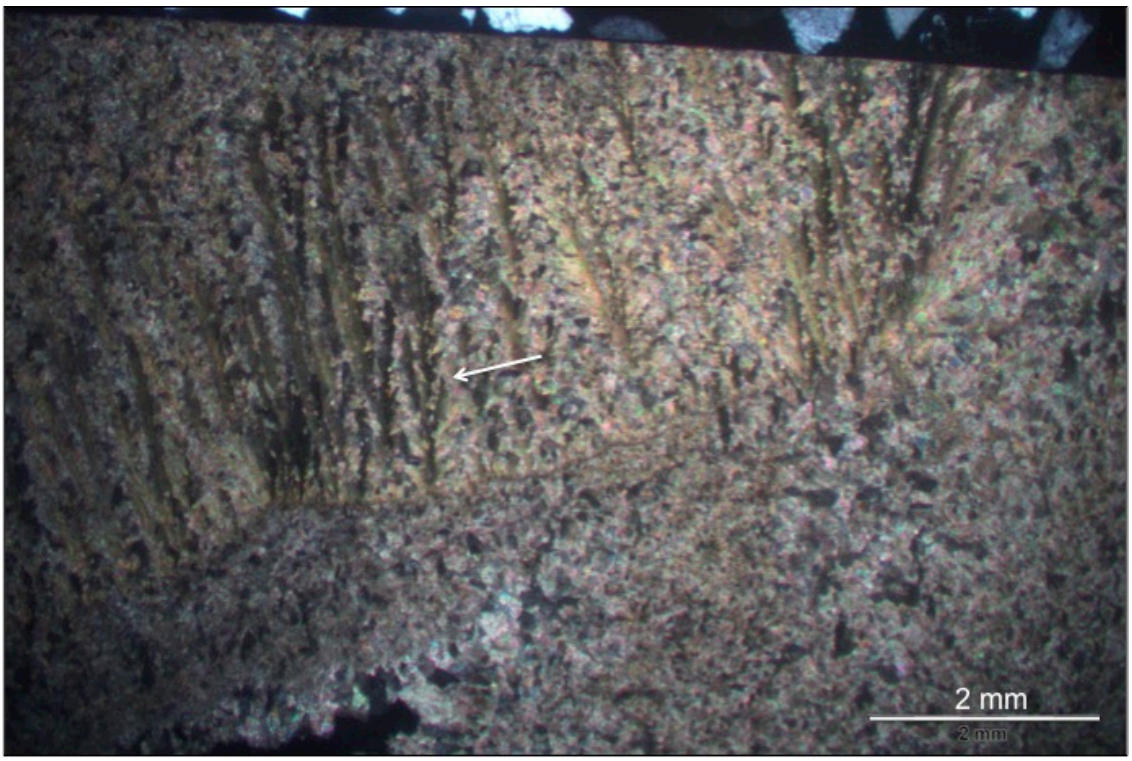

Figure 35: Photomicrograph in cross-polarized light of feather dendrites (white arrow). The feather dendrites have elongate central stalks in which small crystal branches initiate.

4.1.4.6.3 Ray Crystal Fans and Crusts

Ray crystal fans are 1 to 5 mm high, single teardrop-shaped features that form with the teardrop vertex at the base (Figure 36). They are composed of radiating calcite crystals and have a sweeping extinction in cross-polarized light. They also have distinct growth lines that are convex upward, away from the fan base. The ray crystal fans can form both laterally continuous layers, and can form around other constituents, such as rafts. When growing on other constituents, they can form on both the top and bottom of the feature. In either instance, they grow perpendicular to the surface on which they are formed.

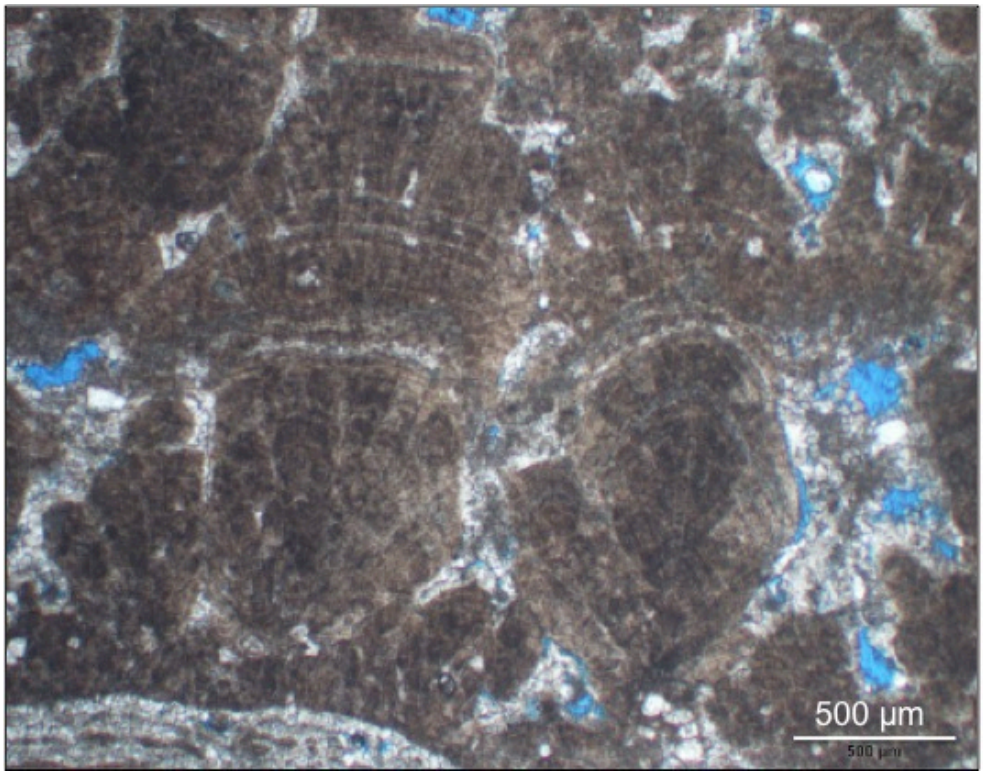

Figure 36: Photomicrograph in plane light of ray crystals. The ray crystals have a teardrop shape.

If the ray crystal fans are closely spaced on a surface, the difference in growth rate between the neighboring fans will affect their morphology. Fans growing at the same speed will grow straight vertically, resulting in tall but not wide fans and a defined contact between two fans (Figure 37). Neighboring fans in which one is growing significantly faster than the other will result in one fan taking over the space of the other fan and truncating its growth.

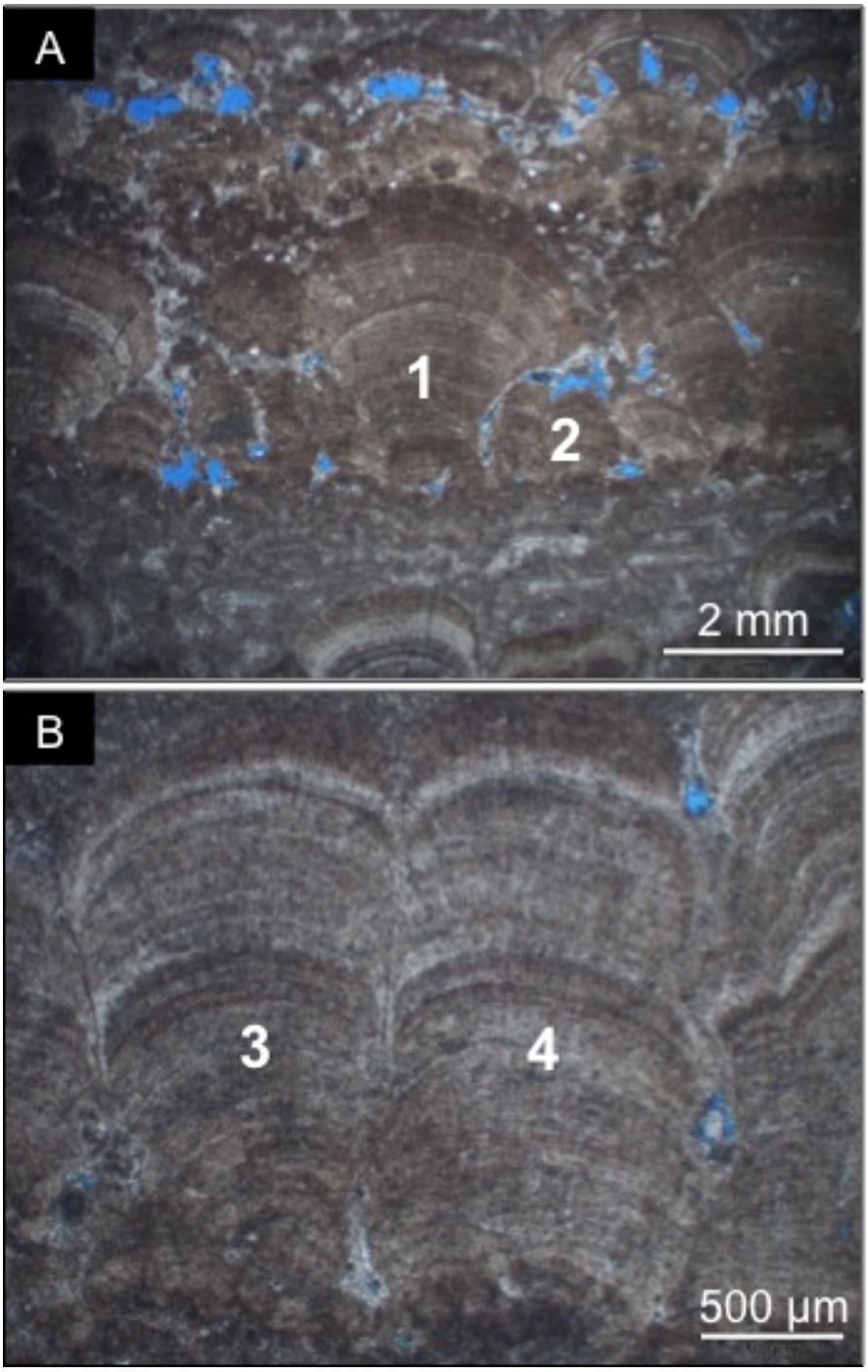

Figure 37: Photomicrographs in plane light of ray crystals. (A) One ray crystal ("1") grew significantly faster than the neighboring ray crystal ("2"), and therefore grew into the space of the neighboring ray crystal. (B) The two neighboring ray crystals ("3" and "4") grew at the same rate, resulting in vertical growth and a straight contact between the two ray crystals. The growth lines within the neighboring crystals match, indicating that they grew at the same time.

Ray crystal crusts are layers of calcite crystals that are forming perpendicular to the surface on which they are growing (Figure 38). They have distinct growth lines that form across the layer and are parallel to the surface on which they are growing. The consistency of the growth lines indicates that the whole layer is growing at the same rate and at the same time. Ray crystal crusts are common on terrace rimstone dams and steeply dipping layers.

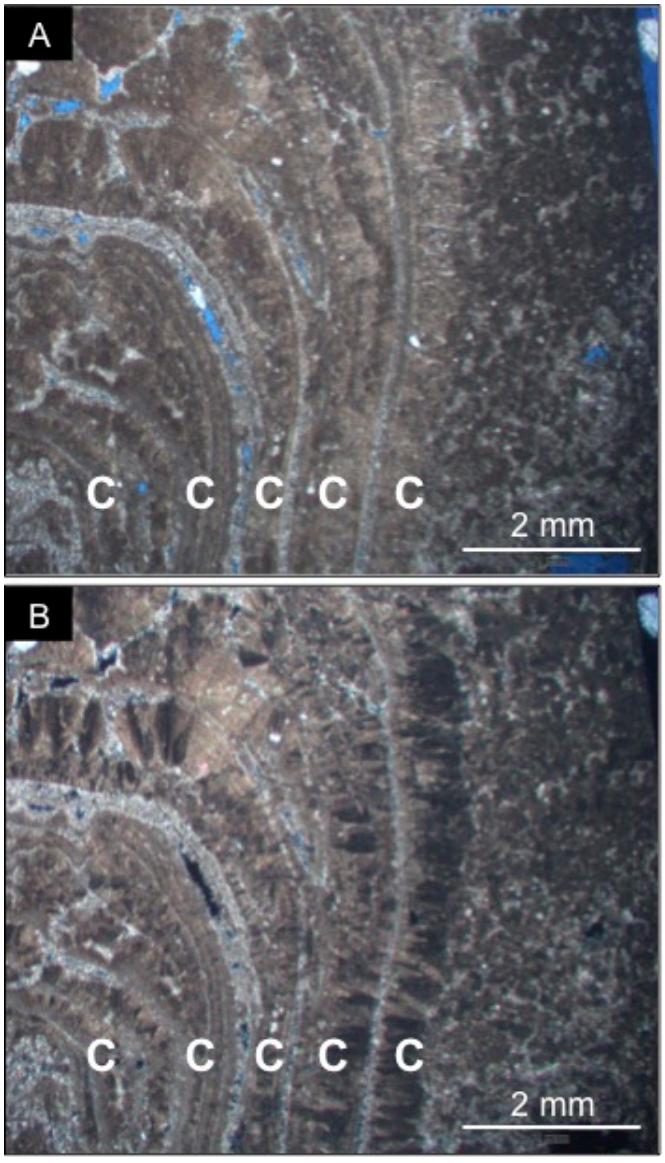

Figure 38: Ray crystal crusts (individual layers marked with a C) forming on the steep part of a rimstone dam. The crystals form perpendicular to the surface they are growing on. (A) Photomicrograph in plane light. (B) Photomicrograph in cross-polarized light.

Ray crystal fans and ray crystal crusts are transitional features, with the most obvious control being slope. An example of this is observed on terrace rimstone dams. Slightly gentler dipping parts of the rimstone dams, such as small shelves, exhibit isolated ray crystal fans. When the slope increases, the isolated ray crystal fans transition into ray crystal crusts. As the slope decreases again, the crusts will transition back into fans (Figure 39).

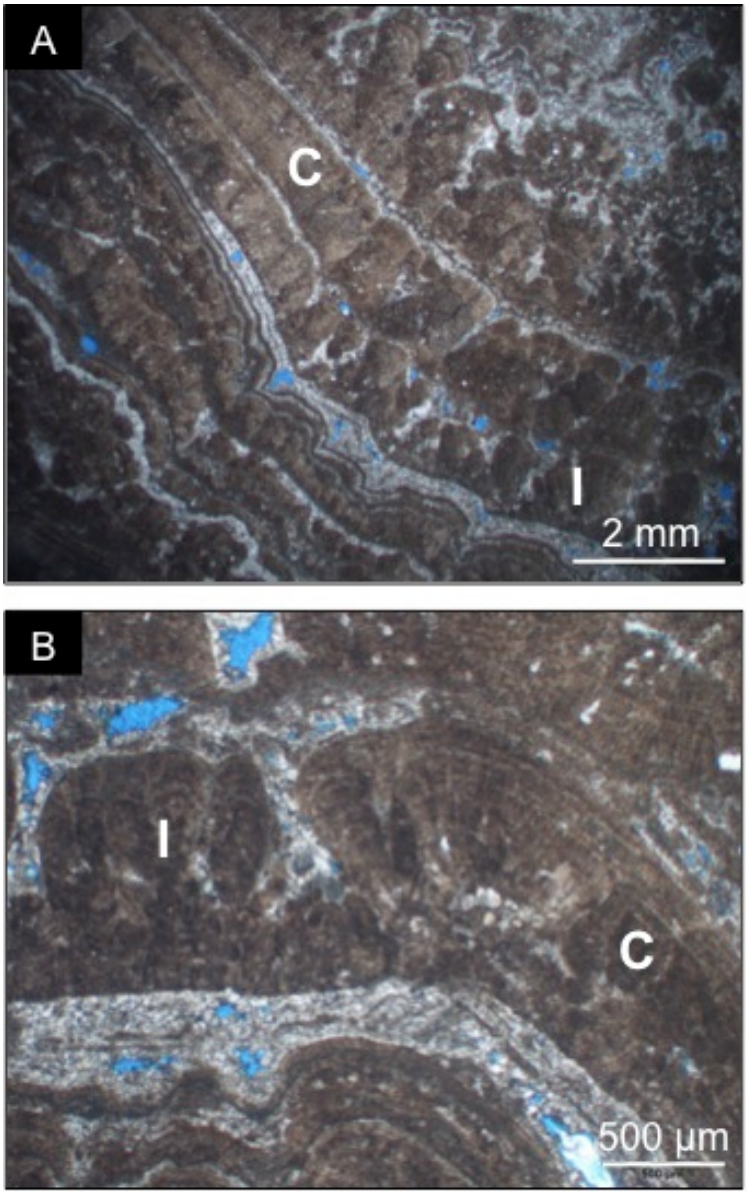

Figure 39: (A) Photomicrograph in plane light showing a terrace rimstone dam that is composed of ray crystal crusts ("C"). As the rimstone dam begins to dip more gently, the crusts transition into isolated ray crystals ("I"). (B) Photomicrograph in plane light showing the transition from isolated ray crystals ("I") to ray crystal crusts ("C").

Ray crystal clusters are amalgamations of individual ray crystal fans. Individual fans will form next to and on top of each other, but will still maintain an overall teardrop shape (Figure 40). The individual ray crystal fans will commonly maintain the crystallographic orientation of the fan on which it is growing. Occasionally the individual ray crystal fans will take on a new crystallographic orientation. Each ray crystal fan displays individual growth laminations, but sometimes they can be traced from one fan in the cluster to another. The ray crystal clusters form on constituents (such as rafts and coated grains), but do not form continuous layers. Similar to the individual ray crystal fans, they form perpendicular to the surface they are growing on. Also similar to the individual ray crystal fans, if the spacing of the ray crystal clusters is close enough, the faster growing cluster will expand into the area of the surrounding cluster and truncate its growth.

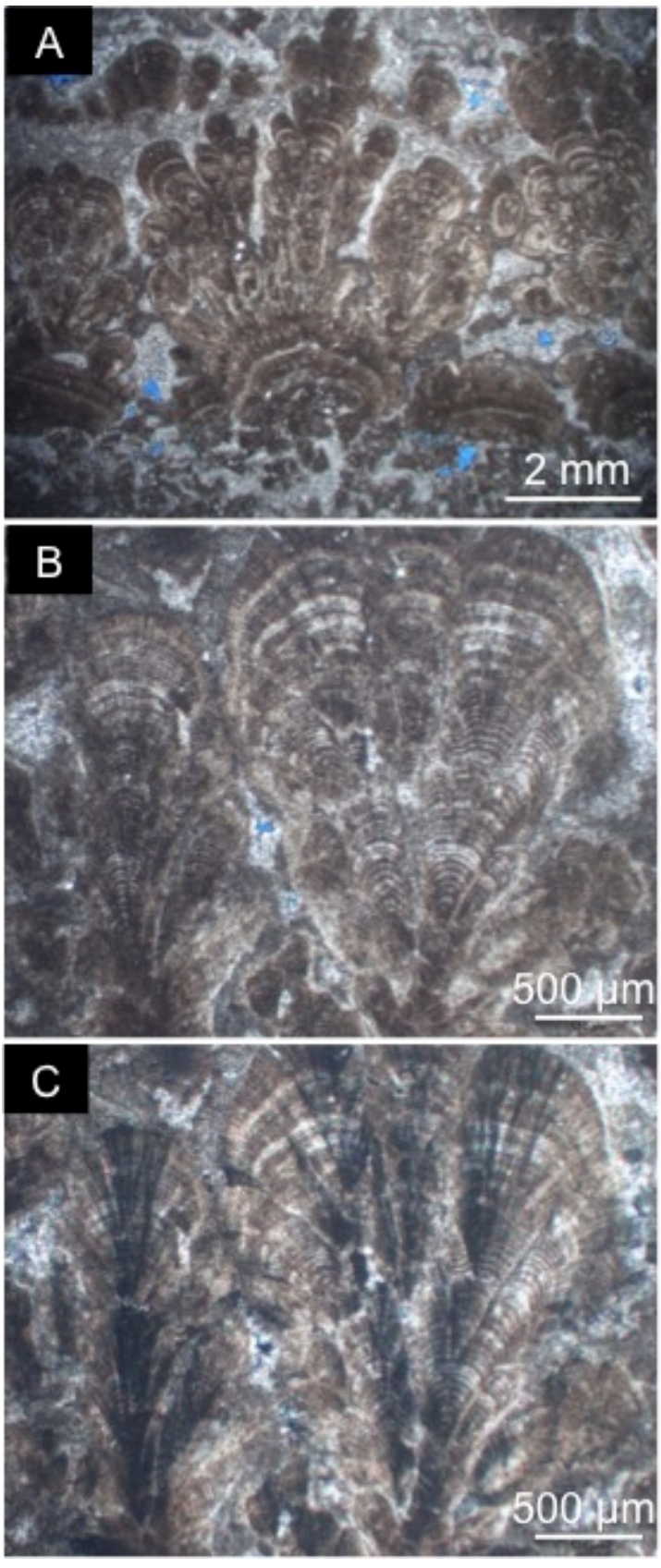

Figure 40: (A) Photomicrograph in plane light showing multiple isolated ray crystal clusters forming on a constituent. (B) Photomicrograph in plane light showing the amalgamation of ray crystals into a cluster. Distinct growth bands are visible. (C) Photomicrograph in cross-polarized light of the same ray crystal cluster as B, showing the extinction of the ray crystals.

4.1.5 Porosity

Within the Gold and Ivory quarries, the porosity is dependent upon the type of constituent, the amount of cementation, and the presence of fractures. Interparticle porosity within travertine deposits is commonly fairly high and can be found surrounding a variety of constituents including, rafts, coated grains, and shrubs. The exact amount of primary porosity is dependent upon the packing and mixture of different constituents found within the layer. The interparticle porosity is highly connected and commonly results in good horizontal permeability. The consistently layered nature of travertine deposits results in anisotropic permeability, as the vertical permeability is hampered by the presence of dense, non-porous layers.

Each constituent exhibits unique differences in the porosity produced. The presence of rafts creates horizontal pores that form underneath the raft (Figure 41). These pores commonly span the entire length of the raft, as the raft shields the pore from sediment or other constituents occluding it. Pisoids can exhibit intraparticle pores, both between cortices and within the nucleus (Figure 27). The leaves of bacterial shrubs also have abundant intraparticle pores, observed as micropores formed by bacteria (Figure 34).

Foam rock intervals are composed of vertical pores that are densely packed within layers. Each vertical pore is surrounded by a micrite border, resulting in the possible isolation of individual pores within a single layer. A number of the pores appear to be open on one end, or broken, which could

increase the permeability within the foam rock layer. Individual foam rock layers are commonly stacked on top of each other, but they are separated by dense micrite layers (Figure 24). This results in permeability that is likely anisotropic, due to the presence of extensive horizontal layering. The lateral extent of the foam rock layers is isolated to individual terrace pools and is bounded by densely crystalline rimstone dams on all sides.

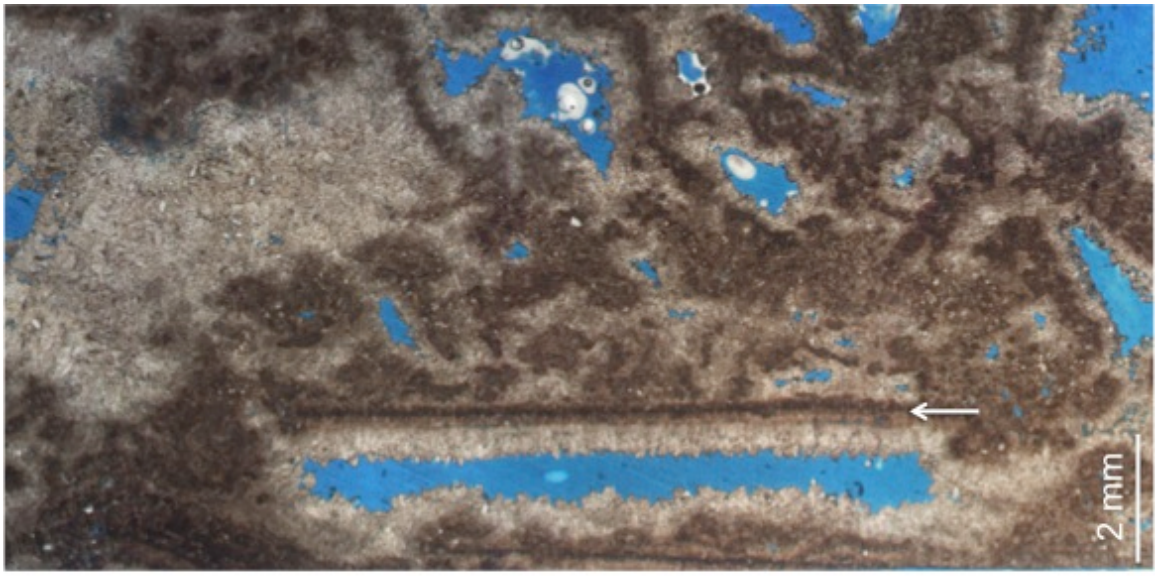

Figure 41: Photomicrograph in plane light showing a 10 mm horizontal pool beneath a raft (white arrow).

Secondary porosity has formed within the Gold and Ivory quarries. It has been observed as both fracture pores and large, vuggy pores (Figure 42). The vuggy pores are mostly found along fractures, as they act as a pathway for fluid movement, resulting in local dissolution of the travertine. Some of the fractures cut across the primary travertine layers and increase the vertical permeability.

Much of the porosity within the Gold and Ivory quarries is reduced or completely occluded by cementation. Quantification of present day porosity within thin section samples indicated a range in porosity from 0.8 to 11.8 percent based on the digital porosity analysis (Figure 43 and 44). The majority of the samples had between 2 and 7 percent porosity (Figure 45). It is important to note that the low porosity percentages can be misleading, as the thin sections were primarily chosen to investigate constituents and observe relationships between them. This likely resulted in the selection of less-porous samples, as large pores within thin sections do not provide much data about constituents.

Figure 42: Fractures vertically cut across the travertine layers (black arrow) resulting in increased vertical permeability. Along the fractures some increased dissolution has occurred resulting in vuggy porosity (white arrow).

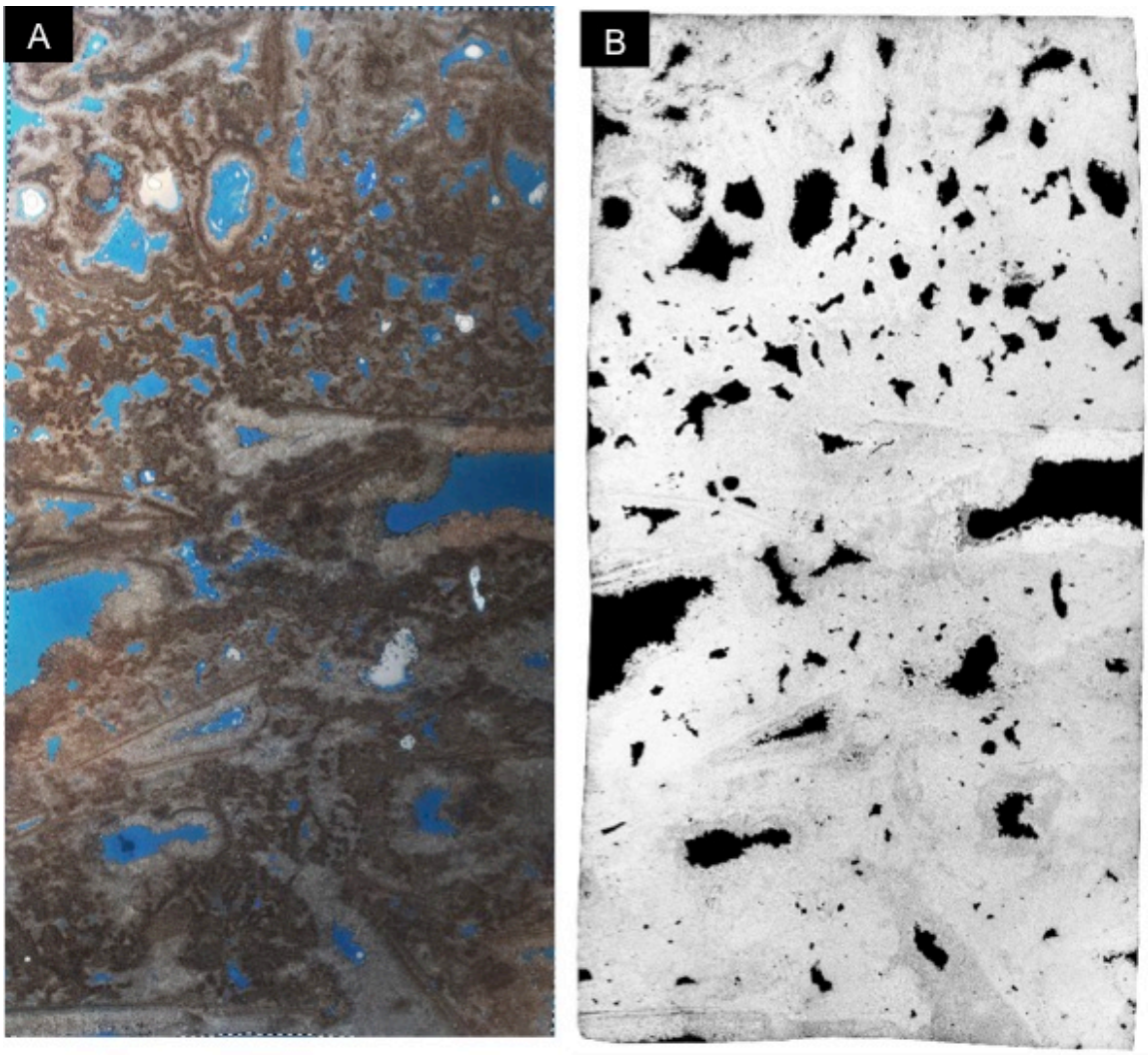

Figure 43: (A) Photomicrograph in plane light of a sample containing foam rock and rafts. This sample has 11.8 percent porosity. (B) Copy of the photomicrograph with the colors inverted to highlight the porosity (in black) in an effort to show the shape of the pores.

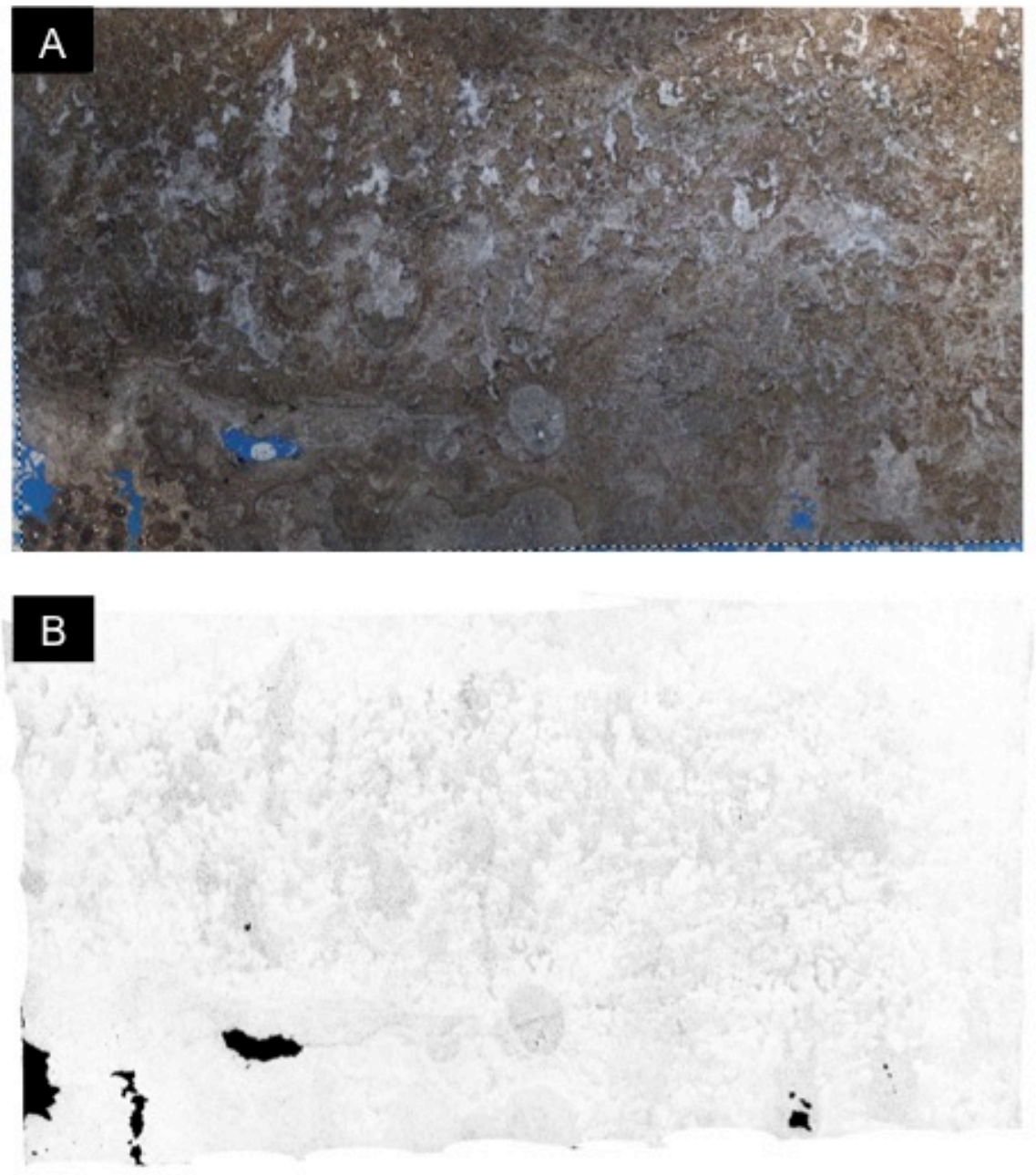

Figure 44: (A) Photomicrograph in plane light of a sample containing foam rock and ray crystal clusters. This sample has 0.9 percent porosity. (B) Copy of the photomicrograph with the colors inverted to highlight the porosity (in black) in an effort to show the shape of the pores.

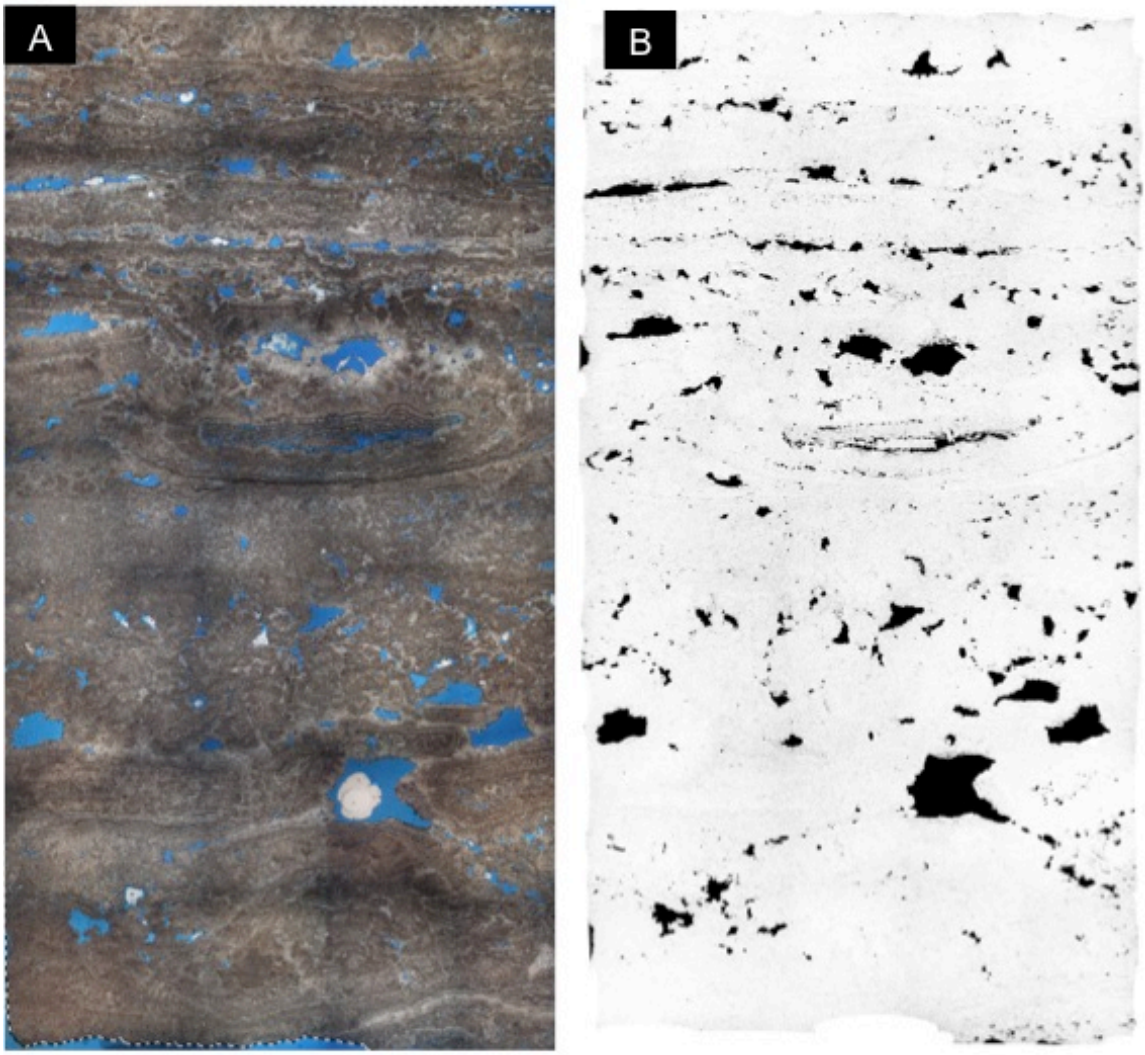

Figure 45: (A) Photomicrograph in plane light of a sample containing pisoids. This sample has 5.3 percent porosity. (B) Copy of the photomicrograph with the colors inverted to highlight the porosity (in black) in an effort to show the shape of the pores. The porosity has a dominantly horizontal orientation.

4.1.6 Depositional Morphologies and Facies

4.1.6.1 Ivory Quarry Facies

Two distinct depositional morphologies are present within the Ivory Quarry: terrace mounds and sloping mounds. The transition between terrace mound and sloping mound morphologies is subtle and can occur both laterally (along a single layer) and temporally (at a single location through time). The terrace mounds can be divided into two components: pools and rimstone dams. The pools are composed of horizontal layers that are bounded on all sides by rimstone dams. The paleo-water depth within the pools was very shallow, commonly only ranging from 0.5 to 3 cm (Figure 46). The pools remained in the same location, resulting in over 1.5 meters of stacked pool layers. The majority of the layers are laterally continuous throughout the extent of a single pool, and commonly can be traced from one pool, down the rimstone dam, and across an adjacent pool (Figure 13). The layers within a pool range in thickness from 0.5 to 5 cm but when traced through multiple pools a single layer can vary in thickness. The thickening of layers in a downstream pool results in the decrease in height of the rimstone dam and ultimately the elimination of a rimstone dam at that location (Figure 14).

The layers in the pool are composed of a range of constituents, including bacterial shrubs, rafts, coated grains, and foam rock. Individual layers can be either dominated by a single constituent or can contain a mixture of constituents. A common sequence observed within a pool layer includes a densely packed

peloidal zone at the base, followed by bacterial shrubs which are then topped with a mixture of small rafts and pisoids (Figure 47). Following the interpretation by Chafetz and Folk (1984), the peloidal zone likely represents the non-growing season and the following bacterial shrubs indicate formation during the growing season. As the pisoids and raft are found between the bacterial shrubs and the peloidal zone of the following layer, they likely indicate a transitional stage between the growing and non-growing seasons.

Figure 46: Paleo-water depth indicated by the difference in height between the layer in the pool and the edge of the same layer in the rimstone dam (white arrows mark the top and bottom of the rim).

In addition to the layers mentioned above, many additional types of layers are present within the pools, such as layers that are composed completely of rafts (Figure 48). These layers indicate that the air-water contact was highly

super-saturated, which causes rapid raft formation. The water was then disturbed, resulting in the breaking up and sinking of the rafts, allowing for preservation. Foam rock layers are also commonly observed within pools. On Ivory Quarry wall E2, all three of the observed pool accumulations have foam rock layers present. When comparing the location of foam rock layers between these three pools, for any stratigraphically equivalent layer, the foam rock layer is commonly only present within one pool. Some minor stratigraphic overlap does occur as the foam rock layer transitions between pools. As foam rock layers are thought to indicate the location of vents, this would suggest that the vent location migrated between the three pools through time (Figure 49).

Rimstone dams are easily identified within the Ivory Quarry. They are composed of near vertical layers that are immediately adjacent to the horizontal pool layers. The shape of the rimstone dam varies from completely straight to convex outward. Individual layers identified within pools can be traced along rimstone dams, but the morphology and thickness of the layer changes abruptly. Rimstone dams are composed of multiple ray crystal crust layers that are only 0.5 to 2 mm thick (Figure 26A). The height of an individual rimstone dam in the Ivory Quarry reaches a maximum of approximately 50 cm. As the rimstone dams commonly occupied the same location for a period of time, it resulted in a zone of rimstone dams that are greater than 1.5 m high.

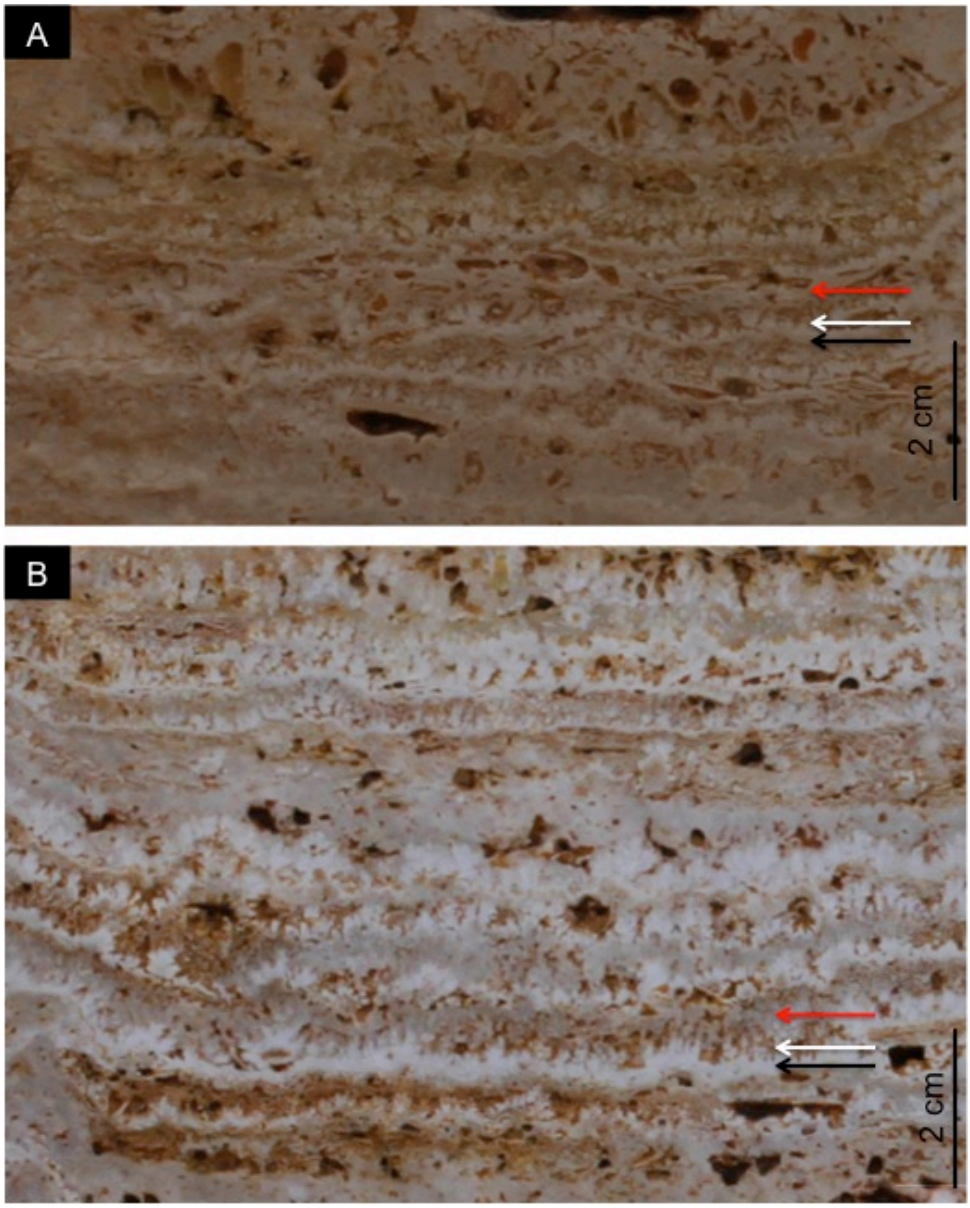

Figure 47: (A and B) Multiple layers of a distinct sequence within two different terrace mound pools. The sequence shows a peloid-rich zone at the base (black arrow), followed by a bacterial shrub interval (white arrow) that is topped with pisoids and rafts (red arrow).

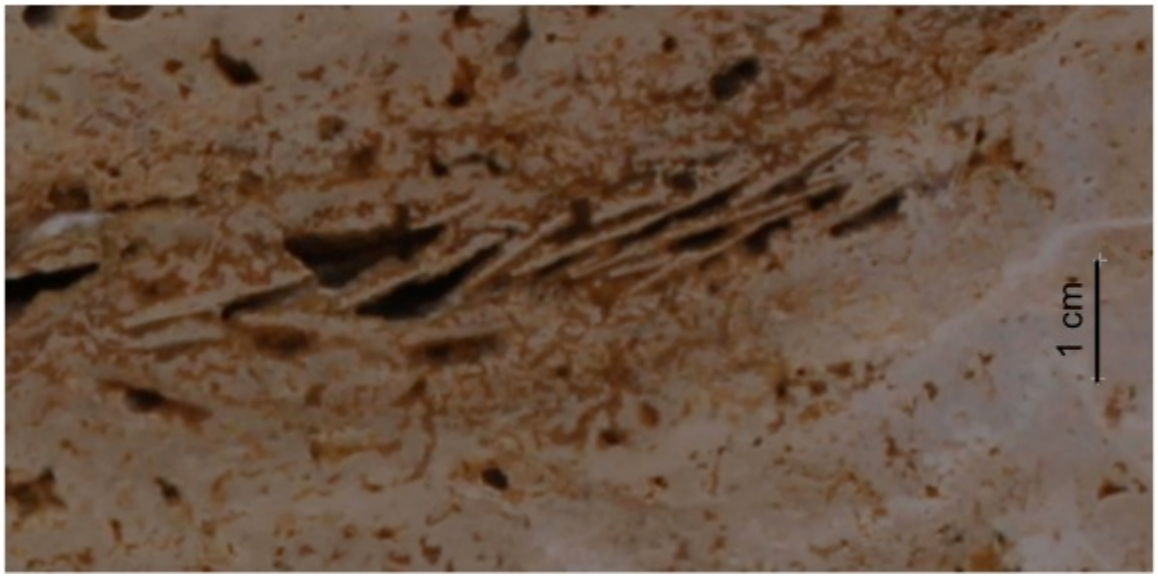

Figure 48: Terrace mound pool layer composed completely of rafts.

Figure 49: Ivory Quarry Wall E2 with the foam rock layers highlighted in blue. Stratigraphically equivalent layers (black lines) show that the foam rock layers migrate between the three pools through time.

The sloping mound morphology within the Ivory Quarry is composed of layers that dip approximately 8 to 19 degrees and have abundant microterrace structures. The length of the microterrace pools is heavily dependent upon the dip of the layer. Layers that have gentler dips have longer microterrace pools, and as the dip steepens, the length of the pool decreases (Figure 50). Some of the constituents within the microterrace pools are similar to that of larger terrace pools, such as raft and pisoids. Others constituents are noticeably different, such as the lack of bacterial shrubs and the presence of ray crystal fans and ray crystal clusters. This change indicates a switch from bacterially influenced to abiotically influenced formation of constituents. This is likely due to the increased flow velocity and thus higher saturation states on the sloping layers as opposed to the ponded water within larger pools. The sloping mound layers also lack foam rock, which indicates that there were no vents present along the layers and that all of the water was coming from a source farther upstream. The microterrace rimstone dams are not stationary for a long period of time, and commonly move locations after only a couple of layers. Layers within the sloping mound morphology occasionally pinch out.

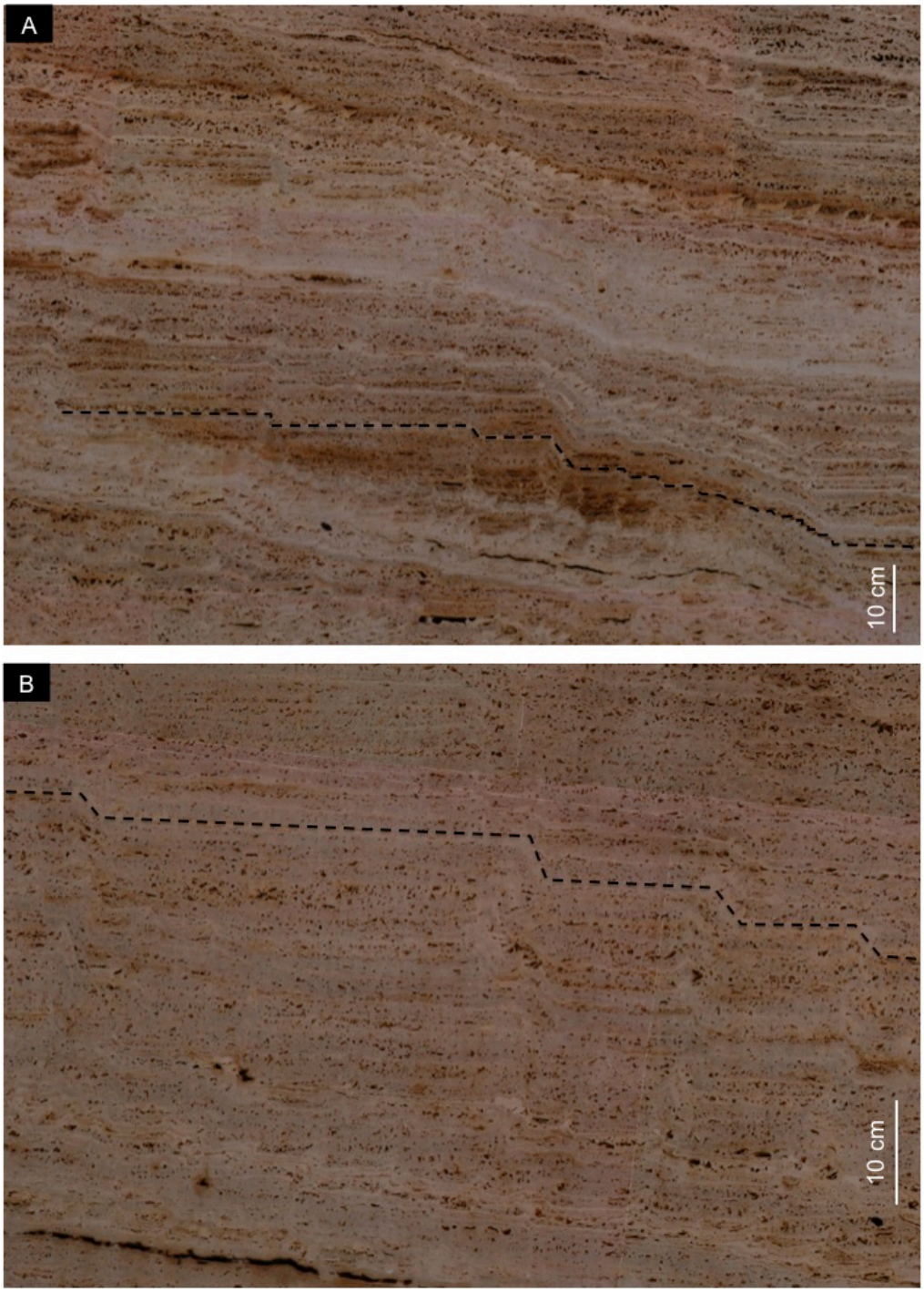

Figure 50: (A and B) Sloping mound with microterraces in which the pool length decreases with increasing slope. A single layer is traced with a dashed black line to emphasize the structure.

4.1.6.2 Gold Quarry Facies

The Gold Quarry has a small zone of terrace mound morphology present on wall D (Figure 51). The distinct rimstone dams are very similar to those seen in the Ivory Quarry, with vertical layers of thin ray crystal crust. The pools have layers that range in thickness form 0.1 to 5 cm. Contrary to the abundant foam rock in the Ivory Quarry pools, the pool in the Gold Quarry terrace mounds only has one small foam rock layer. The majority of the layers appear massive and do not have highly distinct constituents.

Most of the Gold Quarry displays a sloping mound morphology. The layers dip between approximately 5 and 12 degrees. A lot of the structure within the Gold Quarry is obscured by the abundant alteration. The sloping mound layers range in thickness from 0.1 to 3 cm. Many of the layers are laterally continuous throughout the quarry, although some of the layers pinch out (Figure 52). The sloping mound layers have small, poorly-defined microterraces. The rimstone dams of the microterraces commonly only form in the same location for a few layers and then disappear (Figure 53). The microterrace pools have small rafts and pisoids, as well as ray crystal fans. The smooth sloping layers that lack microterraces exhibit feather dendrites. The sloping mound layers have a slight undulating appearing, but have an overall downslope dip. The lows formed in the undulating layers are the location of localized ponding.

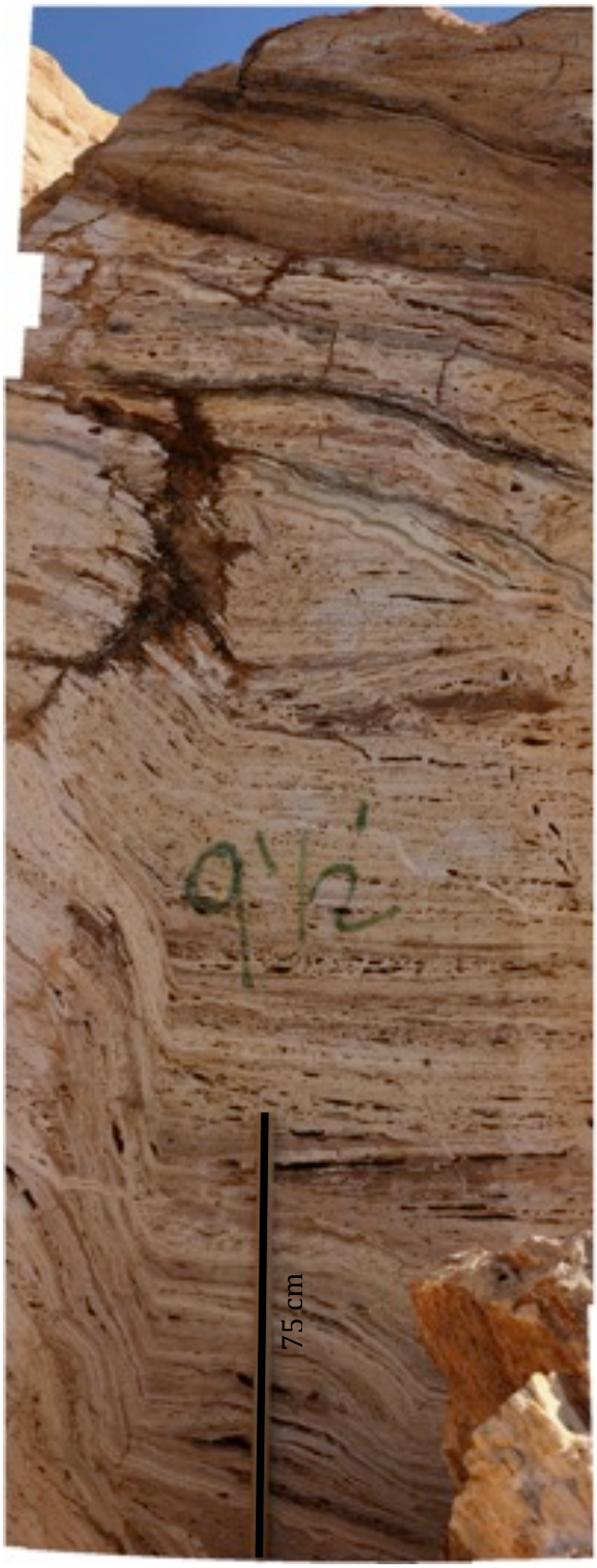

Figure 51: Terrace mound morphology in the Gold Quarry. The image shows a rimstone dam in the bottom left corner and an adjacent terrace pool. The "9 ½" was written on the wall for quarry activities.

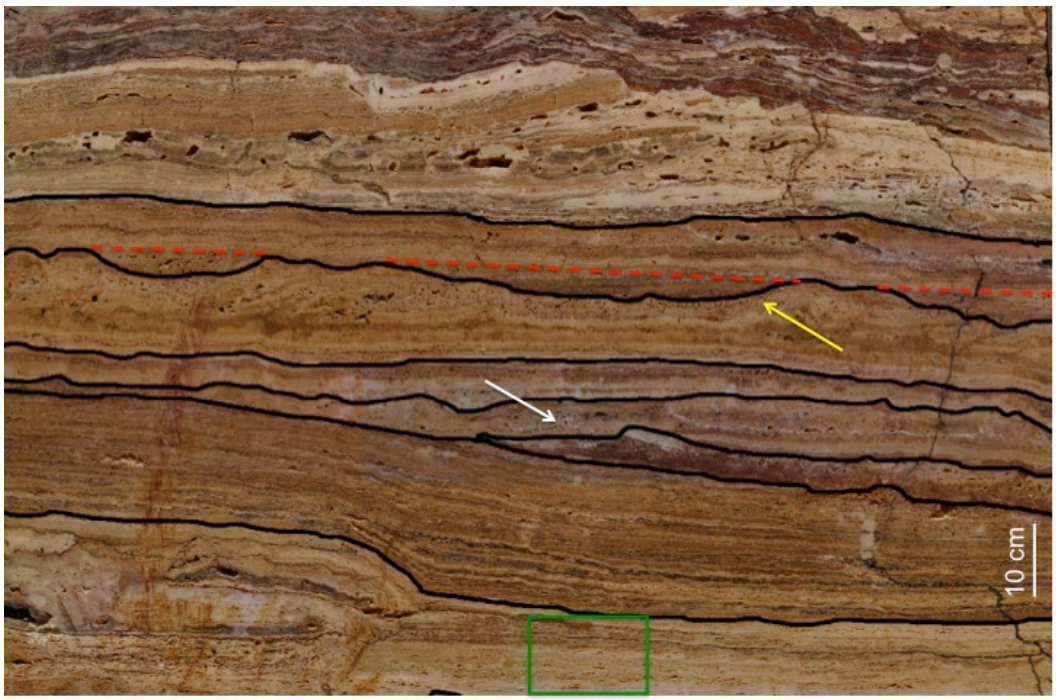

Figure 52: Gold Quarry Wall B showing a sloping mound morphology. The layers are dipping between 4 and 10 degrees. Multiple features can be observed, including microterraces (green box at the bottom indicates the location of Figure 53), a breccia layer pinching out (white arrow), and an undulating sloping layer (yellow arrow). The tops of the depression-fills in the undulating layer are highlighted with a red dashed line.

Figure 53: Image of Gold Quarry Wall B showing microterraces on a sloping mound layer. The structure of the microterraces is traced with black dashed lines.

4.2 Conglomerates

The presence of conglomerates interbedded within the travertine indicates cyclic changes that result from paleo-environmental variance. A significant and prolonged increase in rainfall can result in the decrease of calcium carbonate saturation within the water, resulting in a hiatus in travertine precipitation. The increase in rainfall could also result in erosion of the travertine due to an increase in the erosional capacity of the fluid.

4.2.1 Gold Quarry Conglomerates

In the Gold Quarry, multiple layers of breccias are interbedded within the travertine deposits. The breccias have a fine-grained, red matrix and are composed of locally ripped-up travertine clasts. The breccia layers range in thickness from less than 0.1 m to 1.6 m and are scattered throughout the entire exposed section within the quarry.

The thickest exposed breccia layer is seen on walls D and E and is 1.6 m thick. The boundary between the breccia and the underlying travertine is obviously erosional, as many of the travertine layers have been truncated and large clasts from the travertine have been ripped-up and incorporated into the breccia (Figure 10). The breccia has a red matrix and in some areas appears matrix-supported and elsewhere it is clast-supported. The clasts within the breccia range in size from 1 mm to 42 cm and are sub-angular to angular. They are composed of locally derived travertine and vein material and range from very

porous, shrubby travertine to densely crystalline vein-fill. The presence of vein-fill clasts within the breccia indicates that the veins formed prior to breccia formation. Another episode of vein formation occurred after the breccia was deposited. This is supported by the evidence of veins cutting through the matrix and clasts of the breccia in multiple orientations. This breccia is dipping at approximately 19 degrees from horizontal and is buried too deeply to be exposed on the other walls in the quarry.

Smaller breccia layers have been identified on walls A, B, C, and F in the lowest exposed 3 meters. One particular breccia can be identified on all four of the above-mentioned walls. Due to the three-dimensional nature of the breccia tongue, it can be seen pinching out at various points along the walls (Figure 54). The breccia ranges up to 0.2 m thick (not taking into account the areas where it is pinching out). It is very similar to the large breccia seen on walls D and E, with a red matrix and locally derived travertine clasts. The clasts range in size from 1 millimeter to 7 cm and are sub-angular to angular. Higher in the stratigraphic section, many additional breccia deposits are present. Detailed characterization of these deposits was not possible due to their high location on the quarry wall, but they generally appear to resemble the other breccia in this quarry.

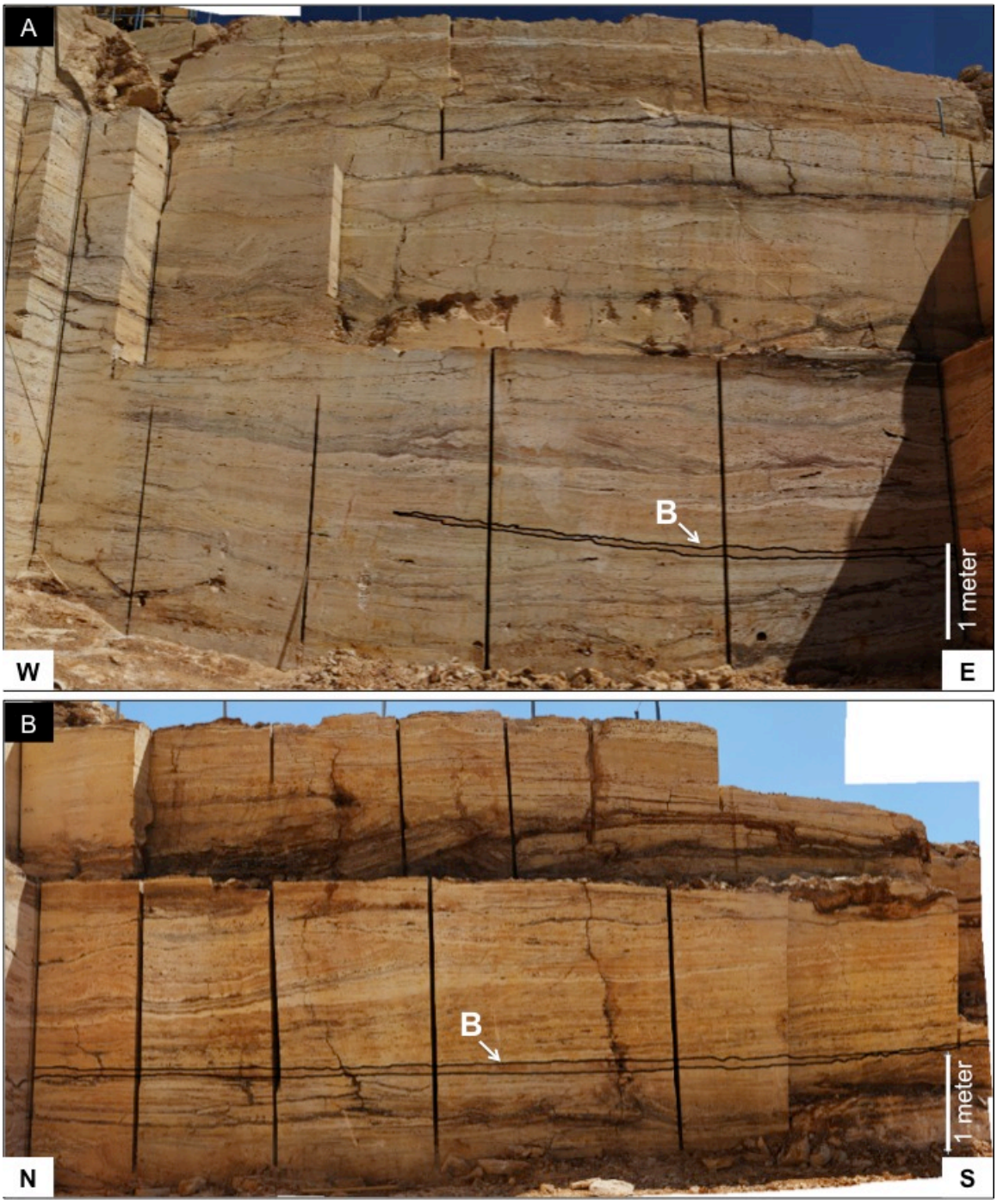

Figure 54: (A) Panoramic image of Gold Quarry- Wall B. The breccia layer is highlighted in black and marked with a "B". The layer can be seen pinching out halfway across the wall. (B) Panoramic image of Gold Quarry- Wall C. The same breccia layer is highlighted in black and marked with a "B". It is continuous across the wall and can be seen dipping slightly to the north.

4.2.2 Ivory Quarry Conglomerates

The Ivory Quarry has fewer breccias interbedded within the main travertine deposit than is seen in the Gold Quarry. The southern walls in the Ivory Quarry (Walls B and C) have a breccia unit at the base of the exposed section. This unit is possibly present under the other walls, but is buried too deep to be visible. The true thickness is unknown, as it is at the base of the unit is covered, but approximately 0.15 m is exposed. It has a cream-colored matrix and is composed of travertine clasts. The clasts range in size from 1 millimeter to 8 cm and are sub-angular to angular.

The main travertine sequence is capped with a thick conglomerate, which is present throughout the entire quarry (Figure 55). The thickness of the conglomerate ranges from 1.9 to 2.7 m, but as it is at the top of the quarry walls, it was likely thicker at the time of deposition and has since been partly eroded. The conglomerate has an abundance of calcium carbonate veins cutting through it, and this likely adds to its overall thickness. Starting on wall E2 and continuing onto wall E3, there is a 0.6 m thick travertine layer within the conglomerate. The thickness of this travertine layer has been subtracted from the thickness of the conglomerate on these walls.

The matrix of the large conglomerate is red, very similar to the breccias in the Gold Quarry. The clasts are composed of both locally and regionally derived material. The regionally derived clasts are from the Madera Limestone and are black in color, sub-rounded to rounded, and range from spherical to elongate.

They range in size from 1 millimeter to 6 cm. The locally derived clasts are travertine and are angular to sub-rounded. The average size range for the travertine clasts is from 1 millimeter to 8 cm, but there is an occasional large rip-up clast that is up to 40 cm. The elongate clasts on walls E2 and E3 exhibit imbrication in which the long axis points towards the interpreted downstream direction (Figure 56). The paleo-flow direction indicated by the imbricated clasts matches the northeastern direction indicated by features in the travertine below the conglomerate.

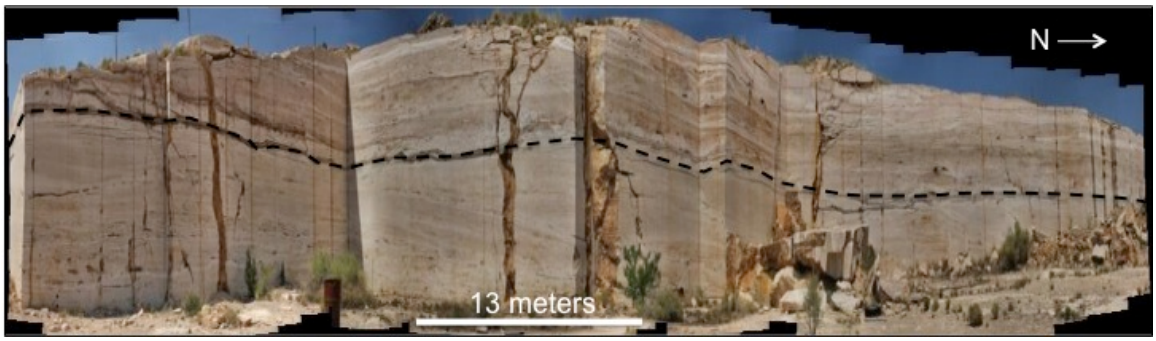

Figure 55: Vertically exaggerated panoramic of the Ivory Quarry. Black dashed lines represent the contact of the conglomerate above and the travertine below. Carbonate veins and minor amounts of travertine are also present above the black dashed line. The conglomerate is laterally continuous across the entire Ivory Quarry.

Figure 56: Imbricated conglomerate clasts on Ivory Quarry- Wall E2. They are composed of both locally and regionally derived material.

4.3 Veins

Fractures are a common occurrence in areas that are undergoing tectonic deformation. The abundance of fractures within an area generally increases with proximity to a fault plane, especially along the hanging wall fault block (Brogi and Capezzuoli, 2009). When comparing the locations of the quarries within the study area to a local fault map (Kelley and Wood, 1946), this finding appears to hold true (Figure 57). The Vista Grande Quarry is located on the hanging wall of a fault, immediately adjacent to the fault plane. The travertine within this quarry is exclusively carbonate vein-fill and is composed of multiple generations of veins cutting across each other at different orientations (Figure 8). The Pink Quarry has primary travertine visible, but it has been completely distorted and displaced by abundant fractures and vein-fill. The original map by Kelley and Wood (1946) did not show a fault in close proximity to the Pink Quarry, but by extending the “C” fault along strike by 350 meters, the location of the Pink Quarry would only be 150 meters from the fault plane (Figure 57). This would account for the abundance of fractures and vein-fill within the Pink Quarry. The Gold Quarry is approximately 300 meters from the fault and exhibits less fractures and vein-fill than the Pink Quarry, but more than the Ivory Quarry which is located 500 meters from the fault.

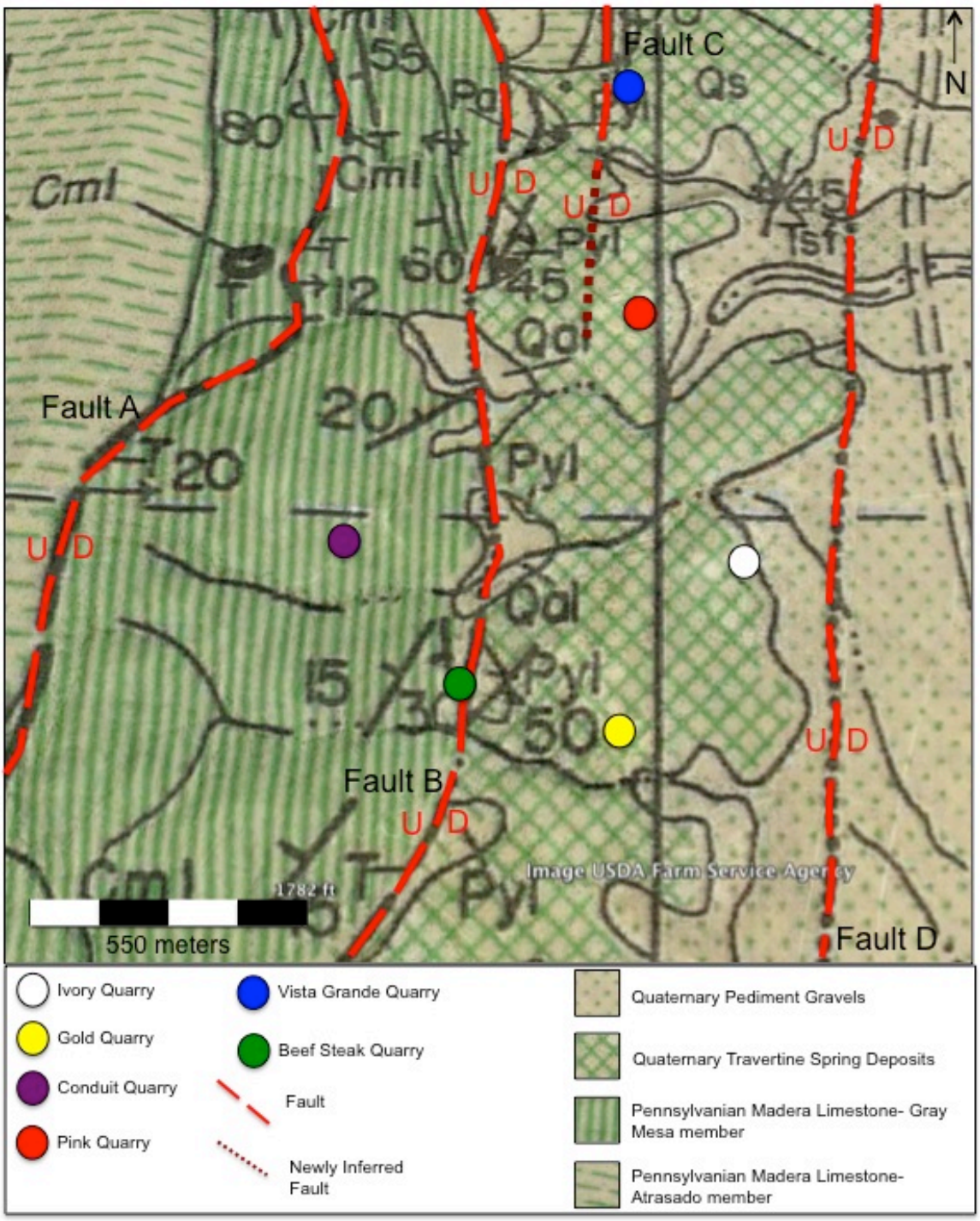

Figure 57: Geologic map modified from Kelley and Wood (1946). Shows location of quarries with respect to the faults mapped within the area.

4.3.1 Gold Quarry Veins

The Gold Quarry has undergone extensive fracturing, which resulted in abundant cross-cutting vein-fill. Two distinct types of veins are present, Type 1 and Type 2. The Type 1 vein-fill are cream and grey in color and they commonly form around a fracture in the center of the vein. The fracture is then surrounded by a grey, bulbous, crystalline layer, which is then surrounded by a less noticeably crystalline, cream-colored layer. The grey layer is either newly formed crystalline material or is more extensively altered travertine than the cream layer. This interpretation is based on its appearance (coarsely crystalline and lacking any remnants of the surrounding travertine) and its proximity to the fracture, which resulted in direct contact with the hydrothermal fluids that passed through the fracture.

Multiple generations of Type 1 fractures have been formed. This is indicated by the observation that some of the vein-fill material has been truncated by, and redeposited as clasts within the breccia layers. This indicates that those veins formed prior to breccia formation. Alternatively, some of the veins cut across the breccia layers, indicating that they formed after breccia formation (Figure 58). The vein-fill of the Type 1 veins is formed by both the recrystallization of the surrounding travertine and the precipitation of new carbonate material within the fracture. The growth of new carbonate material has resulted in the shifting and rotating of some of the travertine layers (Figure 59).

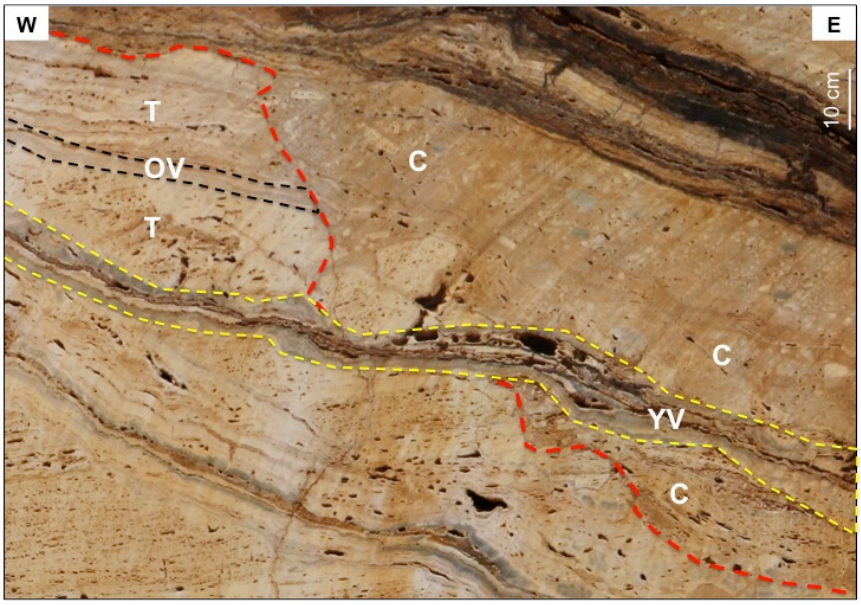

Figure 58: Image of Gold Quarry- Wall D. The travertine (T) and older generations of vein-fill (OV) have been eroded and incorporated as clasts within the conglomerate (C). A younger generation of vein formation (YV) occurred after the conglomerate was deposited, indicated by the veins cutting the conglomerate. The red dashed line indicates the erosional contact between the travertine and the conglomerate. The black dashed line highlights a vein-fill that has been eroded. The yellow dashed line indicates a younger generation of vein-fill that cuts the conglomerate.

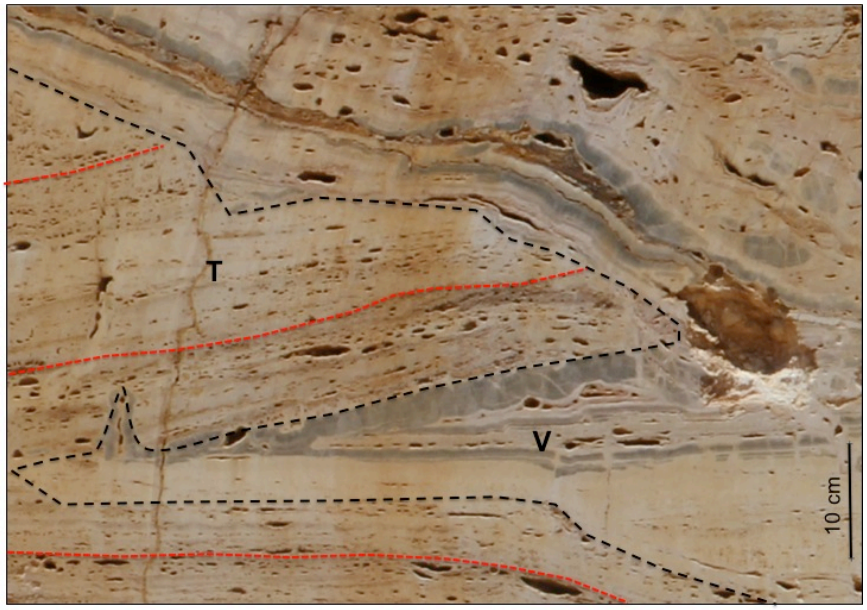

Figure 59: Gold Quarry- Wall D. Distinct travertine layer (marked with "T") rotated upward due to vein growth beneath it (marked with "V"). The dashed black line marks the boundary of the vein-fill and the dashed red lines mark layers within the travertine.

The Type 2 veins are dark red in color and can be separated into two groups: main veins and connecting veins. The main veins are large, laterally continuous veins that are formed along zones of weakness. These veins can be seen on all of the walls in the quarry and follow depositional dip. The connecting veins are smaller veins that formed perpendicular to the main veins, cutting up section through the travertine. These veins connect multiple layers of main veins with each other. The connecting veins are formed due to the build up of pressure in the main vein, forcing the fluids to find another path to flow. On wall F, five main veins can be identified. The veins are evenly distributed throughout the stratigraphic section, occurring approximately 1 to 1.5 meters vertically apart (Figure 60). The veins commonly form at or near the base of breccia layers, as these are zones of weakness, but not all breccia layers are associated with the red veins (Figure 61). The Type 2 veins are very soft and are used by the quarry operator as a floor for the travertine slabs.

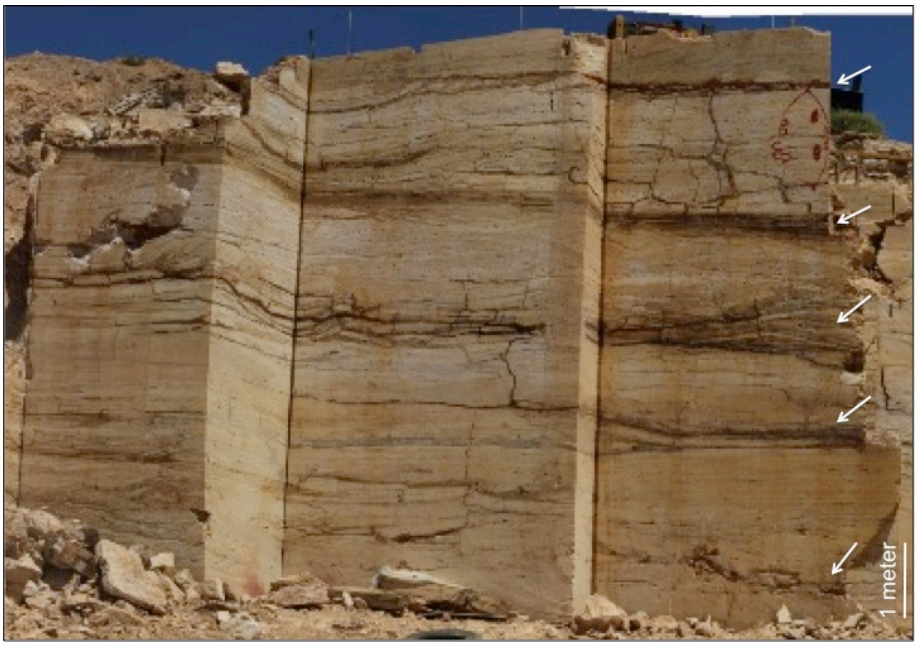

Figure 60: Gold Quarry-Wall F showing the consistent spacing of the red veins. The white arrows point to the vein locations.

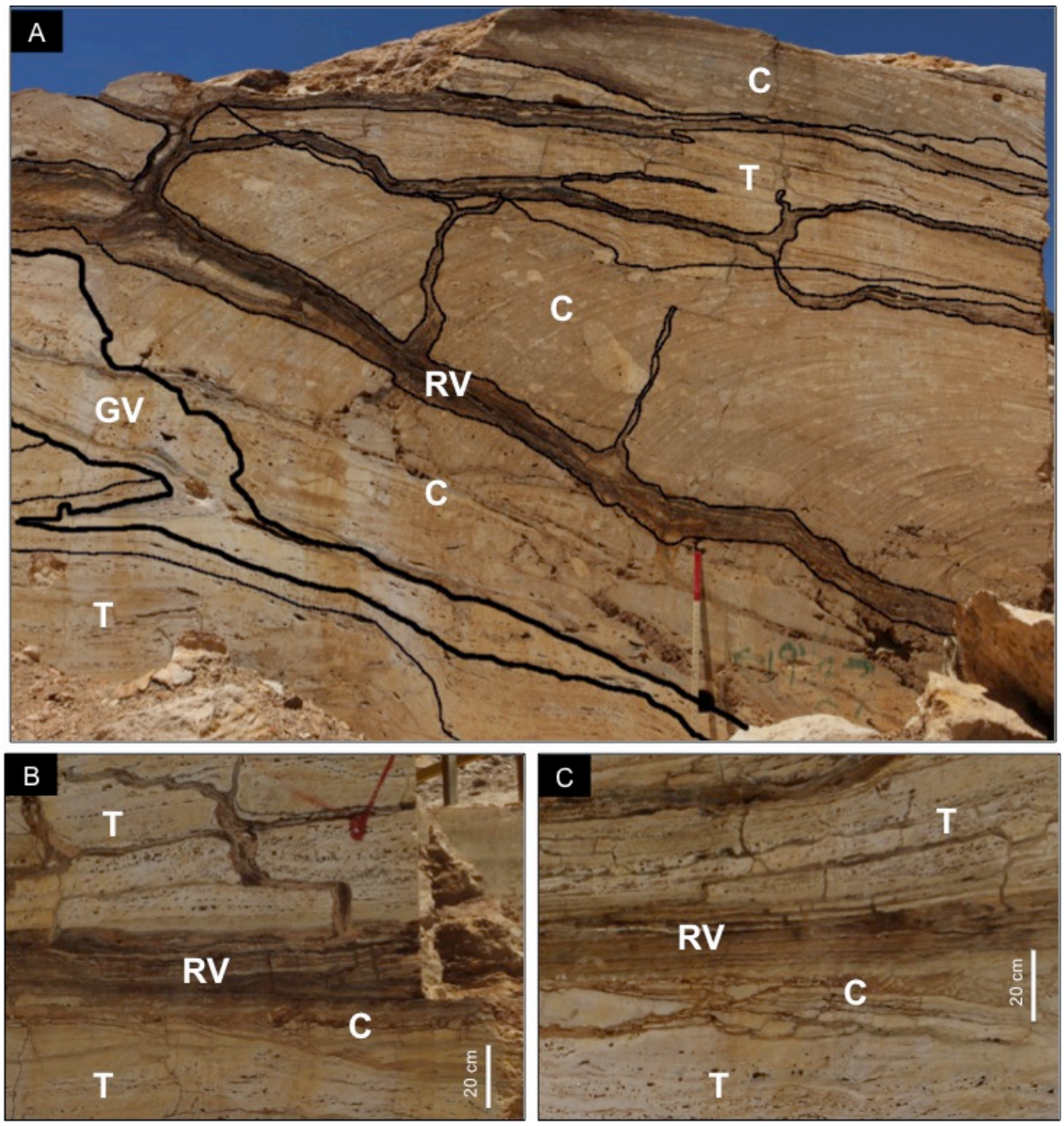

Figure 61: (A) Gold Quarry- Wall D shows a red vein ("RV") that formed in a conglomerate layer ("C"). It has both distinct main veins and connecting veins. The travertine ("T") is separated from the conglomerate by a grey vein (GV). Meter stick for scale with the top 20 cm colored in red. (B-C) Gold Quarry- Wall F has main red veins forming along thin conglomerate layers and connecting veins cutting across the travertine.

4.3.2 Ivory Quarry Veins

The Ivory Quarry has undergone moderate fracturing, but the fractures are less abundant than in the Gold Quarry. On walls A, B, and C, the bottom 1.5 meters of exposure has been extensively cut by veins (Figure 62). The veins are a mixture of cream- and grey-colored zones, with the grey colored areas being significantly more crystalline and indicating significantly more alteration. Many of the veins have extensive vuggy porosity. The veins display two main orientations; large veins that formed along depositional dip, following specific layers and occasional cutting across those layers and smaller veins that formed perpendicular to depositional dip and connected to the large veins. Above this interval, there is a 1.5 to 2.5 m (depending on the wall) zone of travertine that exhibits little cross-cutting by veins.

At the top of the travertine there is a large zone cut by many veins that extends across the entire quarry. These veins formed at the erosional surface between the travertine and the overlying conglomerate, as this surface is a weak zone compared to the surrounding material (Figure 63). The veins in this zone have a variety of colors, ranging from cream to red to grey to black. Veins can be seen truncating and destroying each other, indicating that this zone has undergone multiple generations of alteration. The conglomerate above the erosional surface has also been extensively cut by veins.

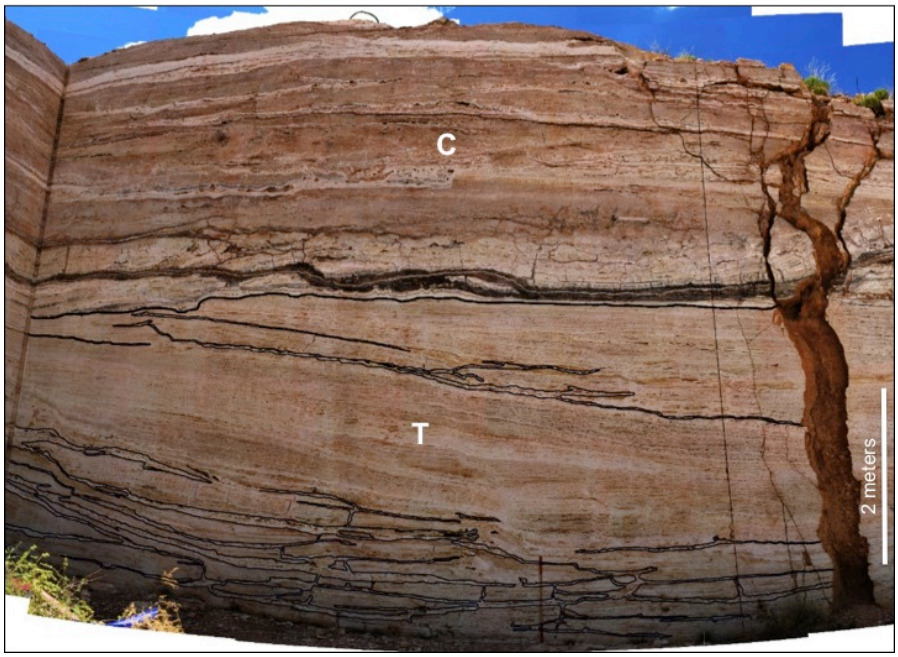

Figure 62: Ivory Quarry- Wall C. The bottom portion of the exposed section has abundant veins breaking up the travertine. The rest of the travertine does not exhibit many veins, until the large vein separating the travertine ("T") and the conglomerate ("C") near the top of the accumulation. The veins are outlined in black.

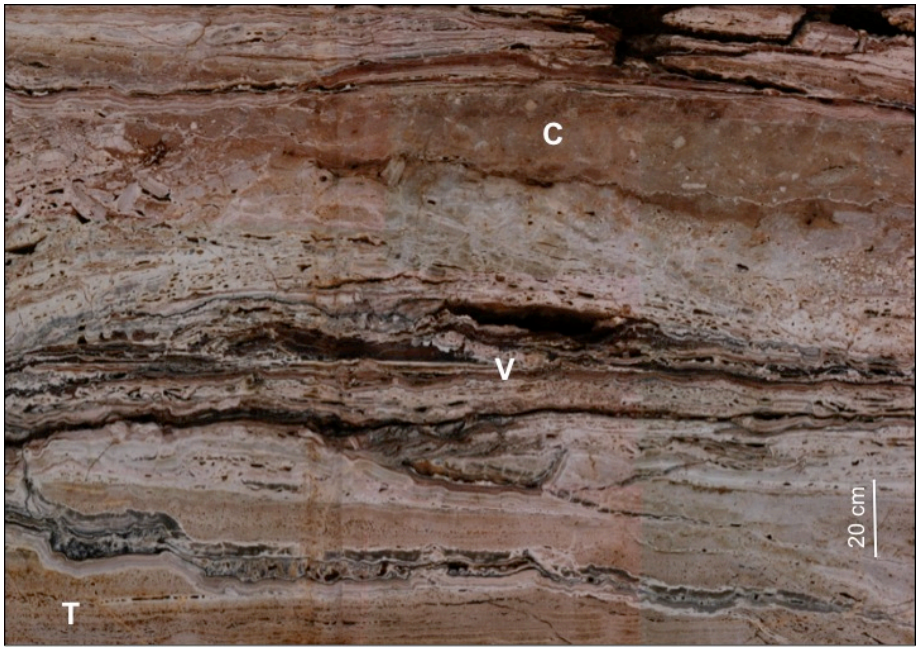

Figure 63: Ivory Quarry- Wall E2 shows a thick zone with many veins ("V") at the contact between the conglomerate ("C") above and travertine ("T") below. The vein zone is composed of multiple generations of veins that cut across each other.

Some of the veins have cut down from the erosional surface, through the top of the travertine and follow along individual layers within the travertine. Occasionally, a vein will cut up or down through the section and begin to follow a new layer. In these areas, it is possible to see that the veins have created new carbonate material instead of just recrystallizing the surrounding travertine. The creation of new material has resulted in the upward shift of blocks of travertine above the vein (Figure 64). The ability of the vein to grow in place and shift blocks of travertine around indicates that the veins formed before abundant overburden.

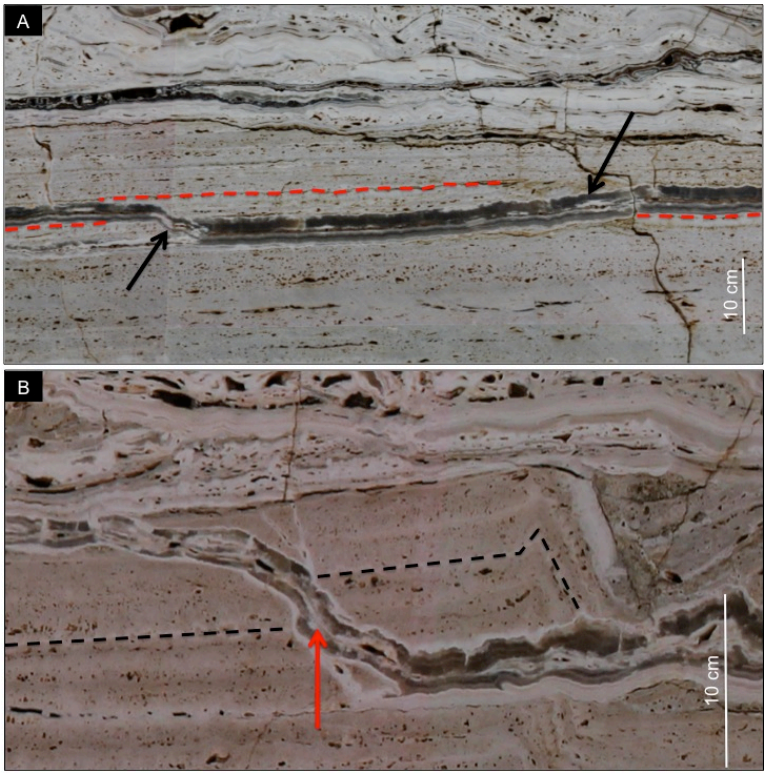

Figure 64: (A) Ivory Quarry- Wall B shows a vein (Black arrows) that is cutting across a distinct travertine layer, indicated by a red dashed line. Precipitation of crystals in the fracture resulted in the upward displacement of the travertine. (B) Ivory Quarry- Wall E3 shows a fragment of travertine that has been upwardly displaced by a vein. The black dashed line indicates an individual layer that has been offset by vein-fill material (red arrow)

CHAPTER 5: SUMMARY AND CONCLUSIONS

5.1 Gold Quarry

The Gold Quarry is located on the hanging wall of a normal fault, approximately 300 meters to the east of the fault plane. It is composed of interbedded primary travertine and conglomerate layers that indicate an east-northeast flow direction. The sloping nature of the paleo-topography resulted in a travertine morphology that was transitional between sloping mound and terrace mound.

The terrace mound morphology is only present within the lowest visible interval within the Gold Quarry. It is likely laterally extensive beneath the entire quarry, but has not been exposed. The terrace mound morphology has alternating rimstone dams and pools. The rimstone dams show a maximum vertical offset of 50 cm and are composed of thin layers of ray crystal crusts that can be traced along the height of the rim. These layers can be traced into the pools and display an abrupt change in characteristics. The pool layers are 0.1 to 5 cm thick and display a variety of constituents such as rafts, pisoids, shrubs, and foam rock.

A sloping mound morphology is abundant within the Gold Quarry. The layers exhibit a thickness of 0.1 to 3 cm and are dipping between 5 and 12 degrees. The sloping mound layers have poorly developed microterraces and occasionally display an undulating habit. The microterrace pools are composed

of rafts, pisoids, and ray crystal fans, whereas the smoothly sloping layers are composed of feather dendrites. Many layers are laterally continuous across the quarry, but some of the layers pinch out.

5.2 Ivory Quarry

The Ivory Quarry is located on the hanging wall of a normal fault, approximately 500 meters to the east of the fault plane. It is composed of interbedded primary travertine and conglomerate layers that indicate a northeast flow direction. The travertine transitions between sloping mound morphology and terrace mound morphology.

The terrace mound morphology is composed of distinct pools and rimstone dams. The pools are composed of horizontal 0.5 to 5 cm layers. A sequence was identified within some of the pool layers, and consists of a dense peloidal zone, followed by bacterial shrubs, which are topped with rafts and pisoids. Foam rock layers were also identified within the pools and were found to occur in different pools at different stratigraphic positions. This indicates that a vent was present in the area and through time. The rimstone dams within the terrace mound morphology are composed of vertically oriented layers of ray crystal crusts. They commonly aggrade, forming thick rimstone dam deposits composed of hundreds of individual layers stacked vertically. Eventually, the rimstone dam decreased in height to the point of non-existence, resulting in a transition to a sloping mound morphology.

The sloping mound morphology is composed of layers that dip between 8 and 19 degrees. Abundant microterraces characterize this morphology, which exhibit constituents similar to the larger-scale features. The microterrace pools do not contain bacterial shrubs and instead contain ray crystal fans. The change in constituents can be attributed to the increased fluid flow along the slope, which favors abiotic precipitation. The location of the rimstone dams rapidly changes along the sloping mound layers and appears to be heavily dependent on the dip of the layer.

5.3 Constituents

The Gold and Ivory quarries are composed of a wide variety of constituents. The rafts within the quarries vary in length but have a fairly consistent thickness. As the rafts break up due to disturbances, the variations in length are expected. The consistent thickness is also expected as a raft can only reach a certain thickness before they sink. The rafts are more abundant within the Ivory Quarry, as it has significantly more terrace pools. The vertical tubes associated with foam rock are elongate in shape and are highly variable in length. They can form in either densely packed layers, or as isolated features. The outline of the bubbles varies significantly in appearance and ranges from thin, concentric layers, to composed of micritic clumps with no obvious layers. Foam rock layers form in terrace pools and are bounded by micrite layers. They are commonly surrounded by microbial mats.

Small coated grains have been identified with a single calcite crystal nucleus and concentric cortices. They form near rimstone dams, as these are sites of consistent agitation. Pisoids range in size from 1 mm to 3 cm and can have a round to elongate shape depending on their nuclei. The cortices surrounding the pisoids are commonly irregular, which can be attributed to either their large size, or the influence of bacteria on their development. Spherulites are small and have fibro-radiating crystals coming from a bacterially derived nucleus. They have been identified among a variety of other constituents, including coated grains and ray crystal fans.

Bacterial shrubs form layers within terrace pools. They are composed of outward-branching micritic clumps that have abundant microporosity due to the influence of bacteria on their formation. Feather dendrites form on smooth, sloping mound surfaces due to the rapid fluid flow down the slope. They form as long crystals with small branches splaying off a central stalk. Ray crystal fans are commonly found in microterrace pools. They have a teardrop shape composed of radiating calcite crystals. As the slope increase, the ray crystal fans will transition into ray crystal crusts. Ray crystal clusters are amalgamations of ray crystal fans and commonly form on other constituents.

5.4 Porosity

Multiple types of pores are present within the Gold and Ivory quarries, including both interparticle and intraparticle. Intraparticle pores is present within the nuclei of pisoids and the leaves of bacterial shrubs. Layers of rafts, shrubs,

and pisoids all have abundant interparticle pores, and consequently have good horizontal permeability. As the travertine layers are well laminated, the permeability is expected to be anisotropic. The presence of fractures cutting across the travertine layers increases the vertical permeability. Porosity varies considerably depending on the amount of cementation that has occurred. The porosity measured within the thin sections from the Gold and Ivory quarries indicated a range from 0.8 percent to 11.82 percent. Although this percentage is likely low due to a bias of choosing less porous samples.

5.5 Gold Quarry Conglomerates and Veins

The conglomerates within the Gold Quarry range in thickness from 0.1 to 1.6 meters. They have a bright red matrix and clasts that are composed of locally derived travertine and Type 1 vein-fill. The thicker breccia layers have clasts that range in size from 1 mm to 42 cm, whereas the thinner breccia layers have clasts that range in size from 1 mm to 7 cm. The breccia layers are laterally continuous across the Gold Quarry and likely indicate changes in the paleo-environmental conditions, such as an increase in rainfall that resulted in erosion of the travertine due to an increase in the erosional capacity of the fluid.

Abundant fractures and vein-fill are present within the Gold Quarry. Two types of veins have been identified, Type 1 and Type 2. The Type 1 vein-fills are filled with a cream to grey calcite and formed along fractures. These veins have formed in multiple generations, as noted by their presence as clasts within breccias and cutting across breccia layers. The Type 1 veins likely formed soon

after travertine deposition, as they have shifted and rotated blocks of travertine. The Type 2 vein-fills are dark red and form along breccia layers. They are laterally continuous throughout the quarry and are evenly spaced throughout the stratigraphic section.

5.6 Ivory Quarry Conglomerates and Veins

The Ivory Quarry contains fewer conglomerates than are present within the Gold Quarry. It has thin breccia layers scattered throughout the exposed travertine section and a 2.7-meter-thick conglomerate at the top. The conglomerate at the top of the travertine has a red matrix and clasts that are composed of both regionally and locally derived material. The regionally derived clasts are smaller and more rounded than the locally derived clasts. The vein-fills within the Ivory Quarry are abundant in the travertine at the base of the exposed section and at the erosional contact between the travertine and the conglomerate. They formed in multiple generations throughout the development of the deposit and likely occurred before abundant overburden emplacement.

5.7 Final Words

This study aimed to provide detailed information regarding both the large-scale and micro-scale features within a travertine deposit. The knowledge gained from the Gold and Ivory quarries can be used in conjunction with other studies to provide a model that will be beneficial in areas where data is limited, such as in the subsurface. The importance of continued research on travertine deposits is

crucial from both an academic and economic perspective, and only with this continued research will the understanding of these intricate systems reach a level similar to that of other better-studied geologic features.

REFERENCES

Austin, G.S., and Barker, J.M., 1990, Commercial travertine in New Mexico: New Mexico Geology, v. 12, p. 49-58.

Baldridge, W.S, Damon, P.E., Shafiqullah, M., and Bridwell, R.J., 1980, Evolution of the central Rio Grande Rift, New Mexico: new potassium-argon ages: Earth and Planetary Science Letters, v. 51, p. 309-321.

Baldridge, W.S., Perry, F.V, and Shafiqullah, M., 1987, Late Cenozoic volcanism of the southeastern Colorado Plateau: I. Volcanic geology of the Lucero area, New Mexico: Geological Society of America Bulletin, v. 99, p. 463-470.

Baldridge, W.S., Perry, F.V., Vaniman, D.T., Nealey, L.D., Leavy, B.D., Laughlin, A.W., Kyle, P., Bartov, Y., Steinitz, G., and Gladney, E.S., 1991, Middle to late Cenozoic magmatism of the southeastern Colorado Plateau and central Rio Grande rift (New Mexico and Arizona, U.S.A.): a model for continental rifting: Tectonophysics, v. 197, p. 327-354.

Barker, J.M., 1986, Travertine: New Mexico Bureau of Mines and Mineral Resources, Open-file Report 229, p. 94-100.

Brogi, A., and Capezzuoli, E., 2009, Travertine deposition and faulting: the fault-related travertine fissure-ridge at Terme S. Giovanni, Rapolano Terme (Italy): International Journal of Earth Sciences, v. 98, p. 931-947.

Buczynski, C., and Chafetz, H.S., 1991, Habit of bacterially induced precipitates of calcium carbonate and the influence of medium viscosity on mineralogy: Journal of Sedimentary Petrology, v. 61, no. 2, p. 226-233.

Chafetz, H.S., in press, Porosity in bacterially induced carbonates: Focus on micropores: AAPG Bulletin

Chafetz, H.S., and Folk, R.L., 1984, Travertines: depositional morphology and the bacterially constructed constituents: Journal of Sedimentary Petrology, v. 54, p. 289-316.

Chafetz, H.S., and Guidry, S.A., 1999, Bacterial shrubs, crystal shrubs, and ray-crystals shrubs: bacterial vs. abiotic precipitation: Sedimentary Geology, v. 126, p. 57-74.

Chafetz, H.S., and Lawrence, J.R., 1994, Stable isotopic variability within modern travertines: Geographie physique et Quaternaire, v. 48, p. 257-273.

Chafetz, H.S., Rush, P.F., and Utech, N.M., 1991, Microenvironmental controls on mineralogy and habit of CaCO3 precipitates: an example from an active travertine system: Sedimentology, v. 38, p. 107-126.

Chen, J., Zhang, D.D., Wang, S., Xiao, T., and Ronggui, H., 2004, Factors controlling tufa deposition in natural waters at waterfall sites: Sedimentary Geology, v. 166, p. 353-366.

Florsheim, J.L., Ustin, S.L., Tang, Y., Di, B., Huang, C., Qiao, X., Peng, H.,

Zhang, M., and Cai, Y., 2013, Basin-scale and travertine dam-scale controls on fluvial travertine, Jiuzhaigou, southwestern China: Geomorphology, v. 180-181, p. 267-280

Folk, R.L., Chafetz, H.S., and Tiezzi, P.A., 1985, Bizarre forms of depositional and diagenetic calcite in hot-spring travertines, central Italy: The Society of Economic Paleontologists and Mineralogists, Carbonate Cements (SP36), p. 349-369.

Folk, R.L., 1993, SEM imaging of bacteria and nannobacteria in carbonate sediments and rocks: Journal of Sedimentary Petrology, v. 63, no. 5, p. 990-999.

Folk, R.L., 1999, Nannobacteria and the precipitation of carbonate in unusual environments: Sedimentary Geology, v. 126, p. 47-55.

Golombek, M.P., McGill, G.E., and Brown, L., 1983, Tectonic and geologic evolution of the Espanola basin, Rio Grande Rift: structure, rate of the extension, and relation to the state of stress in the western United States: Tectonophysics, v. 94, p. 483-507.

Google Earth, www.googleearth.com

Guo, L., and Riding, R., 1992, Aragonite laminae in hot water travertine crusts, Rapolano Terme, Italy: Sedimentology, v. 39, p. 1067-1079.

Guo, L., and Riding, R., 1993, Origin and diagenesis of quaternary travertine

shrub fabrics, Rapolano Terme, central Italy: Sedimentology, v. 41, p. 499-520.

Guo, L., and Riding, R., 1999, Rapid facies changes in Holocene fissure ridge hot spring travertines, Rapolano Terme, Italy: Sedimentology, v. 46, p. 1145-1158.

Guo, X., and Chafetz, H.S., 2012, Large tufa mounds, Searles Lake, California: Sedimentology, v. 59, p. 1509-1535.

Hammer, Ø., Dysthe, D.K., and Jamtveit, B., 2010, Travertine terracing: patterns and mechanisms: Geological Society of London Special Publications: Tufas and Speleothems: Unravelling the Microbial and Physical Controls, v. 336, p. 345-355.

Hancock, P.L., Chalmers, R.M.L., Altunel, and E., Cakir, Z., 1999, Travitonics: using travertines in active fault studies, Journal of Structural Geology, v. 21, p. 903-916.

Hermance, J.F. and Neumann, G.A., 1991, The Rio Grande rift: new electromagnetic constraints on the Socorro magma body: Physics of the Earth and Planetary Interiors, v. 66, p. 101-117.

Ingersoll, R.V., 2001, Structural and stratigraphic evolution of the Rio Grande Rift, northern New Mexico and southern Colorado: International Geology Review, v. 43, p. 867-891.

Jones, B., and Renaut, R.W., 1994, Crystal fabrics and microbiota in large pisoliths from Laguna Pastos Grandes, Bolivia: Sedimentology, v. 41, p. 1171-1202.

Jones, B., and Renaut, R.W., 1995, Noncrystallographic calcite dendrites from hot-spring deposits at Lake Bogoria, Kenya: Journal of Sedimentary Research, v. A65, no. 1, p., 154-169.

Keller, G.R., Khan, M.A, Morgan, P., Wendlandt, R.F, Baldridge, W.S., Olsen, K.H., Prodehl, C., and Braile, L.W., 1991, A comparative study of the Rio Grande and Kenya rifts: Tectonophysics, v. 197, p. 355-371.

Kelley, V.C., and Wood, G.H., 1946, Geology of the Lucero uplift, Valencia, Socorro, and Bernalillo Counties, New Mexico: U.S. Geologic Survey, Oil and Gas Investigations, Preliminary Map 47, scale 1:63,360.

Kil, Y., and Wendlandt, R.F., 2007, Depleted and enriched mantle processes under the Rio Grande rift: spinel peridotite xenoliths: Contrib. Mineral Petrol, v. 154, p. 135-151.

Love, K.M., and Chafetz, H.S., 1988, Diagenesis of laminated travertine crusts, Arbuckle Mountains, Oklahoma: Journal of Sedimentary Petrology, v. 58, p. 441-445.

McLemore, V.T., Broadhead, R.F., Barker, J.M., Austin, G.S., Klein, K., Brown, K.B., Murray, D., Bowie, M.R., and Hingtgen, J.S., 1986, A preliminary mineral-resource potential of Valencia County, northwestern New Mexico:

New Mexico Bureau of Mines and Mineral Resources, Open File Report 229.

Morgan. P., and Golombek, M.P., 1984, Factors controlling the phases and styles of extension in the Northern Rio Grande Rift: New Mexico Geological Society Guidebook, 35th Field Conference, p. 13-19.

Morgan, P., Seager, W.R., and Golombek, M.P., 1986, Cenozoic thermal, mechanical, and tectonic evolution of the Rio Grande Rift: Journal of Geophysical Research, v. 91, p. 6263-6276.

Newell, D.L., Crossey, L.J., Karlstrom, K.E., and Fischer, T.P., 2005, Continental-scale links between the mantle and groundwater systems of the western United States: evidence from travertine springs and regional He isotope data: GSA Today, v. 15, p. 4-10.

Pedley, H.M., 1990, Classification and environmental models of cool freshwater tufas: Sedimentary Geology, v. 68, p. 143-154.

Pentecost, A., 1990, The formation of travertine shrubs: Mammoth Hot Springs, Wyoming: Geological Magazine, v. 127, no. 2, p. 159-168.

Pentecost, A., 1995, The Quaternary travertine deposits of Europe and Asia Minor: Quaternary Science Reviews, v. 14, p. 1005-1028.

Pentecost, A., 2005, Travertine: Springer-Verlag, Berlin

Rainey, D.K., and Jones, B., 2009, Abiotic versus biotic controls on the

development of the Fairmont Hot Springs carbonate deposits, British Columbia, Canada: Sedimentology, v. 56, p. 1832-1857.

Riding, R., 2000, Microbial carbonates: the geological record of calcified bacterial-algal mats and biofilms: Sedimentology, v. 47, p. 179-214.

Slack, P.D., Davis, P.M., Baldridge, W.S., Olsen, K.H., Glahn, A., Achauer, U., and Spence, W., 1996, The upper mantle structure of the central Rio Grande rift region form teleseismic P and S wave travel time delays and attenuation: Journal of Geophysical Research, v. 101, p. 16003-16023.

Taylor, P.M., and Chafetz, H.S., 2004, Floating rafts of calcite crystals in cave pools, central Texas, U.S.A.: Crystal habit vs. saturation state: Journal of Sedimentary Research, v. 74, no. 3, p. 328-341.

Tucker, M. E., and Wright. V. P., 1990, Carbonate sedimentology: Blackwell Scientific Publications, 492 p.

Verrecchia, E.P., Freytet, P., Verrecchia, K.E., and Dumont, J.L., 1995, Spherulites in calcrete laminar crusts: biogenic CaCO3 precipitation as a major contributor to crust formation: Journal of Sedimentary Research, v. A65, no. 4, p. 690-700.

Wilson, D., Aster, R., West, M., Ni, J., Grand, S., Goa, W., Baldridge, W.S., Semken, S., and Patel, P., 2005, Lithospheric structure of the Rio Grande Rift: Nature, v. 433, p. 851-855.

Wright, H.E., 1946, Tertiary and Quaternary geology of the lower Rio Puerco Area, New Mexico: Bulletin of the Geological Society of America, v. 57, p. 383-456.

Zhang, D.D., Zhang, Y., Zhu, A., and Cheng, X., 2001, Physical mechanisms of river waterfall tufa (travertine) formation: Journal of Sedimentary Research, v. 71, p. 205-216.

APPENDIX I: GOLD QUARRY MEASURED SECTIONS

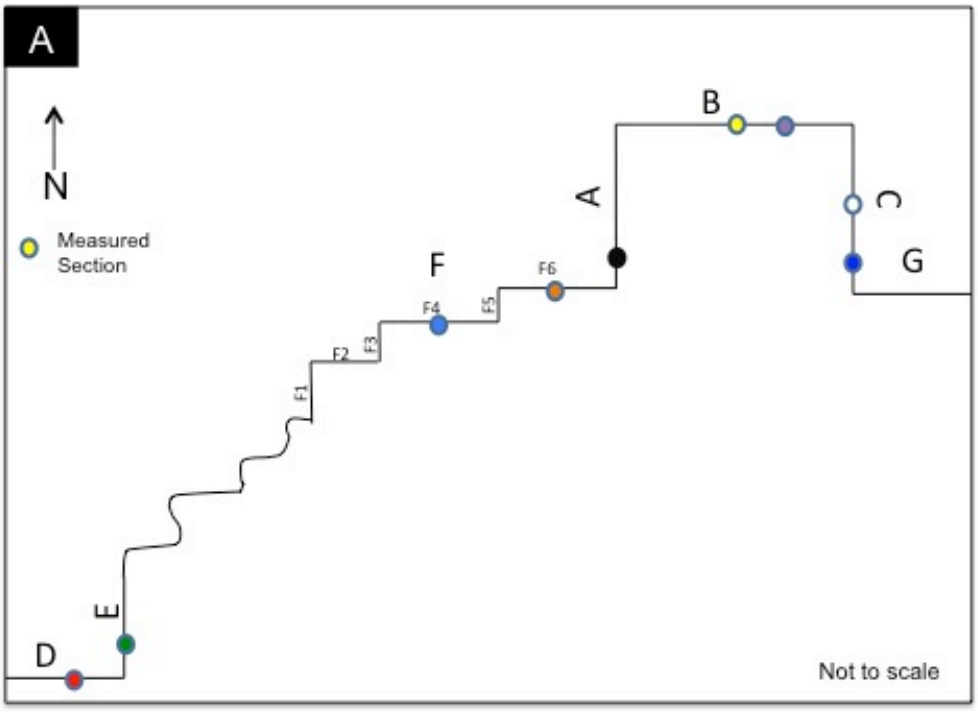

Gold Quarry Wall D- Section 2
Gold Quarry Wall F- Block 6
Gold Quarry Wall B- Block 4
Gold Quarry Wall E- Section 1
Gold Quarry Wall A- Section 1
Gold Quarry Wall C- Block 3
Gold Quarry Wall F- Block 4
Gold Quarry Wall B- Block 3
Gold Quarry Wall C- Block 4

Stratigraphic section legend

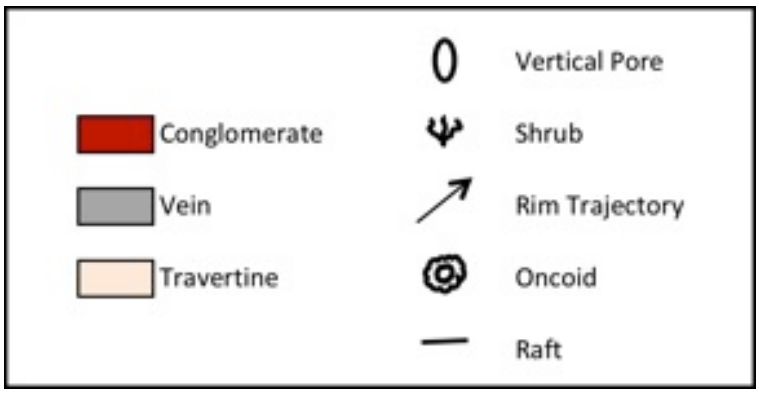

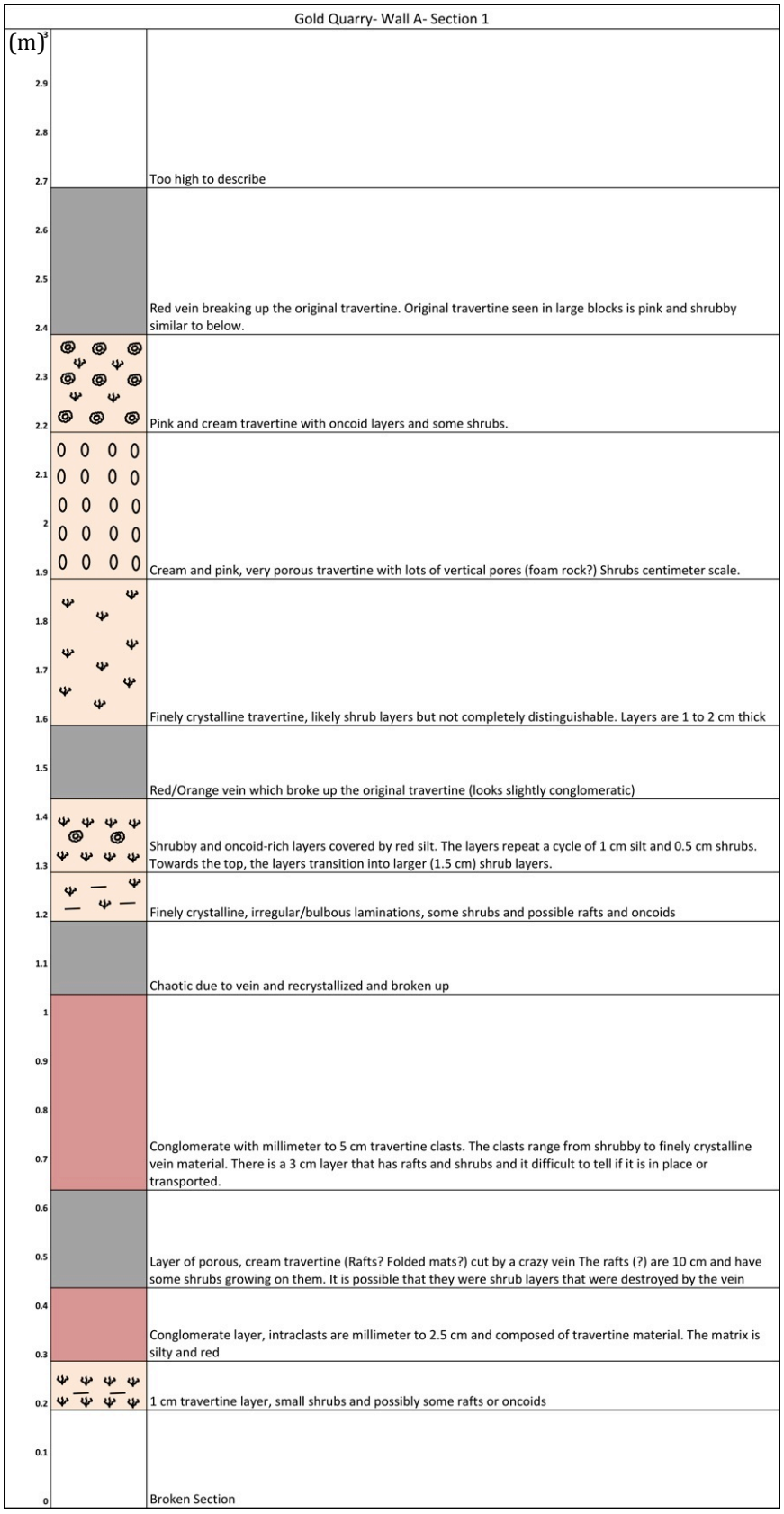
Gold Quarry- Wall A- Section 1
(m)3
2.9
2.8
2.7
2.6
2.5
2.4
2.3
2.2
2.1
2
1.9
1.8
1.7
1.6
1.5
1.4
1.3
1.2
1.1
1
0.9
0.8
0.7
0.6
0.5
0.4
0.3
0.2
0.1
0
Too high to describe
Red vein breaking up the original travertine. Original travertine seen in large blocks is pink and shrubby similar to below.
Pink and cream travertine with oncoid layers and some shrubs.
Cream and pink, very porous travertine with lots of vertical pores (foam rock?) Shrubs centimeter scale.
Finely crystalline travertine, likely shrub layers but not completely distinguishable. Layers are 1 to 2 cm thick
Red/Orange vein which broke up the original travertine (looks slightly conglomeratic)
Shrubby and oncoid-rich layers covered by red silt. The layers repeat a cycle of 1 cm silt and 0.5 cm shrubs. Towards the top, the layers transition into larger (1.5 cm) shrub layers.
Finely crystalline, irregular/bulbous laminations, some shrubs and possible rafts and oncoids
Chaotic due to vein and recrystallized and broken up
Conglomerate with millimeter to 5 cm travertine clasts. The clasts range from shrubby to finely crystalline vein material. There is a 3 cm layer that has rafts and shrubs and it difficult to tell if it is in place or transported.
Layer of porous, cream travertine (Rafts? Folded mats?) cut by a crazy vein The rafts (?) are 10 cm and have some shrubs growing on them. It is possible that they were shrub layers that were destroyed by the vein
Conglomerate layer, intraclasts are millimeter to 2.5 cm and composed of travertine material. The matrix is silty and red
1 cm travertine layer, small shrubs and possibly some rafts or oncoids
Broken Section

Gold Quarry- Wall B- Block 3

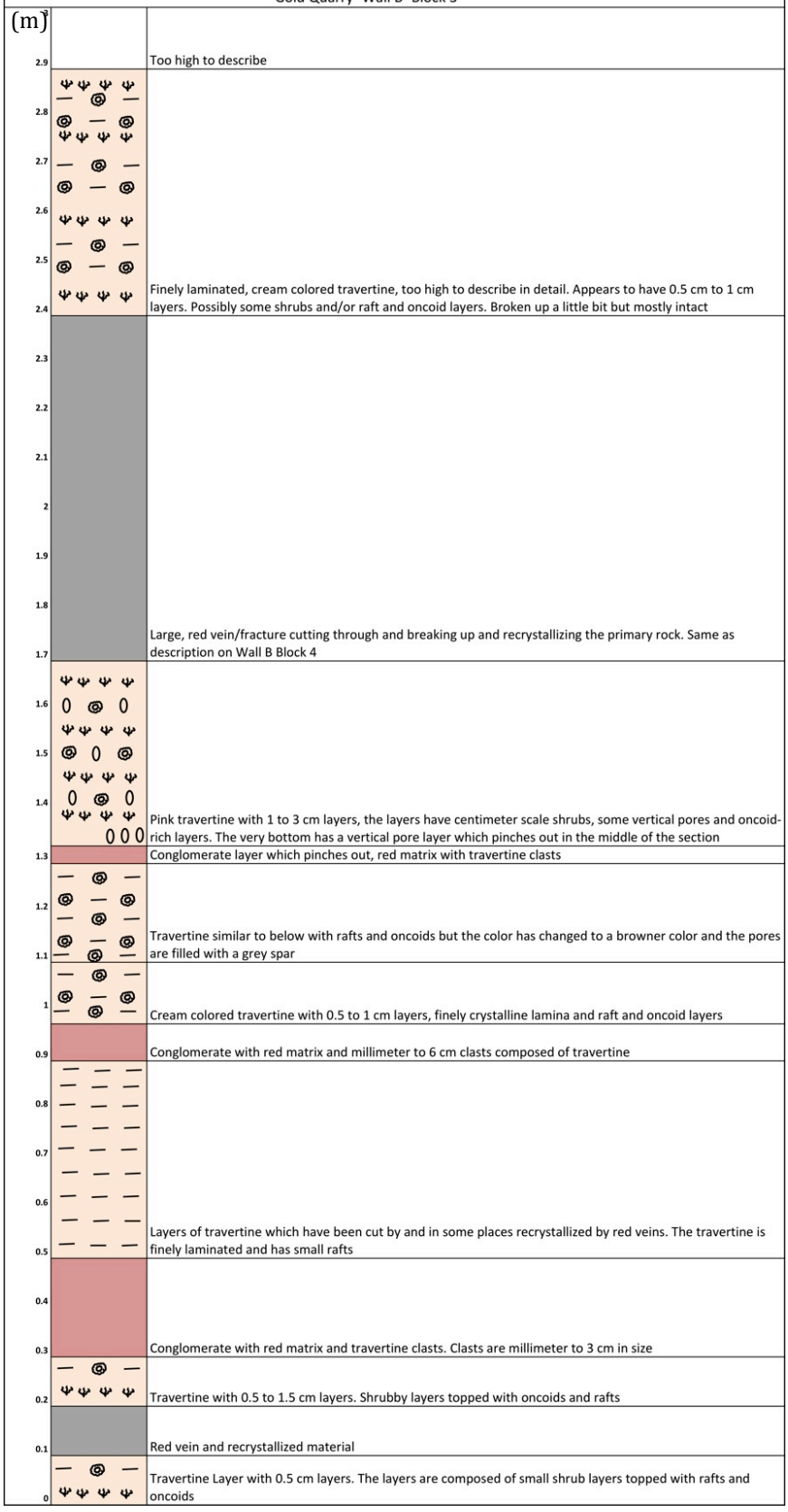

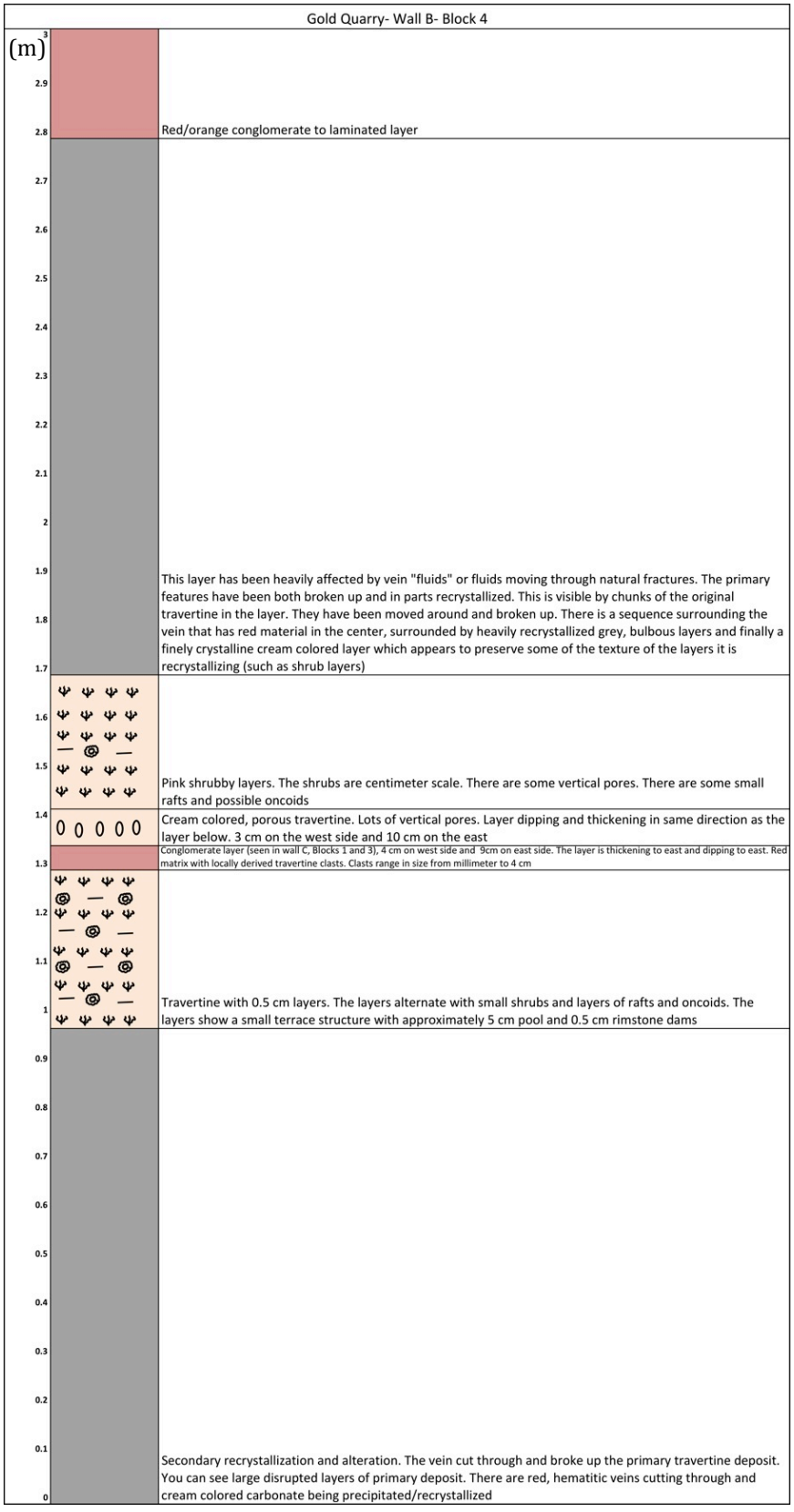
Gold Quarry- Wall B- Block 4
(m)
3
2.9
2.8
2.7
2.6
2.5
2.4
2.3
2.2
2.1
2
1.9
1.8
1.7
1.6
1.5
1.4
1.3
1.2
1.1
1
0.9
0.8
0.7
0.6
0.5
0.4
0.3
0.2
0.1
0
Red/orange conglomerate to laminated layer
This layer has been heavily affected by vein "fluids" or fluids moving through natural fractures. The primary features have been both broken up and in parts recrystallized. This is visible by chunks of the original travertine in the layer. They have been moved around and broken up. There is a sequence surrounding the vein that has red material in the center, surrounded by heavily recrystallized grey, bulbous layers and finally a finely crystalline cream colored layer which appears to preserve some of the texture of the layers it is recrystallizing (such as shrub layers)
Pink shrubby layers. The shrubs are centimeter scale. There are some vertical pores. There are some small rafts and possible oncoids
Cream colored, porous travertine. Lots of vertical pores. Layer dipping and thickening in same direction as the layer below. 3 cm on the west side and 10 cm on the east
Conglomerate layer (seen in wall C, Blocks 1 and 3), 4 cm on west side and 9cm on east side. The layer is thickening to east and dipping to east. Red matrix with locally derived travertine clasts. Clasts range in size from millimeter to 4 cm
Travertine with 0.5 cm layers. The layers alternate with small shrubs and layers of rafts and oncoids. The layers show a small terrace structure with approximately 5 cm pool and 0.5 cm rimstone dams
Secondary recrystallization and alteration. The vein cut through and broke up the primary travertine deposit. You can see large disrupted layers of primary deposit. There are red, hematitic veins cutting through and cream colored carbonate being precipitated/recrystallized

Gold Quarry- Wall C- Block 3

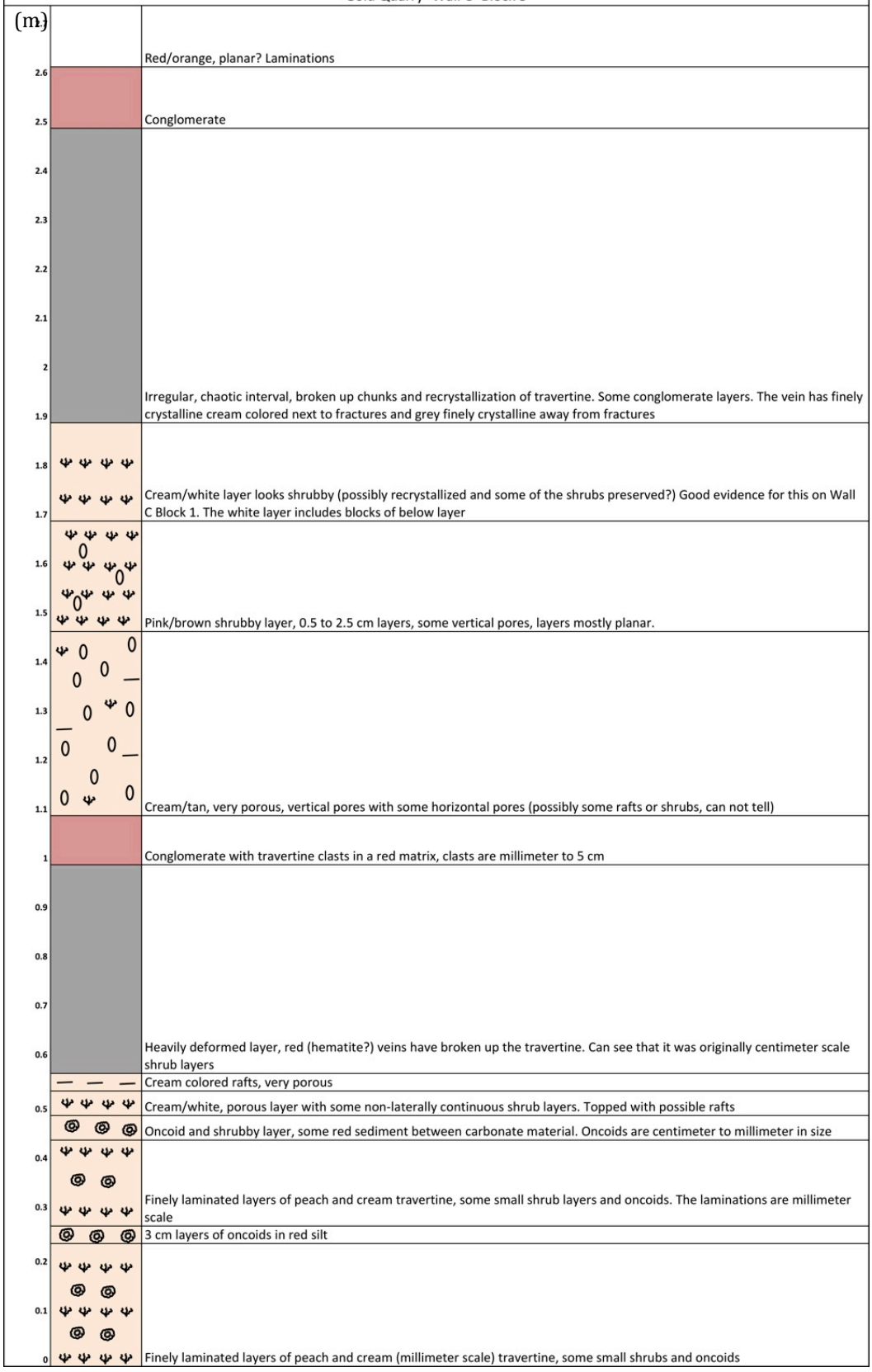

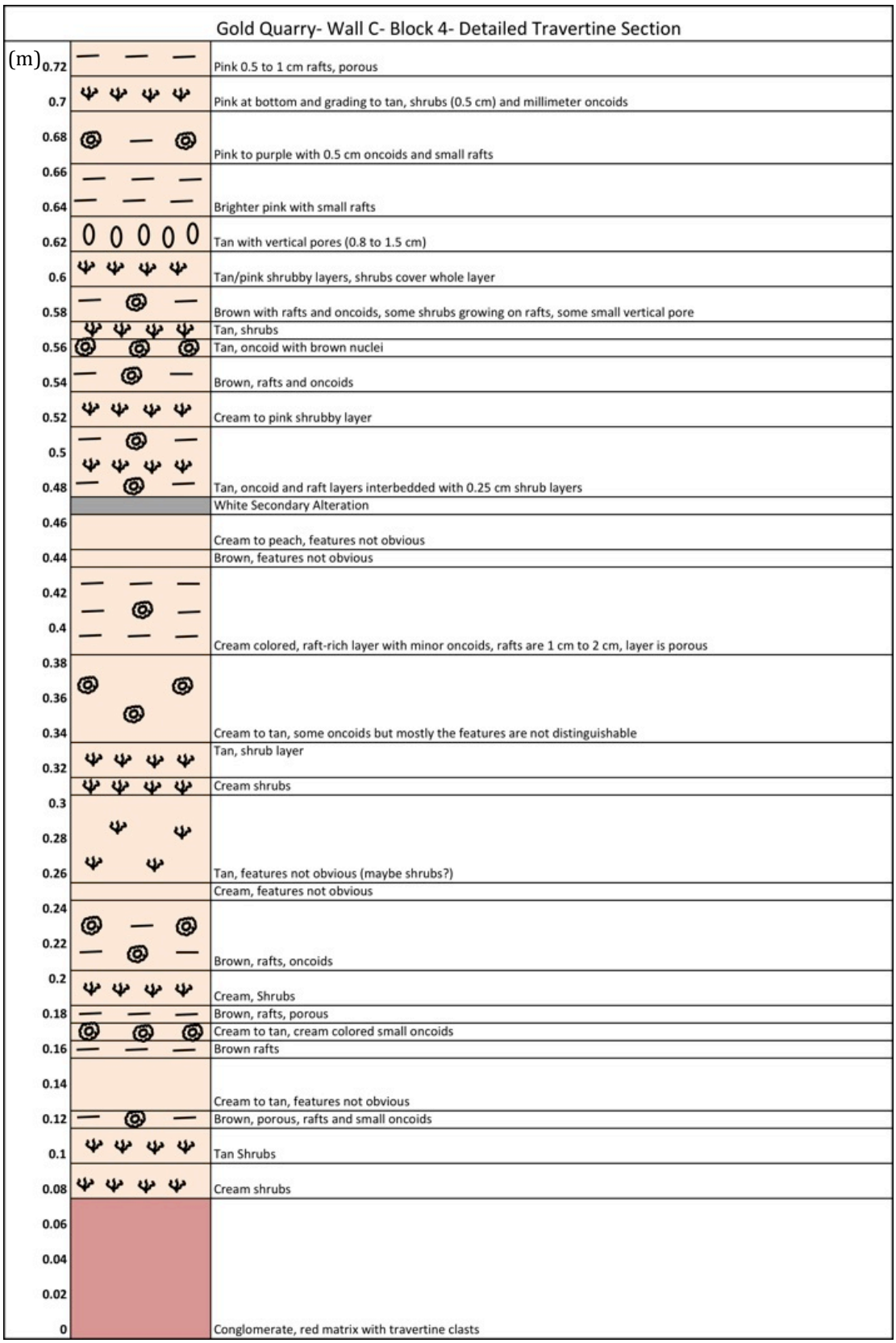
Gold Quarry- Wall C- Block 4- Detailed Travertine Section
(m)
0.72
0.7
0.68
0.66
0.64
0.62
0.6
0.58
0.56
0.54
0.52
0.5
0.48
0.46
0.44
0.42
0.4
0.38
0.36
0.34
0.32
0.3
0.28
0.26
0.24
0.22
0.2
0.18
0.16
0.14
0.12
0.1
0.08
0.06
0.04
0.02
0
Pink 0.5 to 1 cm rafts, porous
Pink at bottom and grading to tan, shrubs (0.5 cm) and millimeter oncoids
Pink to purple with 0.5 cm oncoids and small rafts
Brighter pink with small rafts
Tan with vertical pores (0.8 to 1.5 cm)
Tan/pink shrubby layers, shrubs cover whole layer
Brown with rafts and oncoids, some shrubs growing on rafts, some small vertical pore
Tan, shrubs
Tan, oncoid with brown nuclei
Brown, rafts and oncoids
Cream to pink shrubby layer
Tan, oncoid and raft layers interbedded with 0.25 cm shrub layers
White Secondary Alteration
Cream to peach, features not obvious
Brown, features not obvious
Cream colored, raft-rich layer with minor oncoids, rafts are 1 cm to 2 cm, layer is porous
Cream to tan, some oncoids but mostly the features are not distinguishable
Tan, shrub layer
Cream shrubs
Tan, features not obvious (maybe shrubs?)
Cream, features not obvious
Brown, rafts, oncoids
Cream, Shrubs
Brown, rafts, porous
Cream to tan, cream colored small oncoids
Brown rafts
Cream to tan, features not obvious
Brown, porous, rafts and small oncoids
Tan Shrubs
Cream shrubs
Conglomerate, red matrix with travertine clasts

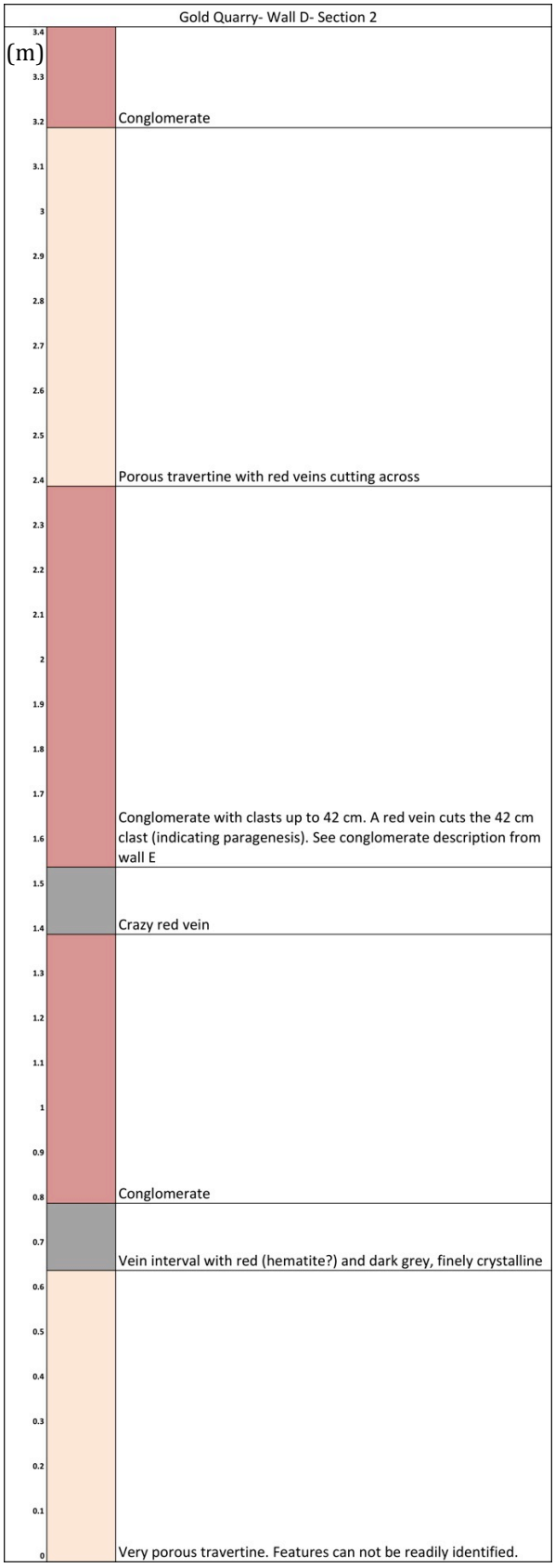
Gold Quarry- Wall D- Section 2
(m)
3.4
3.3
3.2
Conglomerate
3.1
3
2.9
2.8
2.7
2.6
2.5
2.4
Porous travertine with red veins cutting across
2.3
2.2
2.1
2
1.9
1.8
1.7
1.6
Conglomerate with clasts up to 42 cm. A red vein cuts the 42 cm clast (indicating paragenesis). See conglomerate description from wall E
1.5
1.4
Crazy red vein
1.3
1.2
1.1
1
0.9
0.8
Conglomerate
0.7
Vein interval with red (hematite?) and dark grey, finely crystalline
0.6
0.5
0.4
0.3
0.2
0.1
0
Very porous travertine. Features can not be readily identified.

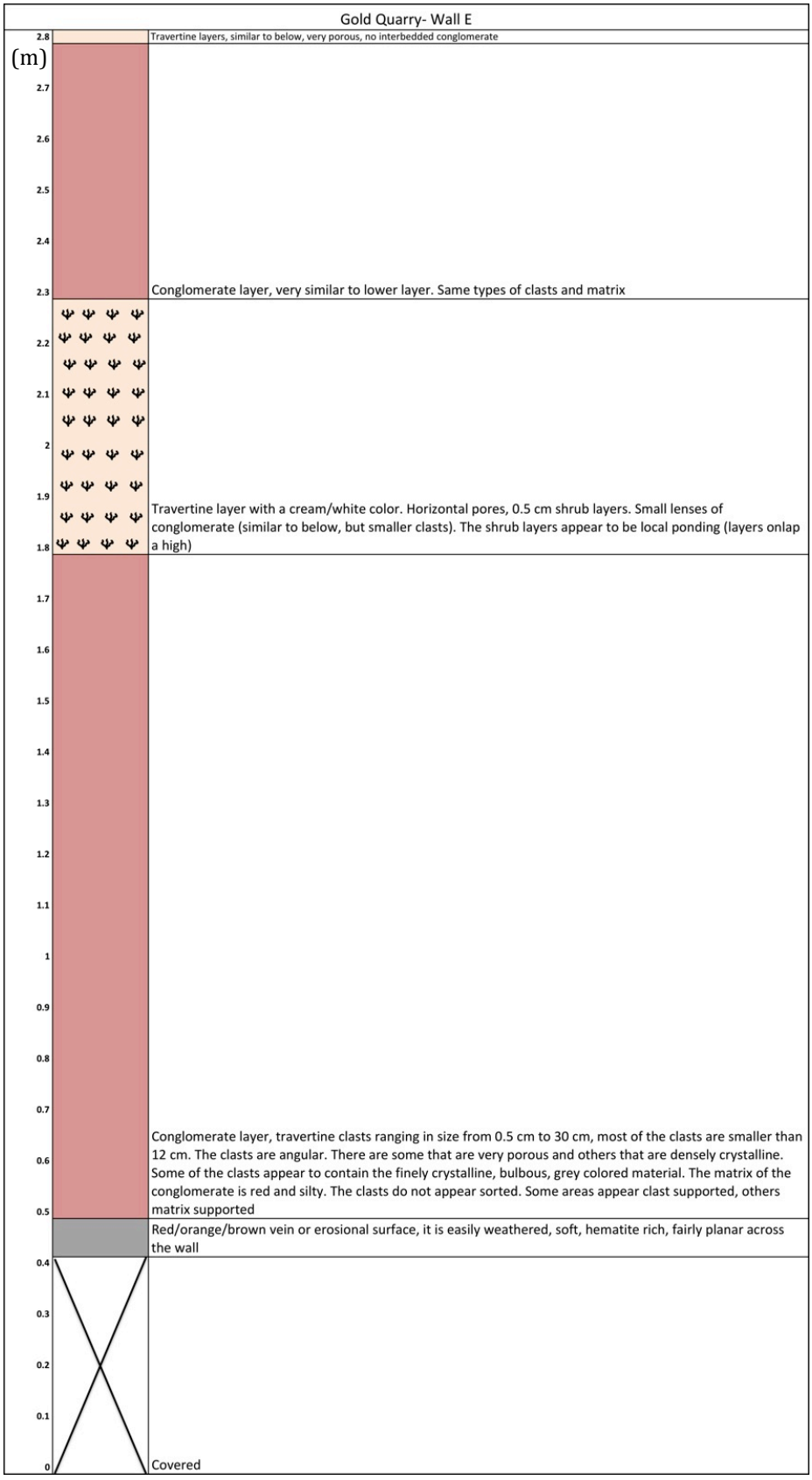
Gold Quarry- Wall E
(m)
2.8
2.7
2.6
2.5
2.4
2.3
2.2
2.1
2
1.9
1.8
1.7
1.6
1.5
1.4
1.3
1.2
1.1
1
0.9
0.8
0.7
0.6
0.5
0.4
0.3
0.2
0.1
0
Travertine layers, similar to below, very porous, no interbedded conglomerate
Conglomerate layer, very similar to lower layer. Same types of clasts and matrix
Travertine layer with a cream/white color. Horizontal pores, 0.5 cm shrub layers. Small lenses of conglomerate (similar to below, but smaller clasts). The shrub layers appear to be local ponding (layers onlap a high)
Conglomerate layer, travertine clasts ranging in size from 0.5 cm to 30 cm, most of the clasts are smaller than 12 cm. The clasts are angular. There are some that are very porous and others that are densely crystalline. Some of the clasts appear to contain the finely crystalline, bulbous, grey colored material. The matrix of the conglomerate is red and silty. The clasts do not appear sorted. Some areas appear clast supported, others matrix supported
Red/orange/brown vein or erosional surface, it is easily weathered, soft, hematite rich, fairly planar across the wall
Covered

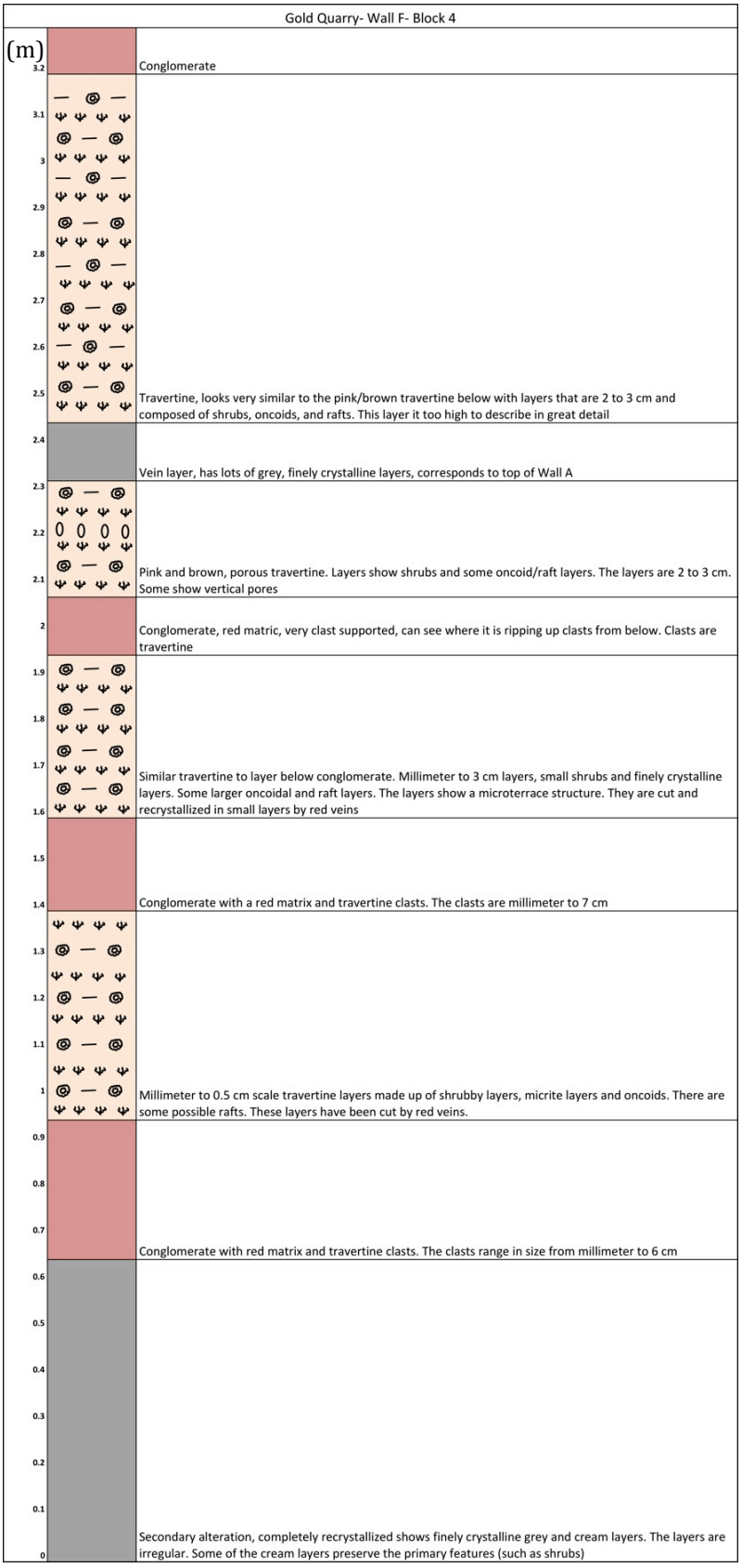
Gold Quarry- Wall F- Block 4
(m)
3.2
3.1
3
2.9
2.8
2.7
2.6
2.5
2.4
2.3
2.2
2.1
2
1.9
1.8
1.7
1.6
1.5
1.4
1.3
1.2
1.1
1
0.9
0.8
0.7
0.6
0.5
0.4
0.3
0.2
0.1
0
Conglomerate
Travertine, looks very similar to the pink/brown travertine below with layers that are 2 to 3 cm and composed of shrubs, oncoids, and rafts. This layer it too high to describe in great detail
Vein layer, has lots of grey, finely crystalline layers, corresponds to top of Wall A
Pink and brown, porous travertine. Layers show shrubs and some oncoid/raft layers. The layers are 2 to 3 cm. Some show vertical pores
Conglomerate, red matric, very clast supported, can see where it is ripping up clasts from below. Clasts are travertine
Similar travertine to layer below conglomerate. Millimeter to 3 cm layers, small shrubs and finely crystalline layers. Some larger oncoidal and raft layers. The layers show a microterrace structure. They are cut and recrystallized in small layers by red veins
Conglomerate with a red matrix and travertine clasts. The clasts are millimeter to 7 cm
Millimeter to 0.5 cm scale travertine layers made up of shrubby layers, micrite layers and oncoids. There are some possible rafts. These layers have been cut by red veins.
Conglomerate with red matrix and travertine clasts. The clasts range in size from millimeter to 6 cm
Secondary alteration, completely recrystallized shows finely crystalline grey and cream layers. The layers are irregular. Some of the cream layers preserve the primary features (such as shrubs)

Gold Quarry- Wall F- Block 6

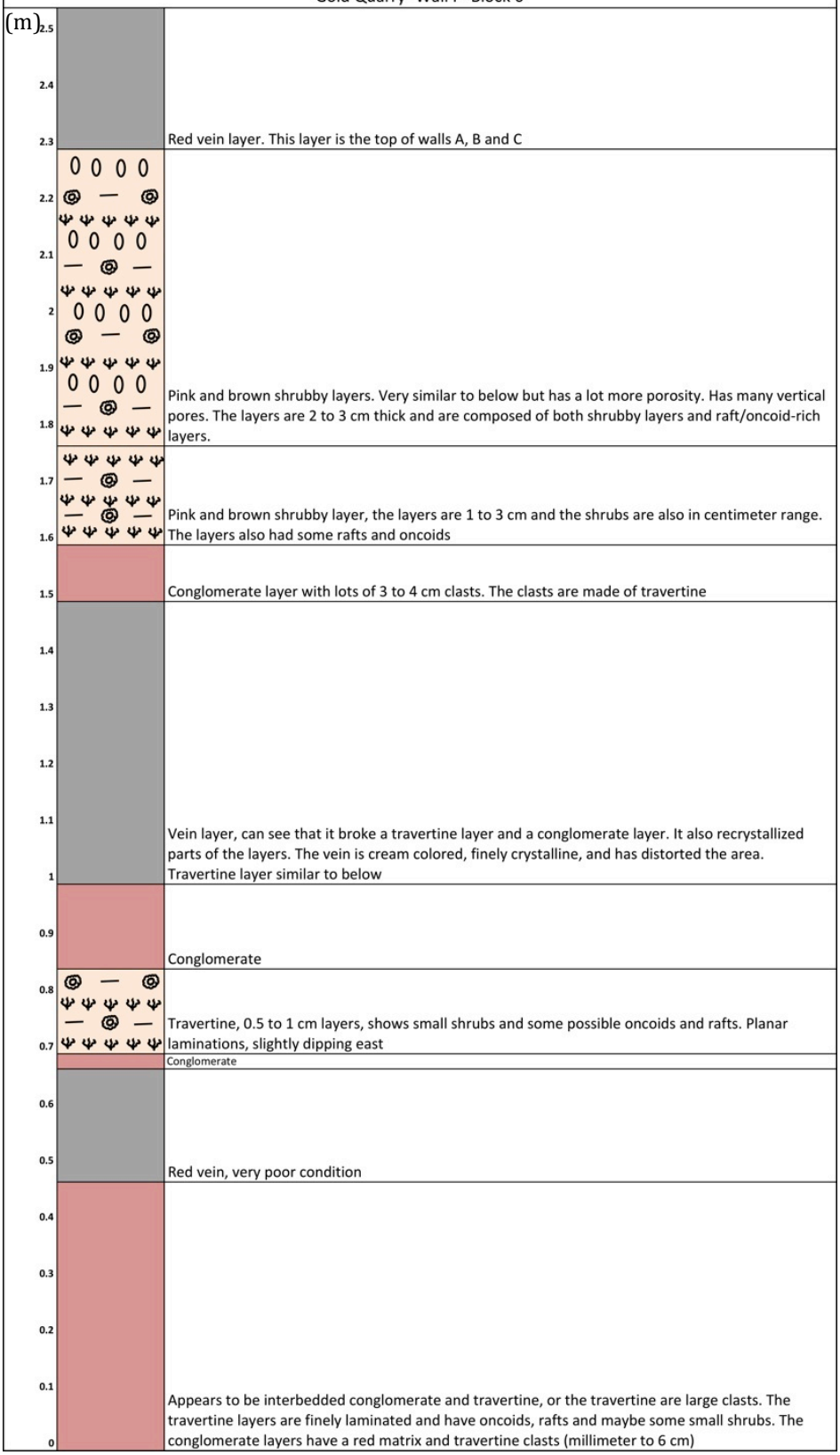

	Red vein layer. This layer is the top of walls A, B and C
	Pink and brown shrubby layers. Very similar to below but has a lot more porosity. Has many vertical pores. The layers are 2 to 3 cm thick and are composed of both shrubby layers and raft/oncoid-rich layers.
	Pink and brown shrubby layer, the layers are 1 to 3 cm and the shrubs are also in centimeter range. The layers also had some rafts and oncoids
	Conglomerate layer with lots of 3 to 4 cm clasts. The clasts are made of travertine
	Vein layer, can see that it broke a travertine layer and a conglomerate layer. It also recrystallized parts of the layers. The vein is cream colored, finely crystalline, and has distorted the area. Travertine layer similar to below
	Conglomerate
	Travertine, 0.5 to 1 cm layers, shows small shrubs and some possible oncoids and rafts. Planar laminations, slightly dipping east
	Conglomerate
	Red vein, very poor condition
	Appears to be interbedded conglomerate and travertine, or the travertine are large clasts. The travertine layers are finely laminated and have oncoids, rafts and maybe some small shrubs. The conglomerate layers have a red matrix and travertine clasts (millimeter to 6 cm)

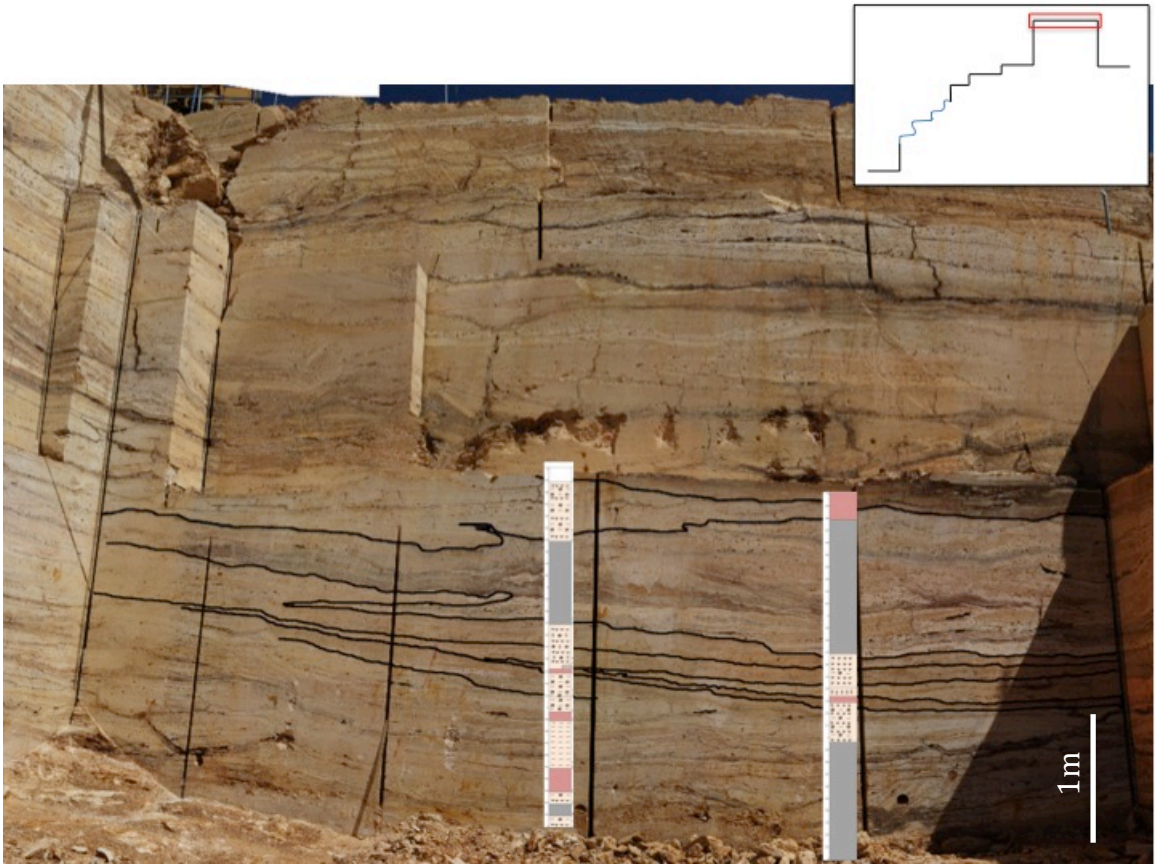

Measured sections Gold Quarry Wall B- Block 3 (left) and Gold Quarry Wall B-Block 4 (right) located on Gold Quarry Wall B. The black lines highlight the structure on the wall.

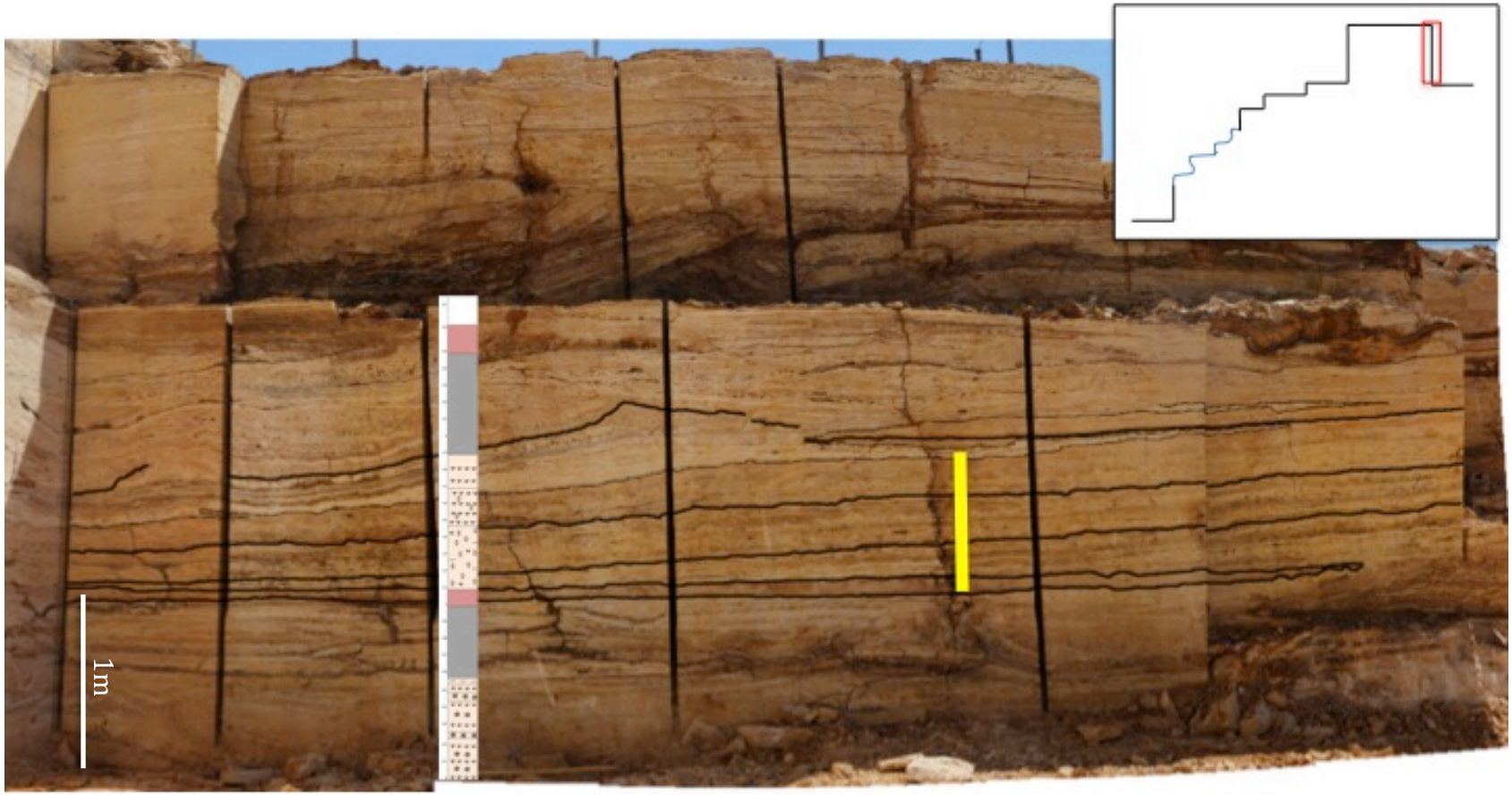

Measured sections Gold Quarry Wall C- Block 3(left) and Gold Quarry Wall C- Block 4- Detailed section (Yellow line)) located on Gold Quarry Wall C. The black lines highlight the structure on the wall.

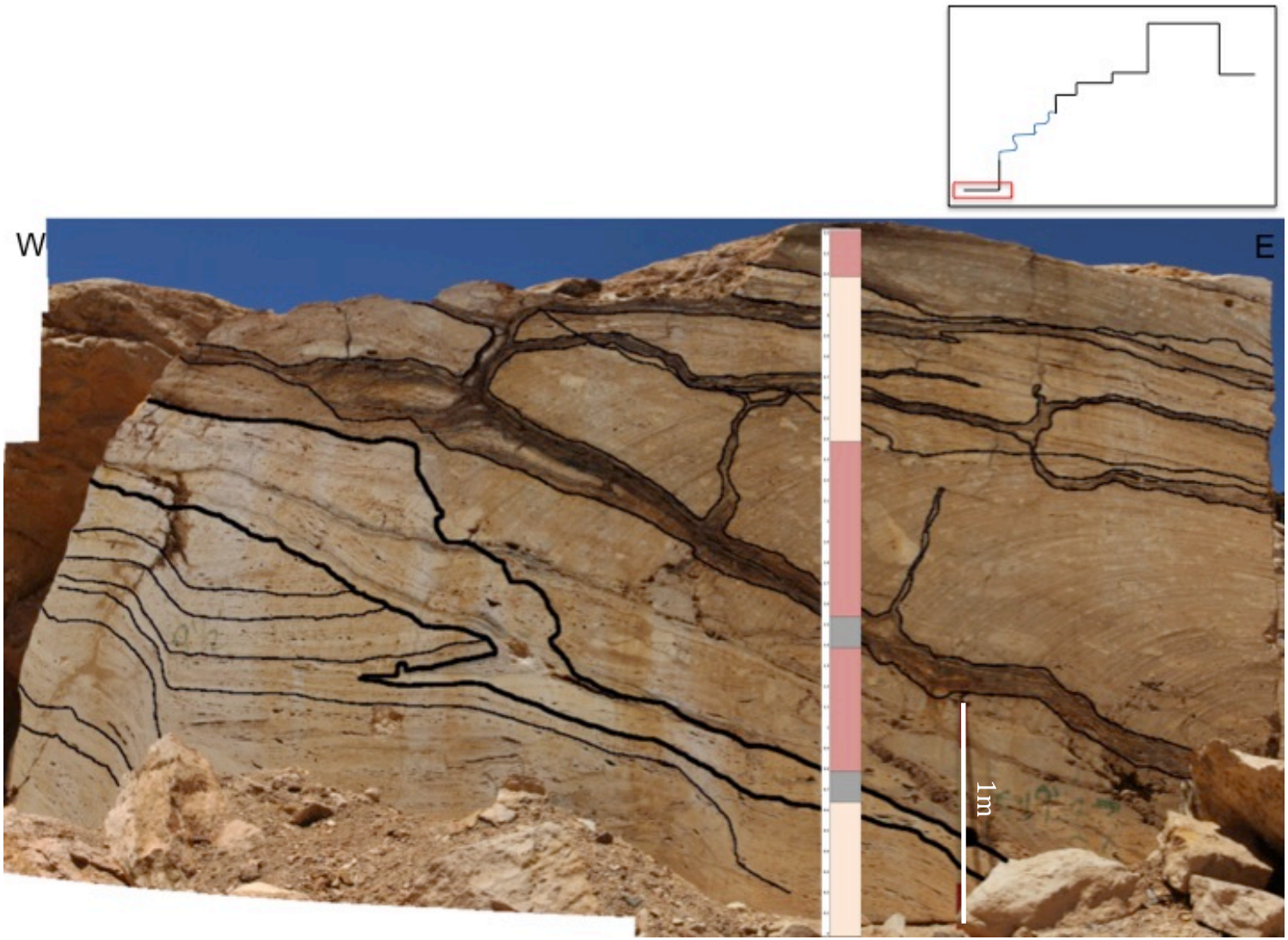

Measured sections Gold Quarry Wall D-Section2 (located on Gold Quarry Wall D. The black lines highlight the structure on the wall.

APPENDIX II: IVORY QUARRY MEASURED SECTIONS

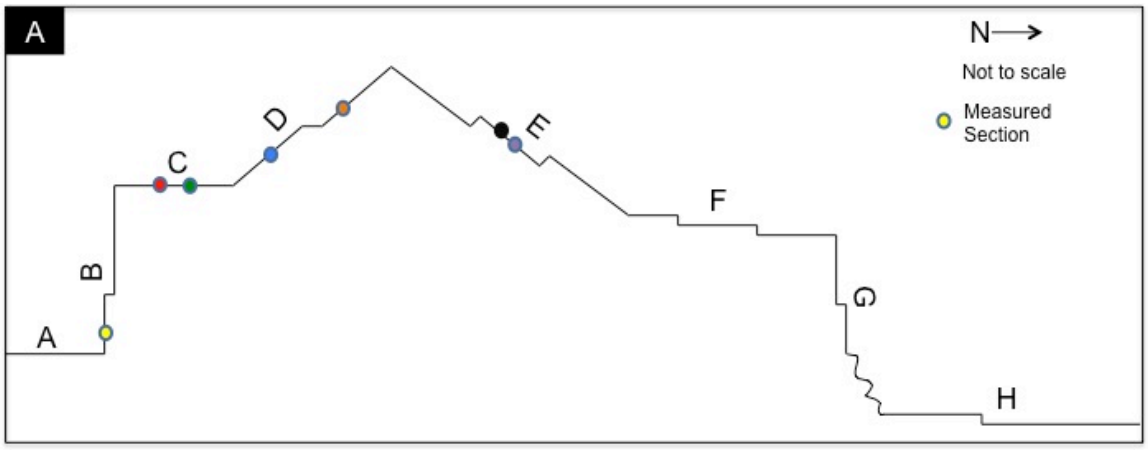

- Ivory Quarry Wall B- Section 1
- Ivory Quarry Wall C- Section 1
- Ivory Quarry Wall C- Section 2
- Ivory Quarry Wall D- Section 1
- Ivory Quarry Wall D- Section 2
- Ivory Quarry Wall E- Section 1
- Ivory Quarry Wall E- Section 2

Ivory Quarry- Wall B- Section 1

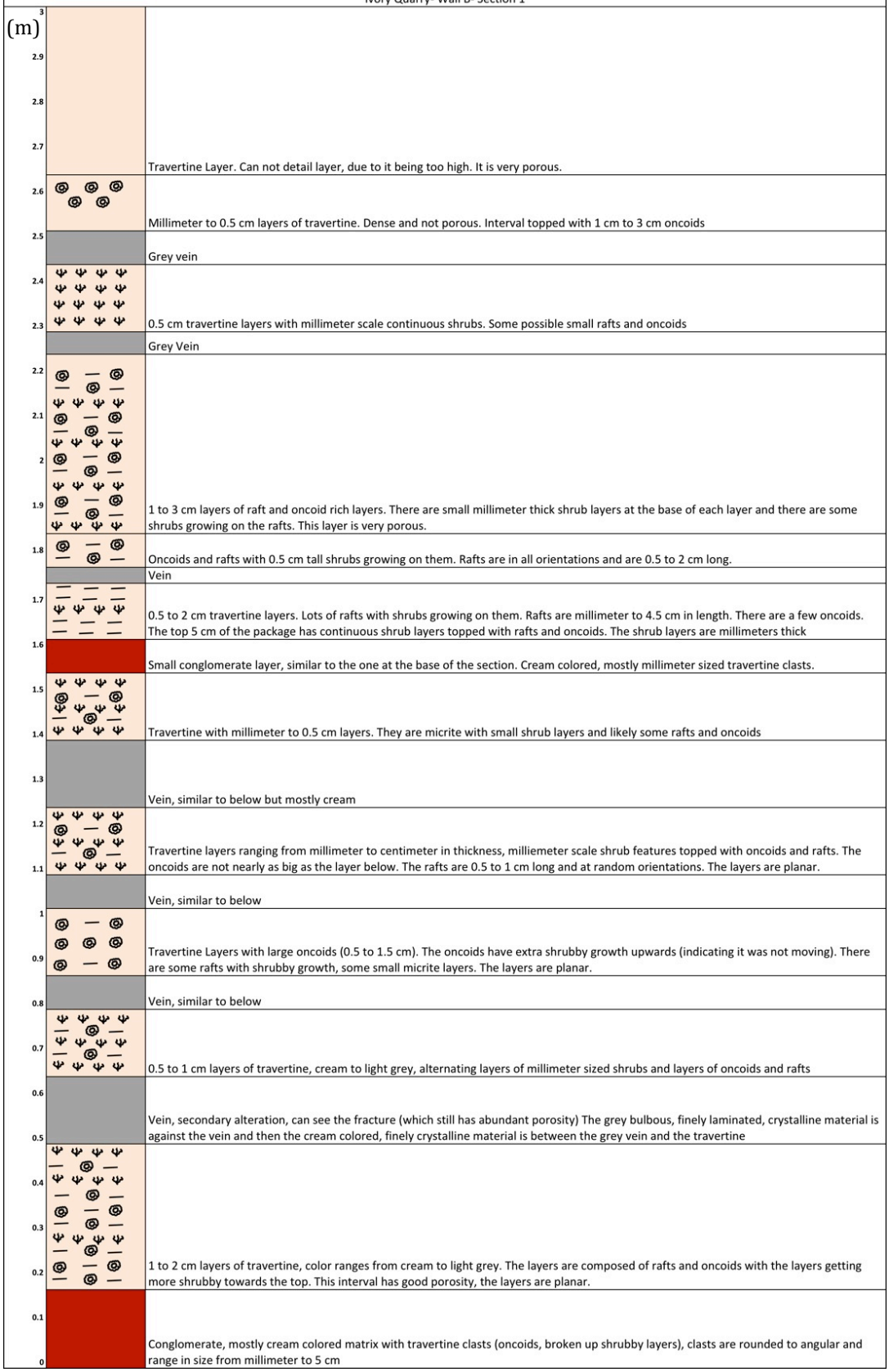

Travertine Layer. Can not detail layer, due to it being too high. It is very porous.

Millimeter to 0.5 cm layers of travertine. Dense and not porous. Interval topped with 1 cm to 3 cm oncoids

Grey vein

0.5 cm travertine layers with millimeter scale continuous shrubs. Some possible small rafts and oncoids

Grey Vein

1 to 3 cm layers of raft and oncoid rich layers. There are small millimeter thick shrub layers at the base of each layer and there are some shrubs growing on the rafts. This layer is very porous.

Oncoids and rafts with 0.5 cm tall shrubs growing on them. Rafts are in all orientations and are 0.5 to 2 cm long.

Vein

0.5 to 2 cm travertine layers. Lots of rafts with shrubs growing on them. Rafts are millimeter to 4.5 cm in length. There are a few oncoids. The top 5 cm of the package has continuous shrub layers topped with rafts and oncoids. The shrub layers are millimeters thick

Small conglomerate layer, similar to the one at the base of the section. Cream colored, mostly millimeter sized travertine clasts.

Travertine with millimeter to 0.5 cm layers. They are micrite with small shrub layers and likely some rafts and oncoids

Vein, similar to below but mostly cream

Travertine layers ranging from millimeter to centimeter in thickness, milliemeter scale shrub features topped with oncoids and rafts. The oncoids are not nearly as big as the layer below. The rafts are 0.5 to 1 cm long and at random orientations. The layers are planar.

Vein, similar to below

Travertine Layers with large oncoids (0.5 to 1.5 cm). The oncoids have extra shrubby growth upwards (indicating it was not moving). There are some rafts with shrubby growth, some small micrite layers. The layers are planar.

Vein, similar to below

0.5 to 1 cm layers of travertine, cream to light grey, alternating layers of millimeter sized shrubs and layers of oncoids and rafts

Vein, secondary alteration, can see the fracture (which still has abundant porosity) The grey bulbous, finely laminated, crystalline material is against the vein and then the cream colored, finely crystalline material is between the grey vein and the travertine

1 to 2 cm layers of travertine, color ranges from cream to light grey. The layers are composed of rafts and oncoids with the layers getting more shrubby towards the top. This interval has good porosity, the layers are planar.

Conglomerate, mostly cream colored matrix with travertine clasts (oncoids, broken up shrubby layers), clasts are rounded to angular and range in size from millimeter to 5 cm

Ivory Quarry- Wall C- Section 1

(m)	
3	2 to 4 cm layers. Each layer appears to be composed of shrubs at the base and rafts at the top but the features are hard to distinguish. The rimstone dam trajectory is backstepping, but other features of the pools and rimstone dams are hard to identify.
2.9	
2.8	
2.7	
2.6	
2.5	
2.4	Tan and cream, 0.5 cm layers at bottom grading to 4 cm layers at top, pools range between 6 cm and 12 cm, rimstone dams are vertical to slightly prograding, layers are shrubby at bottom and rafts on top (within each layer)
2.3	
2.2	Tan, features are not easily distinguishable, porous, large pools, layer thins significantly to left of section (5 cm at left, 12 cm at right)
2.1	
2	Tan and cream colored, 3 to 4 cm pools, very prograding rimstone dams, pools are shrubby topped with rafts
1.9	Tan colored, porous travertine, features are not distinguishable but look similar to below (shrubs with raft layers on top), 10 cm pools
1.8	
1.7	
1.6	2 to 3 cm layers with centimeter thick shrubby layers topped with rafts and some possible encrusted bubbles and vertical pores
	Conglomerate layer with millimeter to 3.5 cm clasts, clasts are of travertine material
1.5	Vein
1.4	0.5 cm shrubby layers of terrace pools. Pools are 6 cm long and rimstone dams trajectory is backstepping. Centimeter sized oncoids on top of layer
1.3	0.5 to 1 cm thick layers of terrace pool deposits. Small micrite to shrubby layer topped with small oncoids and rafts. The pools are approximately 10 cm long and the rimstone dmas have a downstream migrating trajectory.
1.2	millimeter laminated micrite and shrub layers with a few oncoids. Layers are planar
1.1	Very porous, cream colored vein
	Oncoid and raft layer
1	millimeter thick micrite and shrub layers, planar
0.9	Porous raft and oncoid rich layers, rafts 0.2 to 2 cm
	Vein
0.8	0.5 cm travertine layers, millimeter shrub, raft, and oncoid layers
0.7	Vein, mostly cream colored, can see some of the primary features (shrubs and oncoids?) which have been destroyed
0.6	Light grey, porous travertine layer. Two 4 cm layers with some oncoids and rafts, other constituents are not obvious
0.5	Vein, similar to below
0.4	0.5 to 1 cm travertine layers, color appears odd (orange/black/brown), the layers are composed of oncoids and rafts
0.3	
0.2	Vein, mostly cream colored, finely crystalline, very dense
0.1	
0	Conglomerate with millimeter to centimeter sized clasts. The clasts are composed of travertine material

Ivory Quarry- Wall C- Section 2- Detailed Section		
0.4		
0.38		Small oncoids and rafts
0.36		Shrubby Layers
0.34		Shrubby layers with rafts and oncoids
0.32		
0.3		0.25 cm sized rafts and oncoids (spar cement?), some shrub growth
0.28	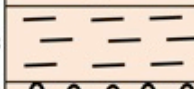	Large rafts (1 to 3 cm), mostly horizontal with some at higher angles. Shrubs growing on top of the rafts and pores underneath
0.26	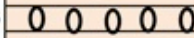	Vertical Pores
0.24	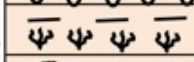	Shrubs and small rafts
0.22		Undistinguishable features, likely rafts and oncoids with shrubs growing on them
0.2	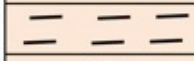	Layer with rafts at random orientations (horizontal to vertical)
0.18		Layer with 0.25 cm to 1 cm oncoids, and some small rafts
0.16	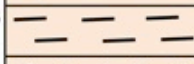	Rafts with shrubs growing on them. Rafts are 1 to 2.5 cm long and 1 mm thick
0.14	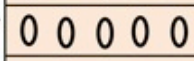	Vertical pores, layer appears shrubby but the features are not fully distinguishable, there appears to be small rafts
0.12		
0.1		Porous travertine layer. It is likely composed of rafts and oncoids but the features are not distinguishable
0.08		
0.06		Very porous layer with large rafts (1 to 2 cm). The rafts are mostly horizontal but some have a little angle. Shrubs are growing on the tops of the rafts
0.04	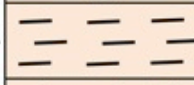	Rafts and possibly small oncoids with shrubs growing on them
0.02	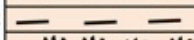	Shrubs growing on rafts and possibly some preserved bubbles
0		Shrubby Layer, 2 one centimeter layers of shrubs

* The detailed section is described from the interval of 1.1 to 1.6 meters on Ivory Quarry Wall C- Section 2

Ivory Quarry- Wall C- Section 2		
(m) 3		
2.9		
2.8		Too high to describe
2.7	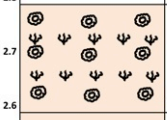	Finely laminated (0.25 to 1 cm) oncoid rich layer with some continuous shrub layers. 2 cm vein cutting through center. Some of the pools have red silt in them (with lots of oncoids), vein gets larger to the left
2.6		
2.5	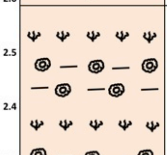	
2.4		
2.3		8 to 10 cm layers that are separated by layer of centimenter micrite and shrubs, layers are very porous and likely composed of rafts and small oncoids, the features are not very distinguishable, weird structure at the base of some layers (rimstone dams?) some preserved bubbles, pools range from approximately 4 to 10 cm but aren't very obvious
2.2		
2.1		1 to 2 cm layers, 1 cm shrubs topped with rafts and some preserved bubbles, cream to peach color, porous
2		0.25 to 1 cm layers, composed of small continuous shrub layers and oncoids (0.5 to 1 cm) pools range in size from 3 cm to 9 cm, the rimstone dams are slightly downstream migrating (approximately 75 degrees from horizontal) Oncoids are very abundant, color is light grey, pink and cream
1.9		
1.8	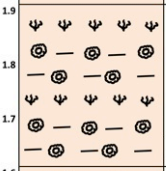	
1.7		2 to 4 cm layers, very porous, mainly composed of rafts and oncoids, shrubs usually grow on top of rafts, there are a few continuous shrub layers (0.5 cm thick). The pores are circular to horizontal and generally follow the layers. Pools are approximately 45 cm long
1.6		
1.5	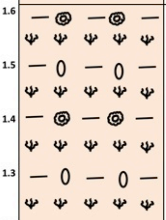	
1.4		
1.3		
1.2		1.5 to 3.5 cm layers, there are 1 cm shrubs, layers of large and small rafts, and a few layers with oncoids and vertical pores, this layer shows a terrace structure with approximately 32 cm pools and downstream migrating rimstone dams (approximately 62 degrees from horizontal)
1.1		Vein
1		Conglomerate layer, cream to orange matrix with oncoids and other travertine clasts
0.9		Finely laminated (millimeter thick) travertine layers, small shrubs and oncoids
0.8		
0.7		
0.6		Vein broken up area, the primary layers (0.5 to 1 cm thick and composed of small shrubs and large oncoids (0.25 to 1.5 cm) are broken up. The vein is porous and recrystallized around in a cream color
0.5	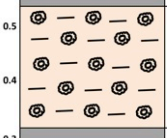	
0.4		3 to 6 cm travertine layers, the layers are mostly raft and oncoid rich, with some shrub growth on them
0.3		Vein
0.2		0.5 to 2 cm travertine layers composed of mainly oncoids and rafts, layer seems slightly altered and color is a little odd (black, brown, orange, cream)
		Cream colored vein
0.1		
0		Conglomerate, cream colored matrix, travertine intraclasts from 1 to 8 cm, locally ripped up (from layer below)

Ivory Quarry- Wall D- Section 1

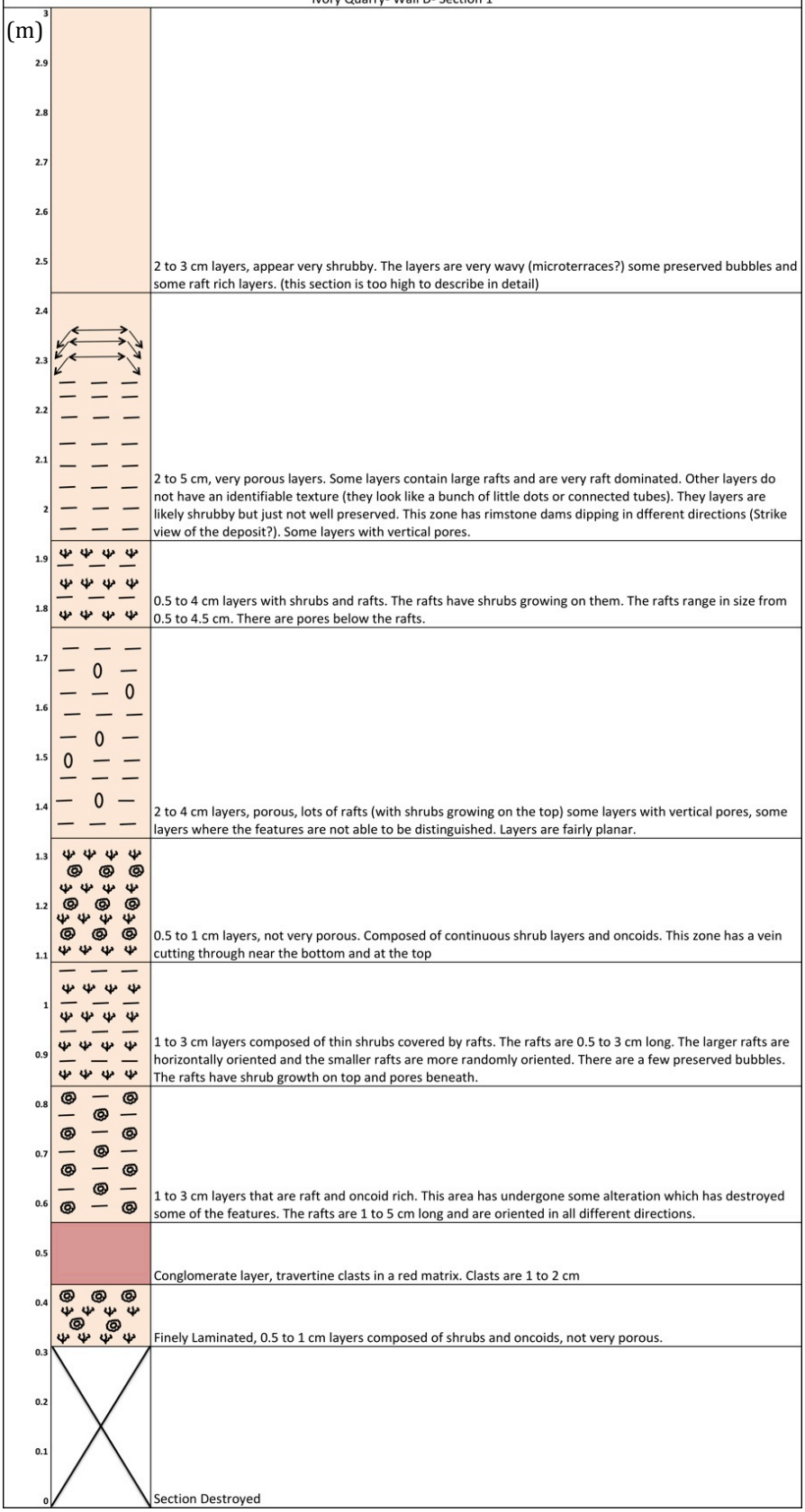

Ivory Quarry- Wall D- Section 2

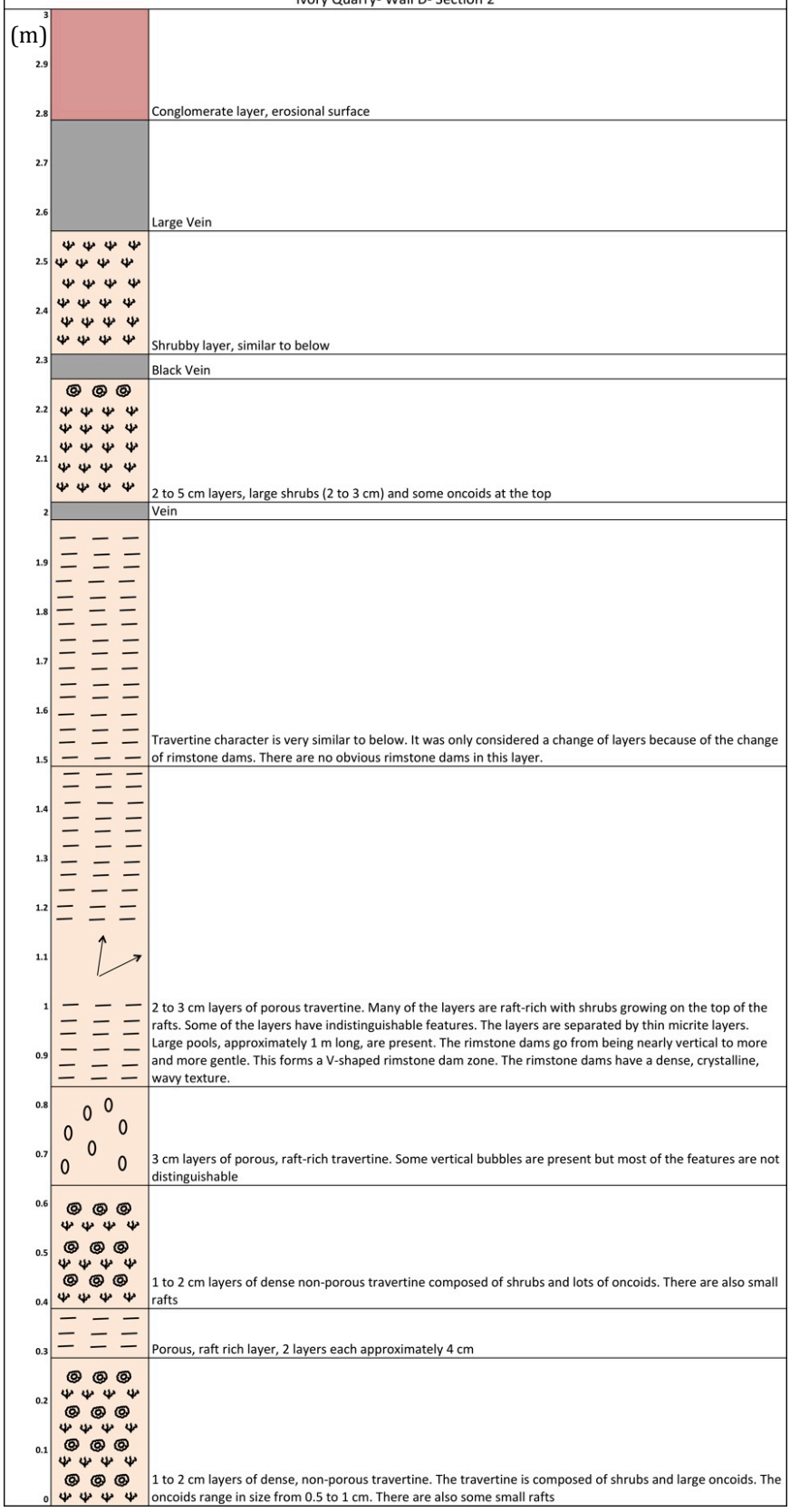

Ivory Quarry- Wall E- Block 2- Section 1

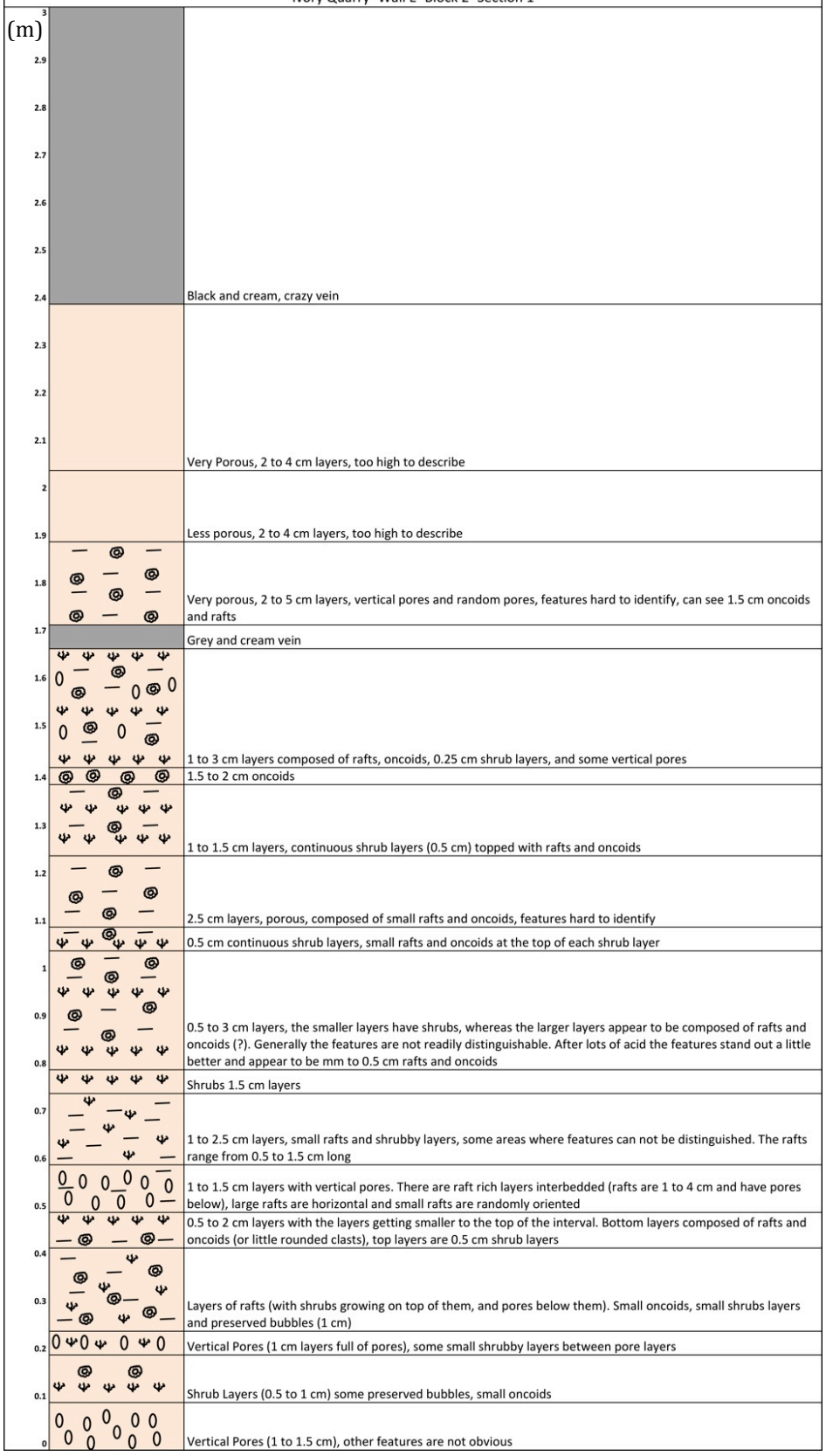

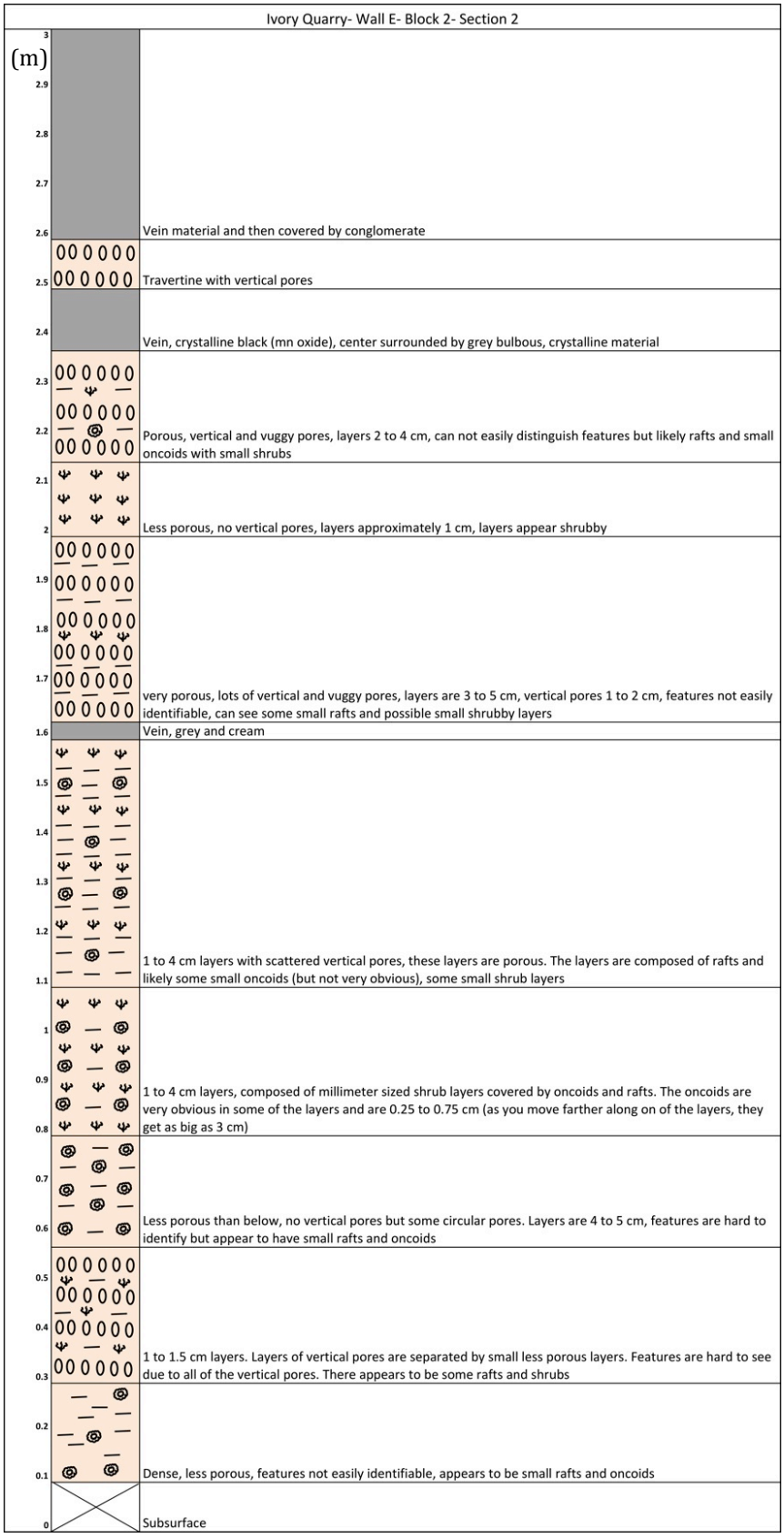
Ivory Quarry- Wall E- Block 2- Section 2
(m)
3
2.9
2.8
2.7
2.6
2.5
2.4
2.3
2.2
2.1
2
1.9
1.8
1.7
1.6
1.5
1.4
1.3
1.2
1.1
1
0.9
0.8
0.7
0.6
0.5
0.4
0.3
0.2
0.1
0
Vein material and then covered by conglomerate
Travertine with vertical pores
Vein, crystalline black (mn oxide), center surrounded by grey bulbous, crystalline material
Porous, vertical and vuggy pores, layers 2 to 4 cm, can not easily distinguish features but likely rafts and small oncoids with small shrubs
Less porous, no vertical pores, layers approximately 1 cm, layers appear shrubby
very porous, lots of vertical and vuggy pores, layers are 3 to 5 cm, vertical pores 1 to 2 cm, features not easily identifiable, can see some small rafts and possible small shrubby layers
Vein, grey and cream
1 to 4 cm layers with scattered vertical pores, these layers are porous. The layers are composed of rafts and likely some small oncoids (but not very obvious), some small shrub layers
1 to 4 cm layers, composed of millimeter sized shrub layers covered by oncoids and rafts. The oncoids are very obvious in some of the layers and are 0.25 to 0.75 cm (as you move farther along on of the layers, they get as big as 3 cm)
Less porous than below, no vertical pores but some circular pores. Layers are 4 to 5 cm, features are hard to identify but appear to have small rafts and oncoids
1 to 1.5 cm layers. Layers of vertical pores are separated by small less porous layers. Features are hard to see due to all of the vertical pores. There appears to be some rafts and shrubs
Dense, less porous, features not easily identifiable, appears to be small rafts and oncoids
Subsurface

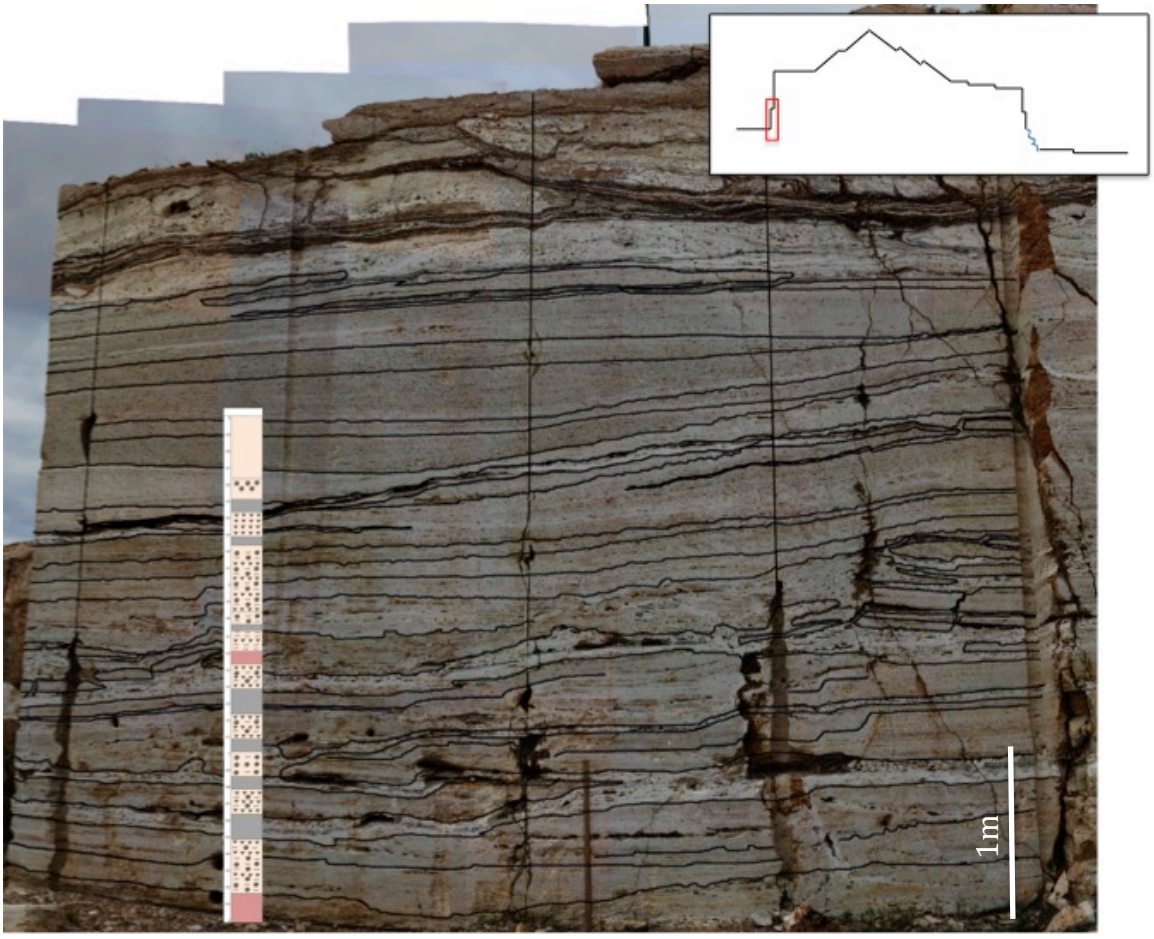

Measured section “Ivory Quarry Wall B- Section 1” located on Ivory Quarry Wall B. The black lines highlight the structure on the wall.

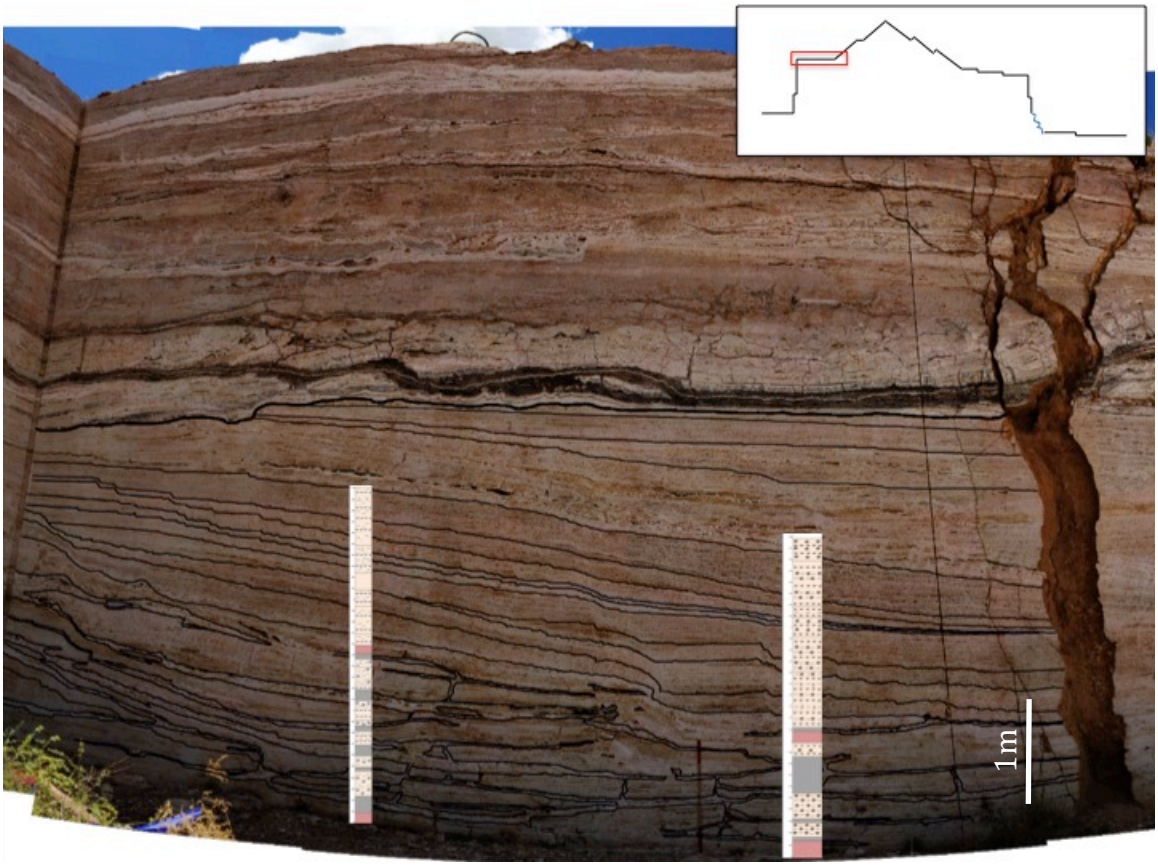

Measured sections Ivory Quarry Wall C- Section 1 (left) and Ivory Quarry Wall C-Section 2 (right) located on Ivory Quarry Wall C. The black lines highlight the structure on the wall.

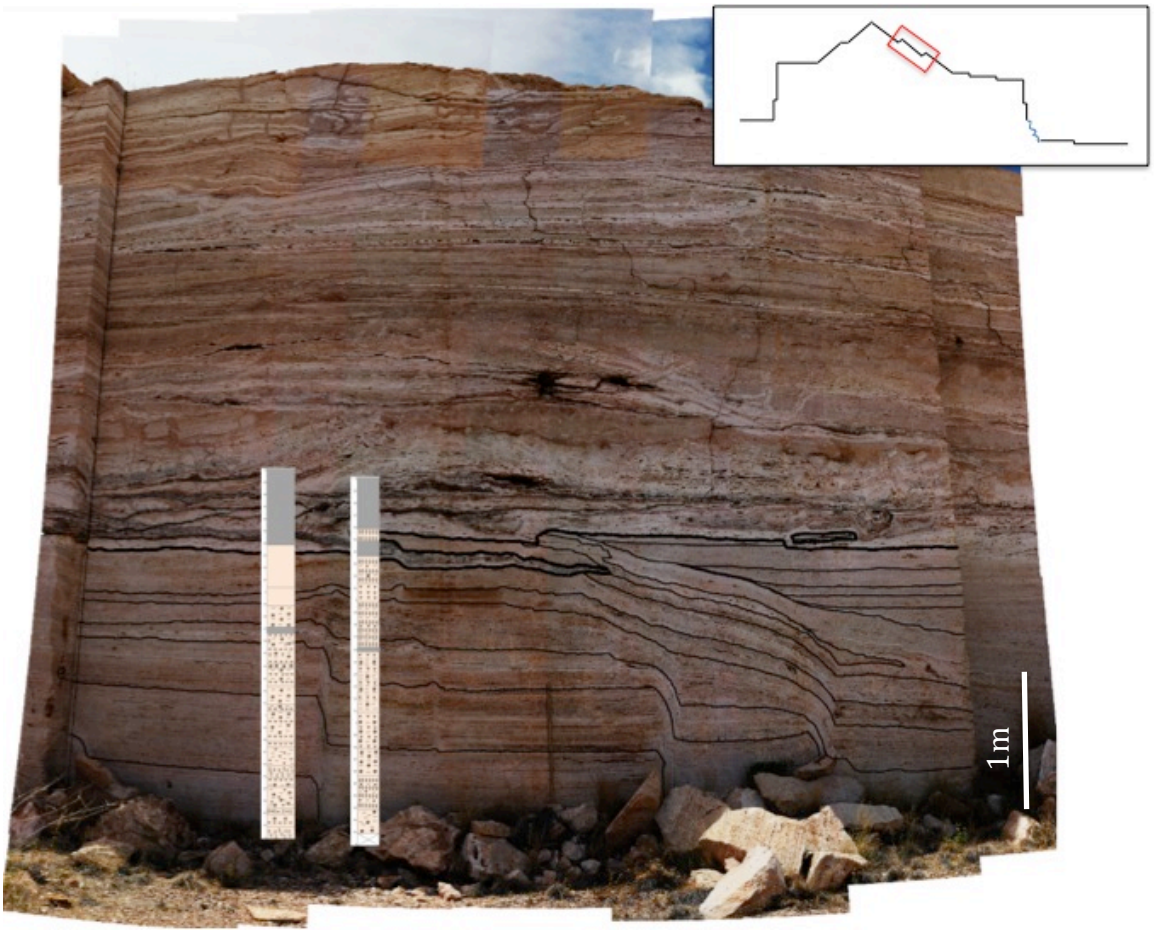

Measured sections Ivory Quarry Wall E- Section 1 (left) and Ivory Quarry Wall E- Section 2 (Right) located on Ivory Quarry Wall E. The black lines highlight the structure on the wall.